

**Synchronizing Rock Clocks of Earth History**K. F. Kuiper, *et al.*Science **320**, 500 (2008);

DOI: 10.1126/science.1154339

***The following resources related to this article are available online at  
www.sciencemag.org (this information is current as of May 15, 2008 ):***

**Updated information and services**, including high-resolution figures, can be found in the online version of this article at:

<http://www.sciencemag.org/cgi/content/full/320/5875/500>

**Supporting Online Material** can be found at:

<http://www.sciencemag.org/cgi/content/full/320/5875/500/DC1>

A list of selected additional articles on the Science Web sites **related to this article** can be found at:

<http://www.sciencemag.org/cgi/content/full/320/5875/500#related-content>

This article **cites 38 articles**, 6 of which can be accessed for free:

<http://www.sciencemag.org/cgi/content/full/320/5875/500#otherarticles>

This article appears in the following **subject collections**:

Geochemistry, Geophysics

[http://www.sciencemag.org/cgi/collection/geochem\\_phys](http://www.sciencemag.org/cgi/collection/geochem_phys)

Information about obtaining **reprints** of this article or about obtaining **permission to reproduce this article** in whole or in part can be found at:

<http://www.sciencemag.org/about/permissions.dtl>

# Synchronizing Rock Clocks of Earth History

K. F. Kuiper,<sup>1,2</sup> A. Deino,<sup>3</sup> F. J. Hilgen,<sup>1</sup> W. Krijgsman,<sup>1</sup> P. R. Renne,<sup>3,4</sup> J. R. Wijbrans<sup>2</sup>

Calibration of the geological time scale is achieved by independent radioisotopic and astronomical dating, but these techniques yield discrepancies of ~1.0% or more, limiting our ability to reconstruct Earth history. To overcome this fundamental setback, we compared astronomical and  $^{40}\text{Ar}/^{39}\text{Ar}$  ages of tephras in marine deposits in Morocco to calibrate the age of Fish Canyon sanidine, the most widely used standard in  $^{40}\text{Ar}/^{39}\text{Ar}$  geochronology. This calibration results in a more precise older age of  $28.201 \pm 0.046$  million years ago (Ma) and reduces the  $^{40}\text{Ar}/^{39}\text{Ar}$  method's absolute uncertainty from ~2.5 to 0.25%. In addition, this calibration provides tight constraints for the astronomical tuning of pre-Neogene successions, resulting in a mutually consistent age of ~65.95 Ma for the Cretaceous/Tertiary boundary.

**A**ccurate and precise measurement of geological time is a prerequisite for understanding Earth's history. Numerical calibration of the geological time scale (GTS) [for example, GTS2004 (1)] is currently based on two independent techniques: astronomical tuning of cyclic sedimentary sequences, which provides a very accurate and high-resolution age model for the youngest Neogene part of the time scale, and radioisotopic dating for older time intervals. However, the various techniques often yield statistically different ages when applied to the same stratigraphic horizons (2, 3).

The radioisotopic dating technique most widely applicable to the late Cenozoic is the  $^{40}\text{Ar}/^{39}\text{Ar}$

method. With careful attention to experimental design, it is possible to achieve analytical precision of 0.2% or better; however, the absolute accuracy of the technique is limited to ~2.5% (4, 5), mainly because of uncertainties in the ages of standards and radioactive decay rates (6).

Several attempts have been made to improve the technique's accuracy by calibrating the  $^{40}\text{Ar}/^{39}\text{Ar}$  dating method to the astronomical method. However, these attempts were limited by uncertainties in identifying the location of magnetostratigraphic boundaries and their correlation to the astronomical polarity time scale (7), assumptions regarding constancy of sedimentation rates (7), complications associated with the use of geochronometers such as biotite (recoil, open-system alteration) and plagioclase (excess argon) (8), problems associated with multigrain sanidine experiments (masking complexities in age distributions) (3), or uncertainties in astronomical time control (3, 9).

We avoid these drawbacks by applying the single-crystal  $^{40}\text{Ar}/^{39}\text{Ar}$  dating method to sanidine

phenocrysts extracted from numerous silicic tephra layers intercalated in an astronomically tuned open marine succession from the Messinian Melilla Basin in Morocco. This basinal succession grades laterally into a marginal carbonate complex; the coarse-grained tephra are derived from the nearby Gourougou volcanic complex (10, 11). The astronomical tuning of the basinal precession-related marl-diatomite cycles is accomplished indirectly, because the sedimentary cycles lack the expression of characteristic details related to precession amplitude and precession-obliquity interference that are common in Mediterranean sapropel sequences (12). Selected planktonic foraminiferal bioevents known to be synchronous throughout the Mediterranean have been identified in the Melilla sections and are correlated to well-tuned Mediterranean reference sections (Fig. 1) (11) that form the core of the standard Neogene time scale (12, 13). The number of sedimentary cycles at Melilla between these biostratigraphic markers is consistent with the number found in these reference sections (11, 12). This indirect approach allows astronomical dating of each tephra layer (Fig. 1).

Uncertainties in the astronomical ages of the radioisotopically dated tephra horizons are contingent on (i) the applied astronomical solutions, including values for tidal dissipation and dynamical ellipticity; (ii) errors in interpolation resulting from the assumption of a constant sedimentation rate between two astronomically tuned calibration points [in this case, cycles are precession tuned and errors are therefore much less than 21 thousand years (ky)]; and (iii) the lag between the orbital forcing and sedimentary expression (we assume that the lag is zero). No exact error can be calculated, but taking these uncertainties into account and provided that the tuning and correlation itself is correct, we estimate that the uncertainty in the astronomical ages for the volcanic ash layers is  $\pm 10$  ky.

<sup>1</sup>Faculty of Geosciences, Department of Earth Sciences, Utrecht University, Budapestlaan 4, 3584 CD Utrecht, Netherlands.

<sup>2</sup>Faculty of Earth and Life Sciences, Institute of Earth Sciences, Vrije Universiteit Amsterdam, De Boelelaan 1085, 1011 HV Amsterdam, Netherlands. <sup>3</sup>Berkeley Geochronology Center, 2455 Ridge Road, Berkeley, CA 94709, USA. <sup>4</sup>Department of Earth and Planetary Science, University of California, Berkeley, CA 94720, USA.

**Table 1.** Recalculated ages of K-T boundary and early Paleocene geomagnetic polarity-reversal boundaries, in Ma. The  $^{40}\text{Ar}/^{39}\text{Ar}$  ages of (36–38) are recalculated relative to the astronomically calibrated age of FCs ( $28.201 \pm 0.046$  Ma). An age of 28.02 Ma for FCs (4) is adopted in GTS2004. Reversal ages in GTS2004 are based on age calibration by spline fit of selected calibration points, including the K-T boundary with an age of 65.5 Ma. Recalculated radioisotopic ages are given with full error estimate. Details on the revised astronomical tuning are given in Fig. 4. The astronomical ages for the reversal boundaries and K-T boundary are calculated by counting the

number of precession cycles from the nearest 100-ky eccentricity maximum/minimum. The age is then calculated by adding or subtracting this number multiplied with the 21-ky precession period to or from the age of the nearest eccentricity maximum or minimum. The astronomical error includes, under the assumption of a correct correlation to the 100-ky eccentricity maximum or minimum, the uncertainty in the 405-ky eccentricity cycle in astronomical solution ( $\pm 40$  ky) [figure 25 in (35)] and an additional error of  $\pm 15$  ky for the uncertainty in the exact position of reversal boundaries. Chron, time interval between polarity reversals of Earth's magnetic field.

Chron / Boundary	GTS2004 (1)	Westerhold et al. (39) Option 1	Westerhold et al. (39) Option 2	Dinarès-Turell et al. (33)	Swisher et al. (36, 37)	Izett et al. (38)	Revised tuning (this study)
Reversal C28n (o)	64.128	$64.028 \pm 0.013$	$64.385 \pm 0.013$	64.460	64.6		$64.698 \pm 0.055$ (64.663)
Reversal C29n (y)	64.432	$64.205 \pm 0.014$	$64.572 \pm 0.016$	64.670	64.9		$64.884 \pm 0.055$ (64.835)
C29n (o)	65.118	$64.912 \pm 0.015$	$65.282 \pm 0.016$	65.549	65.4		$65.724 \pm 0.055$ (65.702)
K-T	$65.50 \pm 0.30$	$65.280 \pm 0.010$	$65.680 \pm 0.010$	65.777	$65.81 \pm 0.14^*$ $65.84 \pm 0.12^\dagger$ $65.99 \pm 0.12^\ddagger$ $65.84 \pm 0.16^\S$	$65.98 \pm 0.105$	$65.957 \pm 0.040$ (65.940)

\*Melt rock of Chicxulub crater.

†Sanidine of Z coal.

‡Sanidine of IrZ coal.

§Haitian tektites.

||Bracketed ages tuned to Va03\_R7 (44).

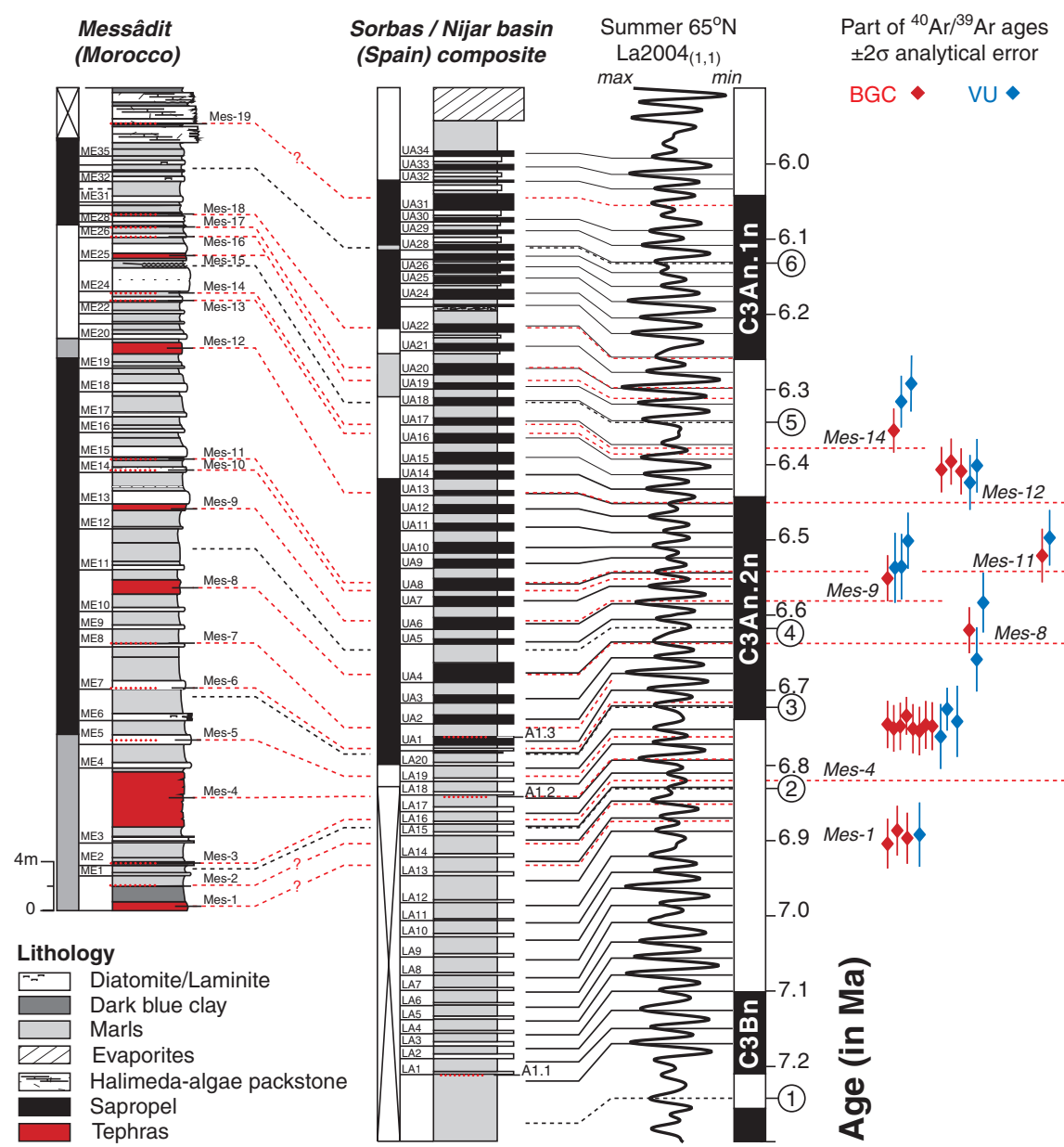
The  $^{40}\text{Ar}/^{39}\text{Ar}$  dating of the Melilla tephra was performed in parallel at the Berkeley Geochronology Center (BGC) and the Vrije Universiteit Amsterdam (VU) (14). In general,  $^{40}\text{Ar}/^{39}\text{Ar}$  ages measured in both laboratories are equivalent within  $2\sigma$  analytical error (table S1), thus confirming a lack of significant interlaboratory bias at this level of confidence. These results can be converted to an astronomically calibrated age for Fish Canyon sandine (FCs) by treating the Melilla sandines as astronomically dated standards and FCs as the unknown (Fig. 2). After incorporating all known sources of error [analytical errors, uncertainty in the astronomical age, and a decay constant of  $5.543 \pm 0.020 \times 10^{-10} \text{ year}^{-1}$  (15)], the intercomparison yielded an age of  $28.198 \pm 0.044$  million years ago (Ma). This approach involves the  $^{40}\text{K}$  total decay constant, but is insensitive

to the value used or its uncertainty. A compilation of the underlying activity data and data updated with new values for other constants led Min *et al.* (5) to determine a value of  $(5.463 \pm 0.214) \times 10^{-10} \text{ year}^{-1}$  and showed the conventionally accepted error to be overly optimistic by an order of magnitude. Nonetheless, from this substantially less accurate (but more realistic) value we calculate an indistinguishable age (with negligibly increased uncertainty) of  $28.201 \pm 0.046$  Ma for FCs. We propose that this result should be the age and uncertainty for FCs, rather than the widely used age of  $28.02 \pm 0.56$  Ma (4). Our age is 0.65% older than the previous one, although given the larger uncertainty of the earlier value the two ages are statistically indistinguishable.

Comparison of our result with the U/Pb zircon age for the Fish Canyon Tuff is meaningless be-

cause of its complex crystallization history, lengthy residence time of zircon, and/or age bias due to Pb loss [for example, see (16–18)]. Comparison of conventional  $^{40}\text{Ar}/^{39}\text{Ar}$  and U/Pb ages for diverse rock types over more than 3 billion years of geological time demonstrates a systematic offset, in which the U/Pb ages are older by 0 to 1% than the  $^{40}\text{Ar}/^{39}\text{Ar}$  ages for the same rocks (19), although scatter in the offset suggests that some of the differences may result from interlaboratory biases or geological complexities. Mundil *et al.* (20) presented U/Pb (zircon) and  $^{40}\text{Ar}/^{39}\text{Ar}$  ages for a suite of volcanic rocks between 130 Ma and 2.1 Ga; these results are likely free of detectable bias due to geological complexities (for example, magma residence time of the zircons, differential closure temperatures, or excess  $^{40}\text{Ar}$ ) or interlaboratory

**Fig. 1.** Astronomical calibration of Messinian Messâdit section in the Melilla-Nador Basin and  $^{40}\text{Ar}/^{39}\text{Ar}$  ages of intercalated tephra. The cycles are tuned to the La2004<sub>(1,1)</sub> solution (35). The main biostratigraphic marker events registered within the studied sections and used for high-resolution correlations are (1) *Globorotalia miotumida* group first regular occurrence (FRO), (2) *G. nicolae* first common occurrence (FCO), (3) *G. nicolae* last occurrence (LO), (4) *G. obesa* FCO, (5) *Neogloboquadrina acostaensis* sinistral/dextral coiling change, and (6) *N. acostaensis* first sinistral influx (11, 12, 43). The phase relation of the sedimentary cycles to orbital parameters is determined using the exact position of bioevents and characteristic planktonic foraminiferal faunal changes associated with the sedimentary cyclicity in the pre-evaporite Messinian Sorbas basin (43). Homogeneous marls in the Moroccan sections correspond to sapropels in Sorbas and other Mediterranean sections (11). Astronomical ages for the tephras are derived by linear interpolation between two astronomically tuned points (that is, three-quarters of the height from the base of the homogeneous interval in each cycle is correlated to the insolation maximum). Weighted mean  $^{40}\text{Ar}/^{39}\text{Ar}$  ages of tephra intercalated in the Messâdit section and analyzed in BGC and VU are shown, calculated relative to an age of 28.02 Ma for FCs (4) (table S1). The  $2\sigma$  error bars include only analytical uncertainties of samples and standards.



errors, and yielded an age of  $28.28 \pm 0.06$  Ma for FCs (21). Thus, our astronomically tuned FCs age of  $28.201$  Ma is consistent at the 95% confidence level with normalization of the  $^{40}\text{Ar}/^{39}\text{Ar}$  to the U/Pb system.

Further confirmation of consistency between the  $^{40}\text{Ar}/^{39}\text{Ar}$  and U/Pb systems based on the proposed revised  $^{40}\text{Ar}/^{39}\text{Ar}$  age of FCs comes from comparison of U/Pb and  $^{40}\text{Ar}/^{39}\text{Ar}$  ages of chondritic meteorites, such as Acapulco (22) and Allende. A ~0.8 to 1% bias between the most accurate  $^{40}\text{Ar}/^{39}\text{Ar}$  (23, 24) and U/Pb (25, 26) ages has classically been interpreted as evidence

for slow cooling after partial melting at  $4555.1 \pm 1.3$  Ma (Acapulco) and formation at  $4566.6 \pm 1.7$  Ma (Allende), as determined by U/Pb dating. With the revised age for the FCs, the K/Ar and U/Pb systems approach concordancy and instead suggest that the parent body of these meteorites cooled rapidly after formation, as suggested by (U+Th)/He (27) and I/Xe (28, 29) studies.

The astronomically calibrated FCs age thus eliminates the documented offset of the conventionally calibrated  $^{40}\text{Ar}/^{39}\text{Ar}$  and U/Pb dating systems in many volcanic rocks. It also has implications for ages of geomagnetic polarity reversals over the past

3 million years (My). Numerous studies in the past two decades have demonstrated apparent consistency between the  $^{40}\text{Ar}/^{39}\text{Ar}$  method and the astronomical dating approach in both sedimentary and volcanic settings, starting from a younger age for FCs or other standards (table S3). This implies that the new FCs age is not consistent with many of these results. For example, recalculating some  $^{40}\text{Ar}/^{39}\text{Ar}$  dates for the Matuyama-Bruhnes reversal relative to our age for FCs yields radioisotopic ages older than the astronomical age [table S3 and references in (14)]. However, the most recent and comprehensive  $^{40}\text{Ar}/^{39}\text{Ar}$  data (30), which suggested that the transition may have been diachronous, are in agreement with our intercalibration.

An important application of the astronomically calibrated  $^{40}\text{Ar}/^{39}\text{Ar}$  method is to provide constraints for the astronomical tuning of pre-Neogene sequences. The prime, first-order target for tuning these older sequences is the 405-ky earth-orbital eccentricity cycle (31, 32). Our method reduces the absolute uncertainty from ~2.5% (or ~1600 ky at 65 Ma) to potentially <0.25% (or <165 ky at 65 Ma), because the uncertainties in absolute amounts of radiogenic  $^{40}\text{Ar}$  and  $^{40}\text{K}$  in the primary standard and the branching ratio of the  $^{40}\text{K}$  decay constant are circumvented using the astronomical age of the Melilla sanidines as the basis for calculating the  $^{40}\text{Ar}/^{39}\text{Ar}$  age. The use of equation 5 of (4) enables calculation of the age of an unknown based on an age for the standard determined by means other than the K-Ar system, and requires only knowledge of the total  $^{40}\text{K}$  decay constant (that is, not the branching ratio). [Full equations are provided in (14)].

We demonstrate the improved age resolution by examining the GTS2004 age of 65.5 Ma for the Cretaceous/Tertiary (K-T) boundary, which marks one of the most important biotic crises in Earth history. The K-T boundary section at Zumaia, Spain, which magnetostratigraphically covers the interval from the younger part of polarity interval C29r well into C26r, has been astronomically tuned and the boundary has been assigned an age of 65.777 Ma (33). The astronomical age of (33) is uncertain for two reasons: (i) the use of the potentially unstable very-long-period 2.4-My eccentricity cycle as the starting point for the tuning; and (ii) the matching of basic marl/limestone cycle packages [the E-cycles of (33)] to successive 100-ky eccentricity minima in the target curve, which is less certain (and stable) than the 405-ky eccentricity minima (fig. S2).

According to (33), the 405-ky cycle is not expressed, or only very weakly present at Zumaia. Nevertheless, this cycle can be identified on photographs, in the field, and in the lithologic log of Zumaia of (33) through differences in the thickness and expression of marls intercalated between 100-ky limestone beds (Fig. 3 and fig. S3). Details of the cycle pattern confirm the phase relations between the sedimentary cycles and eccentricity as inferred by (33). Small-scale precession-related cycles are less well developed in the limestone beds of eccentricity-related cycles, indicating that these beds indeed correspond to eccentricity minima be-

**Fig. 2.** Astronomically calibrated FCs age. The  $^{40}\text{Ar}/^{39}\text{Ar}$  ages of the ash layers are converted to an astronomically calibrated age for FCs by using the Melilla sanidines as astronomically dated standards and the FCs as the unknown. Instead of doing this exercise for each tephra horizon separately, we included all reliably (both isotopic and astronomical) dated tephra to prevent an a priori bias to one of the astronomically dated tephra. However, the calibrated age is an inverse-variance weighted

mean age; thus, tephra mes4, with the highest number of replicate analyses and the most precise data, dominates the final outcome. We include only the single-crystal fusion data (displayed here with  $1\sigma$  analytical error), and ages with  $P > 0.1$ . Incremental heating experiments on selected sanidine fractions confirm the thermally undisturbed nature of the samples (14). We calculate an astronomically calibrated FCs age for each experiment propagating only analytical uncertainties. The weighted mean FCs age and standard analytical error for BGC and VU data are displayed separately and as a combined-age probability diagram. The  $28.201 \pm 0.012$  Ma age for FCs is converted to an intercalibration factor of  $R_{\text{FCs},\text{astro}}^{\text{FCs}}$  of  $4.3644 \pm 0.0018$  for a  $T_{\text{astro}}$  at 6.500 Ma. This translates to  $28.201 \pm 0.046$  Ma, including decay-constant uncertainties and the uncertainty in the astronomical ages of  $\pm 10$  ky.

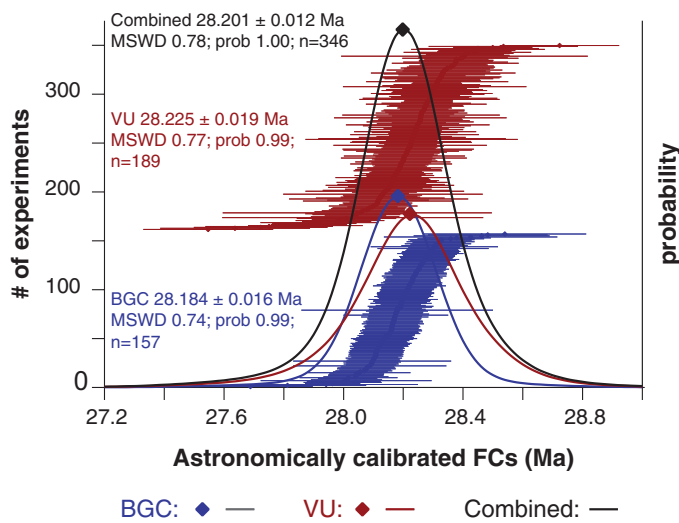
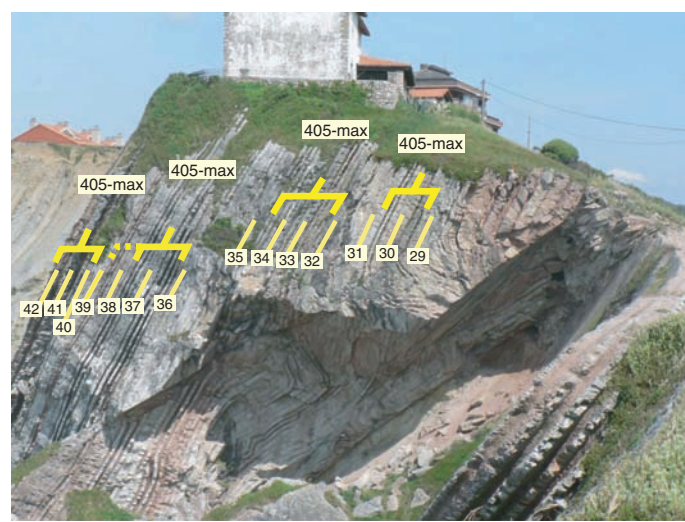


**Fig. 3.** Photo of the upper part of the Zumaia section below the San Telmo chapel. Both the 100-ky limestone beds 29 to 42 of (33) and the large-scale clusters of precession-related basic cycles that mark successive 405-ky eccentricity maxima are indicated (see also figs. S3, a to d). The phase relation with eccentricity is unambiguous: The marly intervals in between the 405- and 100-ky limestone beds often reveal distinct precession-related cycles, which is consistent with eccentricity maxima because eccentricity determines precessional amplitude. Eccentricity minima are marked by weakly developed precession-related cycles and are dominated by limestone beds.



cause eccentricity modulates the precession signal's amplitude.

The K-T boundary at Zumaia lies at the base of a prominent limestone-dominated interval that

**Fig. 4.** Tuning of the K-T boundary section at Zumaia. Modified tuning of the Zumaia section following (33) that is consistent with the proposed intercalibration and takes the expression of the 405-ky eccentricity cycle into account. Close inspection of the lithological log suggests that cycle bundles 1 to 14 should be tuned one 100-ky eccentricity minimum older than in (33) if the Va03\_R7 solution is used for the tuning (note that the differences with the La2004 solution are larger). Crosses to the right of the lithological column mark midpoints of limestone-dominated parts of the 100-ky cycle that correlate with 100-ky eccentricity minima. The boundaries between the 100-ky cycles represent midpoints of the more marly intervals. Solid lines mark correlation lines in intervals in which the identification of the ~100- and 405-ky cycles is rather straightforward; dashed lines mark correlation lines in intervals in which the identification of the 405-ky cycle is less clear but supported by the number of ~100-ky and precession-related cycles. A conservative estimate of the absolute uncertainty in the 405-ky cycle around 65 Ma is  $\pm 40$  ky (35). The estimated uncertainty of  $\sim 165$  ky in the astronomically calibrated  $^{40}\text{Ar}/^{39}\text{Ar}$  method at the K-T boundary gives a combined estimate of  $\pm 200$  ky. This is sufficient to pinpoint the correct 405-ky maximum, because the astronomically calibrated  $^{40}\text{Ar}/^{39}\text{Ar}$  ages (Table 1 and table S4) for the K-T boundary correspond closely to a 405-ky eccentricity minimum, leaving no space for tuning the K-T boundary interval one 405-ky eccentricity minimum older (K-T  $\sim 66.4$  Ma) or younger (K-T  $\sim 65.6$  Ma). Starting from the eccentricity tuning, the astronomical age of the K-T boundary arrives at 65.957 or 65.940 Ma for the La2004 and Va03\_R7 solutions, respectively, using the average precession period (21 ky) at that time and the number of precession-related cycles (2.5) below cycle 2b, the oldest tuned 100-ky eccentricity minimum.

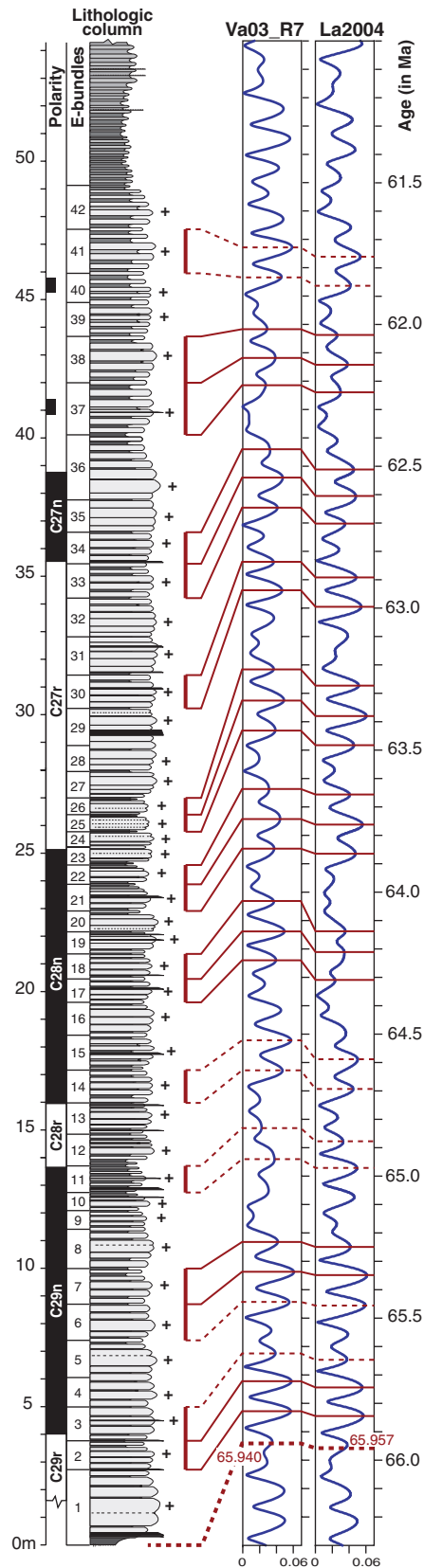
corresponds to a 405-ky eccentricity minimum. Successive 405-ky minima have ages of  $\sim 65.2$ ,  $\sim 65.6$ ,  $\sim 66.0$ , and  $\sim 66.4$  Ma; thus, the challenge is to identify the correlative minimum. The error in

the astronomical solution is on the order of 40 ky at 65 Ma [(34) and figure 25 in (35)]. To pinpoint this minimum, we recalculated published  $^{40}\text{Ar}/^{39}\text{Ar}$  ages for the K-T boundary interval with our astronomical FCs age of 28.201 Ma.

Single-crystal sanidine  $^{40}\text{Ar}/^{39}\text{Ar}$  dates on tephra horizons are available for the same magnetostratigraphic interval in continental sections in Montana (36). Haitian K-T boundary tektites and Chixulub crater melt rock have also been dated by the  $^{40}\text{Ar}/^{39}\text{Ar}$  technique (37, 38). These ages recalculated relative to our FCs age of 28.201 Ma range from 65.8 to 66.0 Ma (Table 1 and table S4). We regard the single-crystal sanidine ages of 65.84 Ma [of Z coal (36)] and especially 65.99 Ma [of IrZ coal (36)] as the best estimates. These ages are considerably greater than the ages reported in GTS2004, which are based on sea-floor anomaly profiles numerically calibrated by means of a limited number of isotopically dated tie points, including the K-T boundary at 65.5 Ma, using an age of 28.02 Ma for FCs. This approach pins the K-T boundary down to the 405-ky eccentricity minimum around 66.0 Ma. Using this calibration as the starting point, the Zumaia section of (33) was retuned, taking the newly recognized 405-ky cycle into account (Figs. 3, 4). The resultant astronomical ages for the K-T boundary and magnetic reversal boundaries are in good agreement with the revised  $^{40}\text{Ar}/^{39}\text{Ar}$  ages (Table 1).

In principle, the revised astronomical age of  $\sim 65.95$  Ma for the K-T boundary can be shifted upward or downward by one 405-ky eccentricity cycle, resulting in ages of either  $\sim 65.56$  or  $\sim 66.4$  Ma (for example, see fig. S4). However, the astronomically recalibrated  $^{40}\text{Ar}/^{39}\text{Ar}$  ages allow us to exclude these ages for the K-T boundary (Table 1 and table S4). Westerhold *et al.* (39) similarly linked the K-T boundary to a 405-ky eccentricity minimum using Fe and magnetic susceptibility records of Ocean Drilling Program cores from the Pacific and Atlantic Ocean and including the Zumaia section in their astrochronological framework. Their preferred tuning options result in ages of 65.28 Ma (option 1) or 65.68 Ma (option 2) for the K-T boundary. A third option (66.08 Ma) was added for consistency with our astronomically calibrated age for FCs, but this option is less favored, because it results in a relatively old age of 56.33 Ma for the Paleocene/Eocene boundary, an age that is difficult to reconcile with existing, though limited, radioisotopic constraints, even when recalculated against our astronomical FCs age. However, our Zumaia tuning results in one extra 405-ky cycle compared with (39) for the interval between the K-T boundary and the top of the normal polarity interval of C28n. Such differences must be resolved before a tuned Paleocene time scale can be finalized. Nevertheless, our intercalibration firmly links the K-T boundary to the 405-ky eccentricity minimum around 66 Ma.

An age of  $\sim 66.0$  Ma for the K-T boundary was previously incorporated in the polarity time scale of Cande and Kent (40). However, this seemingly identical age was interpreted to be a spurious result from the chemical preparation of volcanic ashes



found intercalated in coal beds. Redating of the sanidine in these ash beds (using an age of 27.83 Ma for the FCs) led to a revised age of ~65.0 Ma for the K-T boundary, which was adopted in (41). The same single-crystal sanidine dates now provide an age of ~65.95 Ma, relative to our FCs age of 28.201 Ma.

We argue that our astronomically calibrated FCs age of 28.201 Ma should be incorporated in the next standard GTS to recalculate all other  $^{40}\text{Ar}/^{39}\text{Ar}$  ages after it is confirmed by independent (intercalibration) studies. Only in this way is a mutually consistent age calibration of the GTS assured. Moreover, our integrated approach may lead to a stable time scale with unprecedented accuracy, precision, and resolution that will not be forced to undergo any further substantial revisions.

#### References and notes

1. F. M. Gradstein, J. G. Ogg, A. G. Smith, *A Geologic Time Scale 2004* (Cambridge Univ. Press, Cambridge, 2004).
2. P. R. Renne, D. B. Karner, K. R. Ludwig, *Science* **282**, 1840 (1998).
3. K. F. Kuiper, F. J. Hilgen, J. Steenbrink, J. R. Wijbrans, *Earth Planet. Sci. Lett.* **222**, 583 (2004).
4. P. R. Renne *et al.*, *Chem. Geol.* **145**, 117 (1998).
5. K. W. Min, R. Mundil, P. R. Renne, K. R. Ludwig, *Geochim. Cosmochim. Acta* **64**, 73 (2000).
6. All errors are stated at the  $2\sigma$  level, unless stated otherwise.
7. P. R. Renne *et al.*, *Geology* **22**, 783 (1994).
8. F. J. Hilgen, W. Krijgsman, J. R. Wijbrans, *Geophys. Res. Lett.* **24**, 2043 (1997).
9. J. Steenbrink, N. Van Vugt, F. J. Hilgen, J. R. Wijbrans, J. E. Meulenkamp, *Palaeogeogr. Palaeoclimatol. Palaeoecol.* **152**, 283 (1999).
10. S. Roger *et al.*, *Earth Planet. Sci. Lett.* **179**, 101 (2000).
11. E. Van Assen, K. F. Kuiper, N. Barhoun, W. Krijgsman, F. J. Sierra, *Palaeogeogr. Palaeoclimatol. Palaeoecol.* **238**, 15 (2006).
12. W. Krijgsman, F. J. Hilgen, I. Raffi, F. J. Sierra, D. S. Wilson, *Nature* **400**, 652 (1999).
13. L. J. Lourens, F. J. Hilgen, J. Laskar, N. J. Shackleton, D. Wilson, in *The Geological Time Scale 2004*, F. M. Gradstein, J. G. Ogg, A. G. Smith, Eds. (Cambridge Univ. Press, Cambridge, 2004), pp. 409–440.
14. Materials and methods are available as supporting material on *Science Online*.
15. R. H. Steiger, E. Jäger, *Earth Planet. Sci. Lett.* **36**, 359 (1977).
16. J. I. Simon, P. R. Renne, R. Mundil, *Earth Planet. Sci. Lett.* **266**, 182 (2008).
17. O. Bachmann *et al.*, *Chem. Geol.* **236**, 134 (2007).
18. M. D. Schmitz, S. A. Bowring, *Geochim. Cosmochim. Acta* **65**, 2571 (2001).
19. B. Schoene, J. L. Crowley, D. J. Condon, M. D. Schmitz, S. A. Bowring, *Geochim. Cosmochim. Acta* **70**, 426 (2006).
20. R. Mundil, P. R. Renne, K. K. Min, K. R. Ludwig, *Eos Transactions American Geophysical Union Meeting Supplement* **87**, Abstract V21A (2006).
21. J. Y. Kwon, K. W. Min, P. J. Bickel, P. R. Renne, *Math. Geol.* **34**, 457 (2002).
22. Acapulco has chondritic chemistry but lacks chondrules owing to early high-temperature metamorphism (42).
23. P. R. Renne, *Earth Planet. Sci. Lett.* **175**, 13 (2000).
24. E. K. Jessberger, B. Dominik, T. Staudacher, G. F. Herzog, *Icarus* **42**, 380 (1980).
25. Y. Amelin, V. Pravdivtseva, *Meteorit. Planet. Sci.* **40**, A16 (2005).
26. A. Bouvier, J. Blachert-Toft, F. Moynier, J. D. Vervoort, F. Albarede, *Geochim. Cosmochim. Acta* **71**, 1583 (2007).
27. K. Min, K. A. Farley, P. R. Renne, K. Marti, *Earth Planet. Sci. Lett.* **209**, 323 (2003).
28. R. H. Nichols, C. M. Hohenberg, K. Kehm, Y. Kim, K. Marti, *Geochim. Cosmochim. Acta* **58**, 2553 (1994).
29. T. D. Swindle, *Meteorit. Planet. Sci.* **33**, 1147 (1998).
30. R. S. Coe, B. S. Singer, M. S. Pringle, X. X. Zhao, *Earth Planet. Sci. Lett.* **222**, 667 (2004).
31. L. J. Lourens *et al.*, *Nature* **435**, 1083 (2005).
32. H. Pälike *et al.*, *Science* **314**, 1894 (2006).
33. J. Dinarès-Turell *et al.*, *Earth Planet. Sci. Lett.* **216**, 483 (2003).
34. H. Pälike, J. Laskar, N. J. Shackleton, *Geology* **32**, 929 (2004).
35. J. Laskar *et al.*, *Astron. Astrophys.* **428**, 261 (2004).
36. C. C. Swisher, L. Dingus, R. F. Butler, *Can. J. Earth Sci.* **30**, 1981 (1993).
37. C. C. Swisher III *et al.*, *Science* **257**, 954 (1992).
38. G. A. Izett, G. B. Dalrymple, L. W. Snee, *Science* **252**, 1539 (1991).
39. T. Westerhold *et al.*, *Palaeogeogr. Palaeoclimatol. Palaeoecol.* **257**, 377 (2008).
40. S. C. Cande, D. V. Kent, *J. Geophys. Res.* **97**, 13917 (1992).
41. W. A. Berggren, D. V. Kent, C. C. Swisher, M.-P. Aubry, *Geochronology, Time Scales and Global Stratigraphic Correlation, SEPM Special Publication* **54**, 129 (1995).
42. T. J. McCoy *et al.*, *Geochim. Cosmochim. Acta* **60**, 2681 (1996).
43. F. J. Sierra, F. J. Hilgen, W. Krijgsman, J. A. Flores, *Palaeogeogr. Palaeoclimatol. Palaeoecol.* **168**, 141 (2001).
44. F. Varadi, B. Runnegar, M. Ghil, *Astrophys. J.* **592**, 620 (2003).
45. The project was funded by grants 750.198.02 and 814.01.004 of the Netherlands Organisation for Scientific Research to K.K., and supported by NSF grant EAR-9903078 to P.R. and A.D.P.R. and A.D.'s work was also supported by the Ann and Gordon Getty Foundation. Mineral separation facilities at VU were provided by Roel van Elsas.

#### Supporting Online Material

[www.sciencemag.org/cgi/content/full/320/5875/500/DC1](http://www.sciencemag.org/cgi/content/full/320/5875/500/DC1)

Materials and Methods

SOM Text

Figs. S1 to S4

Tables S1 to S4

References

18 December 2007; accepted 6 March 2008

10.1126/science.1154339

materials the sum of Poisson's ratios for lateral dimension changes exceeds unity, so they increase density when stretched and, inversely, expand in at least one direction when hydrostatically compressed (1). If a lateral dimension expands during stretching, the associated Poisson's ratio is negative and the material is called auxetic (2). Recent interest in this counterintuitive behavior originated from pioneering discoveries that partially collapsed foams and honeycombs (2, 3), fibrillar polymers (4), and polymer composites (5) can be auxetic.

Poisson's ratio was unknowingly used 2000 years ago in the empirical selection of cork for wine bottle stoppers. Cork stoppers have a near-zero Poisson's ratio for radial directions when subjected to orthogonal uniaxial stress (6). A positive Poisson's ratio makes a stopper difficult to insert but easy to remove, and the reverse occurs for a negative Poisson's ratio.

Carbon nanotube sheets (buckypaper) were fabricated (7, 8) by filtration of aqueous dispersions of single-walled nanotubes (SWNTs) (9) and multiwalled carbon nanotubes (MWNTs) (10) produced by chemical vapor deposition, a technique reminiscent of ancient methods for making writing paper by drying a fiber slurry. The SWNTs are seamless cylinders of graphite

## REPORTS

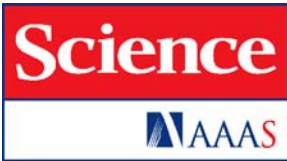
# Sign Change of Poisson's Ratio for Carbon Nanotube Sheets

Lee J. Hall,<sup>1</sup> Vitor R. Coluci,<sup>2</sup> Douglas S. Galvão,<sup>2</sup> Mikhail E. Kozlov,<sup>1</sup> Mei Zhang,<sup>1\*</sup> Sócrates O. Dantas,<sup>3</sup> Ray H. Baughman<sup>1†</sup>

Most materials shrink laterally like a rubber band when stretched, so their Poisson's ratios are positive. Likewise, most materials contract in all directions when hydrostatically compressed and decrease density when stretched, so they have positive linear compressibilities. We found that the in-plane Poisson's ratio of carbon nanotube sheets (buckypaper) can be tuned from positive to negative by mixing single-walled and multiwalled nanotubes. Density-normalized sheet toughness, strength, and modulus were substantially increased by this mixing. A simple model predicts the sign and magnitude of Poisson's ratio for buckypaper from the relative ease of nanofiber bending and stretch, and explains why the Poisson's ratios of ordinary writing paper are positive and much larger. Theory also explains why the negative in-plane Poisson's ratio is associated with a large positive Poisson's ratio for the sheet thickness, and predicts that hydrostatic compression can produce biaxial sheet expansion. This tunability of Poisson's ratio can be exploited in the design of sheet-derived composites, artificial muscles, gaskets, and chemical and mechanical sensors.

When stretched, most materials contract in both lateral dimensions to decrease stretch-induced volume change. The ratio of percent lateral contraction to percent ap-

plied tensile elongation is the Poisson's ratio. Some rubbers have Poisson's ratios of about 0.5 for both lateral directions, so their volume does not appreciably change upon stretching. In very rare



[www.sciencemag.org/cgi/content/full/320/5875/500/DC1](http://www.sciencemag.org/cgi/content/full/320/5875/500/DC1)

## Supporting Online Material for **Synchronizing Rock Clocks of Earth History**

K. F. Kuiper, A. Deino, F. J. Hilgen, W. Krijgsman, P. R. Renne, J. R. Wijbrans

Published 25 April 2008, *Science* **320**, 500 (2008)

DOI: 10.1126/science.1154339

**This PDF file includes:**

Materials and Methods

SOM Text

Figs. S1 to S4

Tables S1 to S4

References

## **Supporting Online Material**

The supporting online material includes:

- Material and Methods with details on data treatment both at BGC and the VU.
- All relevant analytical information (tables S1, S2, fig. S1).
- Age and error equations for astronomically calibrated standard.
- $^{40}\text{Ar}/^{39}\text{Ar}$  ages for the Matuyama- Bruhnes geomagnetic polarity reversal (table S3).
- Details of revised astronomical tuning of the K-T boundary (figs. S2-4).
- Comments on existing controversy of the relation between Chixculub impact crater and K-T boundary event.
- Details on  $^{40}\text{Ar}/^{39}\text{Ar}$  data of the K-T boundary (table S4).
- References.

## **Material and Methods**

Volcanic levels intercalated in cyclic sedimentary sequences of marl and diatomites were sampled during joint field campaigns. Mineral separations and  $^{40}\text{Ar}/^{39}\text{Ar}$  analyses were performed independently both at the Vrije Universiteit Amsterdam (VU) and the Berkeley Geochronology Center (BGC). All samples were irradiated in the OSU TRIGA reactor CLICIT facility in several batches ranging from 7-20 hours irradiation time. At BGC single crystals of sanidine were either fused or incrementally heated. J-values are calculated by a planar regression over the irradiations discs. At the VU single crystals of sanidine were fused. J values are calculated by a 2<sup>nd</sup> order polynomial regression over the vial height. The neutron flux monitor FCs of  $28.02 \pm 0.28$  Ma (*S1*) is used in all irradiations apart from VU37, which used 85G003 of  $28.34 \pm 0.28$  Ma (*S1*). Residuals calculated for J-values are on the order of 0.1% both at BGC and the VU, in practice a slightly higher uncertainty ( $\pm 0.2\text{-}0.3\%$  1 $\sigma$  uncertainty in J) is arbitrarily used in the age calculations. Decay constants of (*S2*) are used in age calculations. Corrections factors for neutron interference reactions are  $2.65 \pm 0.022 \times 10^{-4}$  for  $(^{36}\text{Ar}/^{37}\text{Ar})_{\text{Ca}}$ ,  $6.95 \pm 0.092 \times 10^{-4}$  for  $(^{39}\text{Ar}/^{37}\text{Ar})_{\text{Ca}}$ ,  $1.22 \pm 0.0027 \times 10^{-2}$  for  $(^{38}\text{Ar}/^{39}\text{Ar})_{\text{K}}$  and  $7.3 \pm 0.92 \times 10^{-4}$  for  $(^{40}\text{Ar}/^{39}\text{Ar})_{\text{K}}$  at BGC and  $2.64 \pm 0.017 \times 10^{-4}$  for  $(^{36}\text{Ar}/^{37}\text{Ar})_{\text{Ca}}$ ,  $6.73 \pm 0.037 \times 10^{-4}$  for  $(^{39}\text{Ar}/^{37}\text{Ar})_{\text{Ca}}$ ,  $1.211 \pm 0.003 \times 10^{-2}$  for  $(^{38}\text{Ar}/^{39}\text{Ar})_{\text{K}}$  and  $8.6 \pm 0.7 \times 10^{-4}$  for  $(^{40}\text{Ar}/^{39}\text{Ar})_{\text{K}}$  at the VU (1 sigma errors). Note that all VU data have been recalculated with BGC correction factors resulting in negligible an age difference of 0.007% or less.

### ***Irradiation and flux monitor procedures at BGC***

Samples were irradiated in the OSU TRIGA reactor CLICIT facility in three different irradiation batches: BGC269 in a 14h irradiation and BGC252 and BGC257 in a 20h irradiation. BGC monitors the horizontal flux gradient over 190mm diameter and 2-3 mm thick aluminum discs (*S1*). All irradiations use FCs.

At BGC J-values are calculated by a planar regression over the disc. After rigorous cleaning of the data set (i.e. omission of all data with  $^{40}\text{Ar}^*$  yields < 98%,  $^{39}\text{Ar} < 0.05 \times 10^{-14}$ ,  $\text{Ca/K} > 1$ , followed by omission of data outside 2 standard deviations) weighted mean J values for each hole containing FCs are used for this regression. If standards (and thus also samples) are measured during different periods, J values are calculated for each period and only combined when they are statistically equivalent. Residuals calculated for the standard positions from these regressions are on the order of 0.1%, in practice a slightly higher uncertainty ( $\pm 0.2\%$  1 $\sigma$  uncertainty in J) is arbitrarily used in the age calculations.

### ***Irradiations and flux monitor procedures at VU***

Samples were irradiated in the OSU Triga reactor CLICIT facility in three different irradiation batches all for 7 hours (VU37, VU41 and VU42). The vertical neutron gradient flux is monitored by irradiating samples and standards in ~80mm long vials. The horizontal flux gradient in the 6mm ID vials is ignored. Irradiation VU37 uses Taylor

Creek Rhyolite sanidine (TCs) and irradiations VU41 and VU42 use FCs as neutron flux monitor.

J-values are calculated using a weighted 2<sup>nd</sup> order polynomial regression. Cleaning of the dataset is less rigorous than at BGC, but <sup>40</sup>Ar\* yields for FCs and TCs are in general higher than 97%. Radiogenic <sup>40</sup>Ar yields lower than 90%, and Ca/K > 1 are omitted. When MSWD > student's T statistic outliers are omitted until MSWD < student's T (at 95% confidence level). Then weighted mean J values and standard errors for each position in the vial are used in the weighted 2<sup>nd</sup> order polynomial regression. Residuals are on the order of 0.1 %, but in practice a slightly higher uncertainty (0.2-0.3% 1 $\sigma$  uncertainty in J) is arbitrarily used in the age calculations.

#### *<sup>40</sup>Ar/<sup>39</sup>Ar analytical procedures at BGC*

Samples and standards are melted using a focused CO<sub>2</sub> laser to extract trapped argon from the crystals. Gasses are exposed to a -130°C cold trap to remove H<sub>2</sub>O and to SAES getters to remove reactive compounds. Samples, standards, blanks and air aliquots are measured during a fixed period of 1800 seconds in ~13 scans. Baseline is measured at masses 35.6 and 36.4 at the beginning and end of an analysis. A series of air measurements (n = 4-8) is typically performed at the beginning and end of a series run (after bake out and before sample change). Further single air pipettes are analyzed every ~10 unknowns. Depending on their behavior blanks are measured every one or two unknowns. <sup>40</sup>Ar/<sup>39</sup>Ar dating procedures at BGC are described in detail elsewhere (S1).

#### *<sup>40</sup>Ar/<sup>39</sup>Ar analytical procedures at VU*

Samples are melted with a 20W continuous wave argon ion laser. Samples and standards are preheated with a defocused laser beam at ~1.8W to remove contaminating volatiles before melting. Gasses are exposed to SAES getters during 300 seconds, followed by measurement of the argon isotopes on a MAP 215-50 mass spectrometer. The mass spectrometer is operated with a modified version of the standard MAP software that allows data collection for argon using a Johnston's SEM collector. Measurements are performed in 10-12 scans in a peak jumping mode from m/e 40 to m/e 35.5 in half mass intervals. Baselines in each scan consist of typically 4-6 integration cycles, <sup>37</sup>Ar and <sup>38</sup>Ar peaks consist of 8-12 integration cycles and <sup>40</sup>Ar, <sup>39</sup>Ar and <sup>36</sup>Ar of 12-16 integration cycles per scan. The mean value of each integration cycle is stored in a raw data file together with the number of scans and the time elapsed since the inlet of the gas into the mass spectrometer. System blanks are generally measured every 3 or 4 steps. The total system blanks are in the range of 1-10 × 10<sup>-17</sup> moles for mass 40, 1-5 × 10<sup>-18</sup> moles for mass 39, 38 and 36 and 1-3 × 10<sup>-17</sup> moles for mass 37. Mass discrimination (1.002-1.0100 per atomic mass unit) was monitored by frequent analysis of <sup>40</sup>Ar/<sup>38</sup>Ar reference gas or <sup>40</sup>Ar/<sup>36</sup>Ar air pipette aliquots. Further details on <sup>40</sup>Ar/<sup>39</sup>Ar dating procedures at VU are described in detail elsewhere (S3, S4).

### ***Data reduction, age calculation and error propagation***

$^{40}\text{Ar}/^{39}\text{Ar}$  ages are calculated with decay constants of Steiger and Jäger (S2) and an age of 28.02 Ma for FCs and 28.34 Ma for TCs (S1). At the VU the in-house developed ArArCALC program is used for reduction of the raw  $^{40}\text{Ar}/^{39}\text{Ar}$  data. Details on procedures and algorithms can be found in Koppers (S5). At BGC the in-house developed argon data acquisition and data reduction program “Mass Spec” (by A. Deino) is used for data reduction. In both BGC and VU regression lines are calculated, in general by exponential fitting of  $^{40}\text{Ar}$  and  $^{39}\text{Ar}$  and linear fits for  $^{38}\text{Ar}$ ,  $^{37}\text{Ar}$  and  $^{36}\text{Ar}$ . Blank correction is done by either a (linear or smoothing) trend through a series of blanks or by bracketing blanks (using linear interpolation). Mass discrimination factors are generally based on linear interpolation.

All analytical information is given in the supplementary tables S1, S2. Ages are calculated with  $1\sigma$  analytical error (i.e. only the error in the  $^{40}\text{Ar}^*/^{39}\text{Ar}_K$  ratio of the sample is included) and  $\pm 1\sigma(J)$  including the error in the  $^{40}\text{Ar}^*/^{39}\text{Ar}_K$  ratio of the standard as well.

### ***Outlier detection***

Approaches in detections of outliers between BGC and VU differ at some points. At BGC data yielding either “low” radiogenic  $^{40}\text{Ar}^*$  (i.e. <97% for unknowns and <98% for FCs), Ca/K ratios > 1 and/or small amounts of  $^{39}\text{Ar}$  ( $<0.05 \times 10^{-14}$  moles) are immediately discarded. Outliers in the remaining data set are first visually assessed and extreme outliers (i.e. >1 Ma younger/older than expected age) are rejected. Next, a 1.5 nMad criteria is used for rejection of outliers, which appeared to be a very efficient semi-quantitative way to recognize outliers.

At the VU data yielding either Ca/K ratios > 1 and/or small amounts of  $^{39}\text{Ar}$  ( $<0.05 \times 10^{-14}$  moles) are also immediately discarded, but criteria for low radiogenic  $^{40}\text{Ar}^*$  yields are less rigorous (i.e. data with  $^{40}\text{Ar}^* < 85\%$  are excluded). “Extreme” outliers (> 1 Ma from expected age) are then omitted. For the remaining data the 1.5 nMad outlier criteria is applied.

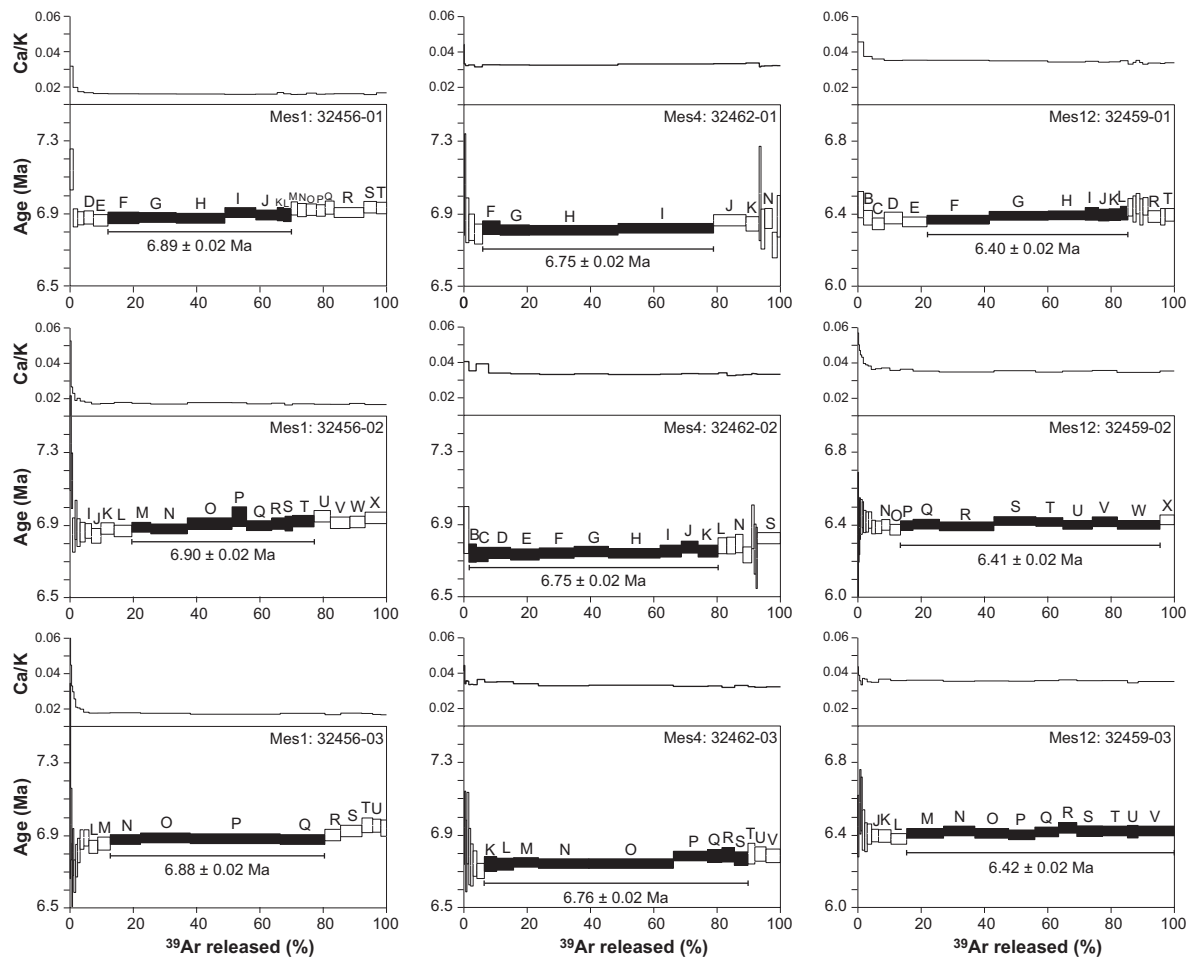


**Figure S1. Incremental heating spectra.**

Incremental heating experiments were performed at BGC on single sanidine crystals of three samples Mes1, Mes4 and Mes12. Analytical data of steps containing less than 2% of the total  $^{39}\text{Ar}$  are listed in the table S2, but are never included in the plateau age. An age plateau is located on basis of MSWD with probability cut-off at 0.95 and the two outermost steps from each side of the plateau must not be significantly different than the weighted mean plateau age at  $1.4\sigma$  (tolerance limit of 1.4). Radiogenic  $^{40}\text{Ar}$  yields are high (>97% for all steps yielding >2%  $^{39}\text{Ar}_K$ ) and Ca/K ratios are constant. The samples do not show complex thermal histories and this implies that total fusions instead of incremental heating experiments are justified (fig. S1). Age spectra are shown with 2 sigma error bars.

**Table S1: Summary of  $^{40}\text{Ar}/^{39}\text{Ar}$  and astronomical ages in the Melilla-Nador Basin.**

Weighted mean ages with  $1\sigma$  analytical errors, including analytical uncertainty in  $J$ , are given for each irradiation. Data are reported using sanidine from the Fish Canyon Tuff (FCs) as a dating standard with a reference age of 28.02 Ma and/or sanidine from the Taylor Creek Rhyolite (TCRs) of 28.34 Ma (*S1*) and decay constants used by convention since 1977 (*S2*). Full analytical data and summary calculations for individual irradiation experiments are available in Table S2. Astronomical ages are given in bold. Published  $^{40}\text{Ar}/^{39}\text{Ar}$  ages of previous studies on the same tephras (*S6-S8*) are listed for completeness, but are not included in the intercalibration.

Lab ID	Irradiation	Age (Ma)	$\pm 1\sigma$ (J)	Prob.	n
<b>Mes1 &gt;6.84 Ma</b>					
32474	BGC252A	6.904	0.016	0.64	8/8
32480	BGC252A	6.887	0.016	0.91	8/8
32486	BGC252A	6.897	0.017	0.75	6/7
01M0165	VU37	6.892	0.021	0.30	8/8
32456-01	BGC252PR-C	6.893*	0.023	0.60	7/20
32456-02	BGC252PR-C	6.901*	0.023	0.22	8/24
32456-03	BGC252PR-C	6.880*	0.024	0.99	4/22
<b>Mes4 = 6.791 Ma</b>					
22009	BGC269A	6.746	0.016	0.15	9/13
22029	BGC269B	6.751	0.016	0.92	11/11
22050	BGC269C	6.748	0.016	0.56	12/12
22071	BGC269D	6.734	0.013	0.92	17/17
22083	BGC269E	6.751	0.016	0.99	7/16
32470	BGC252A	6.754	0.016	0.43	8/8
32476	BGC252A	6.746	0.016	0.54	8/8
32482	BGC252A	6.748	0.016	0.37	9/9
01M0170/191	VU37	6.762	0.022	0.00	4/4
01M0379	VU41	6.725	0.014	0.90	9/10
02M0267	VU42	6.742	0.024	0.72	10/10
32462-01	BGC252PR-C	6.753*	0.023	0.85	4/16
32462-02	BGC252PR-C	6.746*	0.023	0.89	10/19
32462-03	BGC252PR-C	6.758*	0.023	0.09	9/22
V2 (S6)		6.72	0.02		10/10
V2 (S6)		6.76	0.02		10/10
Me-5 (S8)		6.73*	0.02		3/3
<b>Mes6 = 6.716 Ma</b>					
01M0171	VU37	6.679	0.024	0.09	6/6
<b>Mes8 = 6.638 Ma</b>					
32529	BGC257PR-C	6.620	0.015	0.65	13/15
01M0192	VU37	6.659	0.021	0.17	5/6
02M0268	VU42	6.584	0.020	1.00	10/10
Me-13 (S8)		6.54	0.04		10/10
<b>Mes 9 = 6.581 Ma</b>					
32533	BGC257PR-C	6.552	0.015	0.07	12/16
00M0239/245/246	VU37	6.537	0.023	0.75	3/3
01M0167	VU37	6.536	0.022	0.72	5/5
02M0270	VU42	6.502	0.019	0.97	9/10
Me-16 (S8)		6.46	0.03		10/10

<b>Mes10 = 6.552 Ma</b>					
02M0272	VU42	6.508	0.021	0.67	6/9
<b>Mes11 = 6.542 Ma</b>					
32531	BGC257PR-C	6.521	0.018	0.17	17/30
00M0160	VU37	6.498	0.018	0.68	4/5
<b>Mes12 = 6.452 Ma</b>					
32472	BGC252A	6.407	0.015	0.68	8/8
32478	BGC252A	6.396	0.015	1.00	7/8
32484	BGC252A	6.409	0.015	0.90	7/8
00M0172/248/168	VU37	6.402	0.018	0.36	6/8
02M0273	VU42	6.424	0.018	0.98	9/10
32459-01	BGC252PR-C	6.396*	0.022	0.68	7/20
32459-02	BGC252PR-C	6.408*	0.021	0.64	8/24
32459-03	BGC252PR-C	6.419*	0.021	0.86	10/22
<b>Mes14 = 6.378 Ma</b>					
32523	BGC257PR-C	6.355	0.015	0.88	11/14
01M0166	VU37	6.317	0.017	0.00	8/8
02M0275	VU42	6.293	0.019	0.51	9/10
<b>Mes15 = 6.336 Ma</b>					
02M0277	VU42	6.267	0.019	1.00	8/8
<b>Mes16 = 6.312 Ma</b>					
02M0279	VU42	6.264	0.017	0.92	10/10
<b>Mes17 = 6.298 Ma</b>					
00M0237/238	VU37	6.231	0.022	0.60	3/3
00M0236	VU37	6.207	0.027	---	1/1
02M0280	VU42	6.247	0.018	0.96	10/10
<b>Mes18 = 6.259 Ma</b>					
02M0302	VU42	6.220	0.018	0.77	9/10
<b>Ifo1 = 6.452 Ma</b>					
02M0304	VU42	6.411	0.016	0.99	8/10
<b>Ifo2 = 6.442 Ma</b>					
02M0303	VU42	6.417	0.016	0.99	8/10
<b>Ifo3 = 6.325 Ma</b>					
32535	BGC257PR-C	6.275	0.014	0.01	15/16
01M0110	VU37	6.276	0.018	0.00	8/8
02M0307	VU42	6.289	0.016	0.37	10/10
<b>Ifo4 = 6.280 Ma</b>					
32537	BGC257PR-C	6.238	0.014	0.05	13/17
01M0113/193	VU37	6.242	0.018	0.12	6/7
02M0308	VU42	6.279	0.018	0.29	10/10
<b>Ifo5 = 6.269 Ma</b>					
32539	BGC257PR-C	6.241	0.014	0.60	13/17
01M0112	VU37	6.229	0.018	0.84	6/6
02M0309	VU42	6.204	0.017	0.99	10/10
<i>Ro-3 (S7)</i>		6.20	0.02		7/11
<b>Iza = 6.794 Ma</b>					
00M0153/01M0190	VU37	6.730	0.017	0.68	6/11

\*weighted mean plateau ages.

**Table S2: Analytical  $^{40}\text{Ar}/^{39}\text{Ar}$  data (pages 9-20).**

Full analytical data and summary calculations for individual irradiation experiments with  $1\sigma$  errors. Ages with  $1\sigma$  analytical errors, including analytical uncertainty in  $J$ , are given for each experiment. Data are reported using sanidine from the Fish Canyon Tuff (FCs) as a dating standard with a reference age of 28.02 Ma and/or sanidine from the Taylor Creek Rhyolite (TCRs) of 28.34 Ma (*S1*) and decay constants used by convention since 1977 (*S2*).

Lab ID#	Laser Power (W)	<sup>39</sup> Ar (moles)	<sup>39</sup> Ar (% of total)	<sup>40</sup> Ar/ <sup>39</sup> Ar ± 1σ		<sup>38</sup> Ar/ <sup>39</sup> Ar (× 10 <sup>-2</sup> ) ± 1σ		<sup>37</sup> Ar/ <sup>39</sup> Ar (× 10 <sup>-2</sup> ) ± 1σ		<sup>36</sup> Ar/ <sup>39</sup> Ar (× 10 <sup>-4</sup> ) ± 1σ		Ca/K	± 1σ		<sup>40</sup> Ar (%)	<sup>40</sup> Ar/ <sup>39</sup> ArK ± 1σ		Age (Ma)	± 1σ excluding error on J	± 1σ including error on J	Omitted because
---------	-----------------	--------------------------	-------------------------------	---	--	---	--	---	--	---	--	------	------	--	----------------------	--	--	----------	---------------------------	---------------------------	-----------------

#### Single crystal incremental heating - BGC

252PR-C: Mes1 (32456) J = 0.005236 ± 0.000016

32456-01A	9.0	3.96E-14	0.97	0.8880	0.0029	1.3490	0.0056	1.6550	0.0210	4.410	0.170	0.03243	0.00042	85.46	0.7583	0.0061	7.149	0.058	0.062	%40Ar* <97
32456-01B	11.0	6.09E-14	1.49	0.7399	0.0017	1.2135	0.0042	1.0412	0.0096	0.332	0.066	0.02041	0.00019	98.79	0.7302	0.0027	6.884	0.025	0.033	
32456-01C	12.0	7.99E-14	1.96	0.7344	0.0015	1.2149	0.0039	0.9177	0.0095	0.153	0.044	0.01799	0.00019	99.49	0.7299	0.0021	6.881	0.019	0.029	
32456-01D	13.0	1.21E-13	2.96	0.7340	0.0016	1.2212	0.0031	0.8890	0.0096	0.131	0.031	0.01742	0.00019	99.57	0.7302	0.0019	6.884	0.018	0.028	
32456-01E	14.0	1.89E-13	4.63	0.7306	0.0015	1.2144	0.0028	0.8639	0.0094	0.074	0.022	0.01693	0.00018	99.80	0.7284	0.0016	6.888	0.015	0.026	
32456-01F	14.5	3.96E-13	9.66	0.7311	0.0014	1.2106	0.0025	0.8565	0.0057	0.039	0.011	0.01679	0.00011	99.94	0.7300	0.0014	6.882	0.014	0.025	
32456-01G	14.5	4.88E-13	11.92	0.7310	0.0014	1.2068	0.0028	0.8538	0.0050	0.031	0.010	0.01673	0.00010	99.97	0.7301	0.0014	6.883	0.013	0.025	
32456-01H	15.0	6.26E-13	15.29	0.7308	0.0013	1.2042	0.0027	0.8513	0.0051	0.035	0.008	0.01669	0.00010	99.96	0.7298	0.0014	6.880	0.013	0.025	
32456-01I	15.0	3.99E-13	9.73	0.7332	0.0014	1.2110	0.0027	0.8428	0.0057	0.005	0.012	0.01652	0.00011	100.08	0.7330	0.0015	6.911	0.014	0.025	
32456-01J	15.5	2.80E-13	6.85	0.7330	0.0014	1.2006	0.0026	0.8469	0.0075	0.035	0.016	0.01660	0.00015	99.95	0.7319	0.0015	6.900	0.014	0.025	
32456-01K	15.5	8.31E-14	2.03	0.7357	0.0016	1.2094	0.0039	0.8934	0.0088	0.120	0.040	0.01751	0.00017	99.62	0.7322	0.0020	6.903	0.019	0.028	
32456-01L	16.0	9.48E-14	2.31	0.7345	0.0016	1.1990	0.0036	0.8569	0.0077	0.089	0.034	0.01680	0.00015	99.74	0.7319	0.0019	6.900	0.018	0.028	
32456-01M	16.0	8.08E-14	1.98	0.7365	0.0015	1.2058	0.0036	0.8382	0.0099	0.035	0.040	0.01643	0.00019	99.96	0.7355	0.0020	6.934	0.018	0.028	
32456-01N	16.5	1.19E-13	2.90	0.7349	0.0016	1.1992	0.0036	0.8410	0.0110	0.012	0.029	0.01648	0.00021	100.05	0.7345	0.0018	6.925	0.017	0.027	
32456-01O	16.5	1.30E-13	3.19	0.7359	0.0015	1.2041	0.0032	0.8760	0.0100	0.034	0.028	0.01717	0.00020	99.96	0.7348	0.0018	6.928	0.016	0.027	
32456-01P	17.0	1.14E-13	2.80	0.7367	0.0015	1.2104	0.0033	0.8440	0.0110	0.076	0.027	0.01653	0.00021	99.79	0.7344	0.0018	6.924	0.016	0.027	
32456-01Q	18.0	1.14E-13	2.79	0.7389	0.0016	1.2099	0.0040	0.8535	0.0090	0.098	0.028	0.01673	0.00018	99.70	0.7360	0.0018	6.939	0.017	0.027	
32456-01R	19.0	3.87E-13	9.45	0.7343	0.0014	1.2050	0.0026	0.8601	0.0057	0.040	0.010	0.01686	0.00011	99.94	0.7331	0.0014	6.912	0.013	0.025	
32456-01S	20.0	1.60E-13	3.92	0.7373	0.0015	1.2082	0.0032	0.8352	0.0093	0.026	0.025	0.01637	0.00018	99.99	0.7365	0.0017	6.943	0.016	0.027	
32456-01T	24.0	1.31E-13	3.19	0.7363	0.0016	1.2129	0.0034	0.8860	0.0120	0.014	0.030	0.01736	0.00023	100.05	0.7359	0.0018	6.937	0.017	0.027	

252PR-C: Mes1 (32456) J = 0.005236 ± 0.000016

32456-02A	2.0	3.97E-16	0.01	6.1250	0.0570	3.4100	0.1100	7.5100	0.9100	188.300	9.800	0.14700	0.01800	9.20	0.5700	0.3000	5.3	2.8	2.793	%40Ar* <97
32456-02B	3.0	1.50E-15	0.06	1.7599	0.0084	1.5820	0.0280	3.4300	0.2900	32.400	2.500	0.06720	0.00570	45.80	0.8060	0.0750	7.6	0.7	0.703	%40Ar* <97
32456-02C	4.0	7.70E-15	0.29	0.8437	0.0030	1.3640	0.0100	2.6810	0.0810	2.220	0.460	0.05260	0.00160	92.50	0.7800	0.0140	7.35	0.13	0.135	%40Ar* <97
32456-02D	5.0	1.32E-14	0.49	0.7663	0.0023	1.2238	0.0073	1.3520	0.0490	0.300	0.260	0.02651	0.00095	99.00	0.7577	0.0080	7.143	0.076	0.079	
32456-02E	5.5	1.89E-14	0.70	0.7462	0.0018	1.2053	0.0065	1.1670	0.0370	0.690	0.160	0.02287	0.00073	97.39	0.7260	0.0051	6.845	0.048	0.053	
32456-02F	6.0	1.85E-14	0.69	0.7393	0.0021	1.2266	0.0066	0.9620	0.0380	0.140	0.180	0.01886	0.00074	99.53	0.7351	0.0057	6.930	0.054	0.058	
32456-02G	6.5	2.74E-14	1.01	0.7559	0.0019	1.2338	0.0057	1.0240	0.0230	0.970	0.120	0.02007	0.00045	96.34	0.7275	0.0040	6.859	0.038	0.043	%40Ar* <97
32456-02H	7.0	3.92E-14	1.45	0.7460	0.0016	1.2130	0.0055	0.9420	0.0200	0.630	0.079	0.01847	0.00039	97.61	0.7275	0.0029	6.859	0.027	0.035	
32456-02I	7.5	5.73E-14	2.12	0.7326	0.0015	1.2097	0.0039	0.9100	0.0190	0.147	0.054	0.01784	0.00036	99.51	0.7283	0.0022	6.866	0.021	0.030	
32456-02J	8.0	7.68E-14	2.85	0.7315	0.0016	1.2090	0.0039	0.8600	0.0160	0.204	0.040	0.01685	0.00031	99.28	0.7255	0.0020	6.840	0.019	0.028	
32456-02K	8.5	1.16E-13	4.29	0.7301	0.0016	1.2038	0.0035	0.8730	0.0120	0.008	0.030	0.01711	0.00023	100.07	0.7299	0.0018	6.881	0.017	0.027	
32456-02L	9.0	1.51E-13	5.59	0.7285	0.0016	1.2215	0.0030	0.9040	0.0100	0.002	0.025	0.01771	0.00020	100.10	0.7285	0.0017	6.869	0.016	0.027	
32456-02M	9.5	1.60E-13	5.94	0.7305	0.0014	1.2142	0.0033	0.8780	0.0110	0.000	0.024	0.01721	0.00022	100.12	0.7306	0.0016	6.888	0.015	0.026	
32456-02N	10.0	3.14E-13	11.61	0.7297	0.0014	1.2118	0.0027	0.8575	0.0069	0.010	0.013	0.01681	0.00014	100.06	0.7294	0.0014	6.877	0.013	0.025	
32456-02O	10.5	5.35E-13	14.05	0.7335	0.0014	1.2146	0.0032	0.8995	0.0098	0.025	0.012	0.01763	0.00019	100.00	0.7328	0.0015	6.908	0.014	0.025	
32456-02P	11.0	4.38E-13	4.69	0.7367	0.0026	1.2092	0.0076	0.8960	0.0310	0.000	0.038	0.01756	0.00061	100.13	0.7369	0.0029	6.948	0.027	0.034	
32456-02Q	11.5	2.11E-13	7.81	0.7322	0.0015	1.2062	0.0029	0.8630	0.0120	0.025	0.016	0.01692	0.00023	100.00	0.7314	0.0015	6.896	0.014	0.026	
32456-02R	12.0	1.13E-13	4.19	0.7342	0.0016	1.2085	0.0035	0.8809	0.0098	0.055	0.030	0.01727	0.00019	99.88	0.7326	0.0018	6.907	0.017	0.027	
32456-02S	12.5	6.50E-14	2.41	0.7361	0.0016	1.2105	0.0040	0.8310	0.0140	0.115	0.052	0.01628	0.00027	99.63	0.7327	0.0022	6.907	0.021	0.030	
32456-02T	14.0	1.87E-13	6.93	0.7355	0.0015	1.2096	0.0029	0.8653	0.0097	0.046	0.020	0.01696	0.00019	99.92	0.7341	0.0016	6.921	0.015	0.026	
32456-02U	16.0	1.40E-13	5.16	0.7370	0.0015	1.2105	0.0031	0.8500	0.0110	0.000	0.026	0.01666	0.00021	100.12	0.7372	0.0017	6.950	0.016	0.026	
32456-02V	19.0	1.62E-13	6.01	0.7356	0.0015	1.2083	0.0032	0.8491	0.0097	0.073	0.022	0.01664	0.00019	99.81	0.7334	0.0017	6.914	0.016	0.026</	

Lab ID#	Laser Power (W)	<sup>39</sup> Ar (moles)	<sup>39</sup> Ar (% of total)	<sup>40</sup> Ar/ <sup>39</sup> Ar ± 1σ	<sup>38</sup> Ar/ <sup>39</sup> Ar (x 10 <sup>-2</sup> ) ± 1σ	<sup>37</sup> Ar/ <sup>39</sup> Ar (x 10 <sup>-4</sup> ) ± 1σ	<sup>36</sup> Ar/ <sup>39</sup> Ar (x 10 <sup>-4</sup> ) ± 1σ	Ca/K	<sup>40</sup> Ar ± 1σ (%)	<sup>40</sup> Ar/ <sup>39</sup> ArK ± 1σ	Age (Ma)	± 1σ excluding error on J	± 1σ including error on J	Omitted because						
32456-03Q	13.0	4.23E-13	14.13	0.7303	0.0015	1.2114	0.0027	0.8888	0.0077	0.026	0.010	0.01742	0.00015	100.00	0.7296	0.0015	6.878	0.014	0.025	
32456-03R	14.0	1.49E-13	4.98	0.7327	0.0015	1.2047	0.0035	0.8490	0.0120	0.019	0.023	0.01665	0.00024	100.02	0.7321	0.0017	6.902	0.016	0.026	
32456-03S	16.0	1.99E-13	6.66	0.7359	0.0014	1.2127	0.0030	0.8945	0.0084	0.051	0.017	0.01753	0.00017	99.90	0.7344	0.0015	6.924	0.014	0.026	
32456-03T	18.0	1.02E-13	3.42	0.7351	0.0019	1.2027	0.0039	0.8850	0.0130	0.000	0.033	0.01734	0.00025	100.47	0.7378	0.0021	6.956	0.020	0.029	
32456-03U	21.0	7.51E-14	2.52	0.7370	0.0016	1.2092	0.0041	0.8550	0.0160	0.000	0.048	0.01676	0.00032	100.17	0.7375	0.0021	6.953	0.020	0.029	
32456-03V	24.0	5.52E-14	1.85	0.7359	0.0016	1.2076	0.0046	0.8460	0.0160	0.000	0.058	0.01658	0.00031	100.11	0.7360	0.0023	6.939	0.022	0.031	
<b>252PR-C: Mes4 (32459) J = 0.005230 ± 0.000016</b>																				
32462-01A	5.0	2.77E-15	0.15	1.2661	0.0046	1.2830	0.0160	2.2540	0.0750	15.600	1.500	0.04420	0.00150	63.70	0.8060	0.0450	7.59	0.42	0.425	
32462-01B	7.0	7.57E-15	0.41	0.7526	0.0025	1.2110	0.0099	1.6960	0.0430	0.340	0.500	0.03324	0.00083	98.80	0.7430	0.0150	7.00	0.14	0.146	
32462-01C	9.0	1.81E-14	0.96	0.7311	0.0019	1.2192	0.0068	1.6460	0.0220	0.310	0.210	0.03226	0.00042	98.91	0.7224	0.0065	6.803	0.061	0.064	
32462-01D	11.0	3.55E-14	1.90	0.7191	0.0016	1.2237	0.0051	1.6650	0.0230	0.050	0.120	0.03263	0.00045	99.99	0.7183	0.0038	6.764	0.036	0.042	
32462-01E	12.0	4.65E-14	2.47	0.7164	0.0016	1.2044	0.0045	1.6090	0.0150	0.091	0.080	0.03154	0.00029	99.81	0.7143	0.0029	6.727	0.027	0.034	
32462-01F	13.0	1.03E-13	5.52	0.7194	0.0016	1.2221	0.0032	1.6670	0.0120	0.067	0.036	0.03266	0.00024	99.91	0.7181	0.0019	6.762	0.018	0.027	
32462-01G	14.0	1.74E-13	9.31	0.7175	0.0014	1.2140	0.0032	1.6640	0.0120	0.051	0.024	0.03261	0.00023	99.98	0.7166	0.0016	6.749	0.015	0.026	
32462-01H	15.0	5.24E-13	27.95	0.7172	0.0014	1.2137	0.0028	1.6583	0.0078	0.047	0.009	0.03250	0.00015	99.99	0.7164	0.0014	6.747	0.013	0.024	
32462-01I	16.0	5.68E-13	30.27	0.7181	0.0014	1.2053	0.0029	1.6944	0.0091	0.037	0.009	0.03321	0.00018	100.04	0.7177	0.0014	6.758	0.013	0.024	
32462-01J	17.0	1.89E-13	10.14	0.7209	0.0015	1.2039	0.0029	1.7015	0.0090	0.000	0.023	0.03335	0.00018	100.29	0.7223	0.0016	6.802	0.015	0.026	
32462-01K	18.0	8.00E-14	4.28	0.7203	0.0015	1.2019	0.0041	1.7220	0.0130	0.025	0.053	0.03374	0.00025	100.09	0.7203	0.0022	6.783	0.020	0.029	
32462-01L	19.0	8.71E-15	0.47	0.7221	0.0025	1.2160	0.0094	1.6070	0.0330	0.000	0.470	0.03150	0.00065	102.30	0.7380	0.0140	6.950	0.130	0.136	
32462-01M	20.0	2.17E-14	1.17	0.7233	0.0020	1.2058	0.0061	1.6320	0.0230	0.230	0.180	0.03199	0.00044	99.25	0.7172	0.0059	6.754	0.055	0.059	
32462-01N	22.0	4.61E-14	2.47	0.7225	0.0015	1.2050	0.0049	1.6400	0.0210	0.000	0.079	0.03214	0.00041	100.23	0.7235	0.0028	6.813	0.027	0.034	
32462-01O	24.0	2.89E-14	1.54	0.7182	0.0017	1.1916	0.0056	1.6480	0.0200	0.370	0.110	0.03229	0.00039	98.65	0.7078	0.0038	6.666	0.036	0.041	
32462-01P	26.0	1.87E-14	1.00	0.7221	0.0021	1.2077	0.0066	1.6450	0.0230	0.000	0.190	0.03225	0.00045	100.46	0.7247	0.0061	6.825	0.057	0.061	
<b>252PR-C: Mes4 (32459) J = 0.005230 ± 0.000016</b>																				
32462-02A	9.0	3.41E-14	1.56	0.7807	0.0059	1.3930	0.0120	2.0570	0.0350	1.770	0.120	0.04031	0.00069	93.51	0.7294	0.0068	6.869	0.064	0.067	
32462-02B	11.0	5.11E-14	2.28	0.7236	0.0017	1.2237	0.0049	1.7900	0.0190	0.288	0.071	0.03508	0.00037	99.02	0.7158	0.0027	6.741	0.025	0.033	
32462-02C	12.0	8.75E-14	3.92	0.7217	0.0018	1.2632	0.0040	1.9920	0.0150	0.261	0.040	0.03904	0.00030	99.15	0.7149	0.0022	6.733	0.020	0.029	
32462-02D	13.0	1.57E-13	7.00	0.7179	0.0015	1.2140	0.0033	1.7250	0.0120	0.087	0.023	0.03381	0.00024	99.84	0.7160	0.0016	6.743	0.015	0.026	
32462-02E	14.0	2.05E-13	9.16	0.7173	0.0014	1.2155	0.0030	1.7030	0.0110	0.096	0.020	0.03339	0.00021	99.80	0.7151	0.0016	6.734	0.015	0.025	
32462-02F	14.5	2.47E-13	10.98	0.7171	0.0014	1.2154	0.0029	1.6850	0.0120	0.062	0.019	0.03302	0.00024	99.93	0.7159	0.0015	6.742	0.014	0.025	
32462-02G	14.5	2.42E-13	10.74	0.7170	0.0014	1.2092	0.0028	1.7030	0.0120	0.026	0.019	0.03339	0.00024	100.08	0.7168	0.0015	6.751	0.014	0.025	
32462-02H	15.0	3.69E-13	16.40	0.7170	0.0014	1.2061	0.0027	1.6854	0.0086	0.063	0.013	0.03303	0.00017	99.93	0.7157	0.0014	6.740	0.013	0.025	
32462-02I	15.0	1.51E-13	6.72	0.7178	0.0014	1.2098	0.0031	1.6940	0.0160	0.051	0.027	0.03321	0.00032	99.98	0.7169	0.0017	6.752	0.016	0.026	
32462-02J	15.5	1.20E-13	5.32	0.7200	0.0015	1.2074	0.0033	1.7100	0.0120	0.045	0.036	0.03352	0.00024	100.01	0.7194	0.0019	6.774	0.017	0.027	
32462-02K	15.5	1.42E-13	6.32	0.7188	0.0015	1.2156	0.0033	1.7030	0.0120	0.083	0.027	0.03337	0.00024	99.85	0.7170	0.0017	6.752	0.016	0.026	
32462-02L	16.0	6.11E-14	2.72	0.7220	0.0015	1.2069	0.0043	1.7320	0.0160	0.085	0.065	0.03396	0.00031	99.85	0.7202	0.0024	6.782	0.023	0.031	
32462-02M	16.0	6.11E-14	2.72	0.7209	0.0015	1.1944	0.0036	1.6520	0.0150	0.038	0.066	0.03238	0.00029	100.03	0.7203	0.0025	6.784	0.023	0.031	
32462-02N	16.5	5.30E-14	2.36	0.7219	0.0015	1.1993	0.0044	1.6700	0.0180	0.036	0.074	0.03272	0.00036	100.04	0.7214	0.0027	6.794	0.025	0.033	
32462-02O	16.5	6.16E-14	2.74	0.7205	0.0015	1.1980	0.0039	1.6820	0.0180	0.214	0.060	0.03297	0.00036	99.31	0.7148	0.0023	6.732	0.022	0.030	
32462-02P	17.0	1.70E-14	0.76	0.7291	0.0019	1.1982	0.0073	1.7130	0.0240	0.000	0.200	0.03358	0.00047	100.39	0.7312	0.0064	6.886	0.060	0.063	
32462-02Q	18.0	1.35E-14	0.60	0.7201	0.0021	1.1747	0.0094	1.7090	0.0250	0.090	0.240	0.03349	0.00049	99.80	0.7182	0.0074	6.763	0.069	0.072	
32462-02R	19.0	1.14E-14	0.50	0.7202	0.0024	1.1903	0.0079	1.6960	0.0410	0.260	0.290	0.03323	0.00080	99.10	0.7131	0.0091	6.715	0.085	0.088	
32462-02S	24.0	1.62E-13	7.21	0.7252	0.0015	1.2012	0.0033	1.6890	0.0110	0.040	0.023	0.03311	0.00022	100.02	0.7247	0.0017	6.824	0.016	0.026	
<b>252PR-C: Mes4 (32459) J = 0.005230 ± 0.000016</b>																				
32462-03A	2.0	4.47E-16	0.02	15.7000	0.1500	2.6980	0.0780	2.1000	1.0000	517.000	13.000	0.04100	0.02000	2.70	0.4300	0.3800	4.0	3.5	3.539	
32462-03B	3.0	1.64E-15	0.07	1.4904	0.0077	1.4280	0.0250	3.9400	0.3300	22.800	1.900	0.07720	0.00640	55.00	0.8200	0.0580	7.72	0.55	0.548	
32462-03C	4.0	3.90E-15	0.17	0.8588	0.0033	1.2770	0.0150	2.2500	0.1100	2.910	0.810	0.04420	0.00210	90.20	0.7740	0.0250	7.29	0.23	0.232	
32462-03D	5.0	8.60E-15	0.38	0.7534	0.0029	1.1980	0.0100	1.7260	0.0580	0.560	0.350	0.03380	0.00110	98.00	0.7370	0.0110	6.94	0.10	0.105	
32462-03E	5.5	9.70E-15	0.43	0.7374																

Lab ID#	Laser Power (W)	<sup>39</sup> Ar (moles)	<sup>39</sup> Ar (%) of total)	<sup>40</sup> Ar/ <sup>39</sup> Ar ± 1σ	<sup>38</sup> Ar/ <sup>39</sup> Ar (x 10 <sup>-2</sup> ) ± 1σ	<sup>37</sup> Ar/ <sup>39</sup> Ar (x 10 <sup>-2</sup> ) ± 1σ	<sup>36</sup> Ar/ <sup>39</sup> Ar (x 10 <sup>-4</sup> ) ± 1σ	Ca/K	Age (Ma) ± 1σ	<sup>40</sup> Ar (%) ± 1σ	Omitted because
excluding error on J including error on J											
<b>252PR-C: Mes12 (32459) J = 0.005248 ± 0.000016</b>											
32459-01A	9.0	6.29E-14	1.85	0.7406	0.0025	1.2821	0.0050	2.3450	0.0190	1.987	0.091
32459-01B	11.0	9.22E-14	2.68	0.6794	0.0016	1.2252	0.0034	1.9260	0.0120	0.159	0.044
32459-01C	12.0	1.31E-13	3.80	0.6747	0.0015	1.2196	0.0030	1.8530	0.0120	0.121	0.030
32459-01D	13.0	1.98E-13	5.76	0.6775	0.0014	1.2115	0.0032	1.8107	0.0097	0.099	0.022
32459-01E	14.0	2.70E-13	7.84	0.6753	0.0013	1.2114	0.0028	1.8172	0.0089	0.099	0.016
32459-01F	14.5	6.73E-13	19.54	0.6762	0.0013	1.2071	0.0029	1.8160	0.0110	0.084	0.007
32459-01G	14.5	6.40E-13	18.56	0.6769	0.0013	1.2052	0.0027	1.7990	0.0073	0.039	0.008
32459-01H	15.0	4.08E-13	11.88	0.6774	0.0013	1.2025	0.0025	1.7651	0.0062	0.040	0.011
32459-01I	15.0	1.40E-13	4.10	0.6796	0.0016	1.2008	0.0044	1.7860	0.0140	0.084	0.028
32459-01J	15.5	1.18E-13	3.42	0.6806	0.0015	1.2138	0.0032	1.7630	0.0140	0.139	0.028
32459-01K	15.5	1.20E-13	3.48	0.6791	0.0014	1.2129	0.0029	1.7710	0.0160	0.081	0.030
32459-01L	16.0	8.48E-14	2.46	0.6799	0.0015	1.2034	0.0039	1.8040	0.0170	0.083	0.045
32459-01M	16.0	5.50E-14	1.59	0.6797	0.0015	1.1983	0.0039	1.7040	0.0180	0.000	0.069
32459-01N	16.5	3.11E-14	0.90	0.6832	0.0017	1.2117	0.0056	1.7550	0.0240	0.110	0.110
32459-01O	16.5	4.08E-14	1.18	0.6795	0.0015	1.2136	0.0048	1.8130	0.0170	0.000	0.091
32459-01P	17.0	3.33E-14	0.97	0.6803	0.0015	1.2091	0.0047	1.7520	0.0230	0.070	0.120
32459-01Q	18.0	5.62E-14	1.63	0.6808	0.0014	1.2073	0.0037	1.7020	0.0190	0.000	0.069
32459-01R	19.0	1.38E-13	3.98	0.6775	0.0015	1.2052	0.0033	1.7340	0.0110	0.062	0.027
32459-01S	20.0	4.69E-14	1.36	0.6828	0.0014	1.2108	0.0051	1.7240	0.0210	0.252	0.065
32459-01T	24.0	1.04E-13	3.02	0.6796	0.0015	1.2073	0.0037	1.7440	0.0180	0.109	0.034
<b>252PR-C: Mes12 (32459) J = 0.005248 ± 0.000016</b>											
32459-02A	2.0	2.01E-16	0.00	43.1700	0.7800	8.6600	0.2700	26.1000	1.9000	1464.000	37.000
32459-02B	3.0	1.06E-15	0.02	1.4660	0.0120	1.9690	0.0450	7.4500	0.5200	24.700	2.800
32459-02C	4.0	4.75E-15	0.10	0.8041	0.0029	1.1840	0.0140	3.6200	0.1500	4.560	0.600
32459-02D	5.0	1.00E-14	0.20	0.7111	0.0023	1.2033	0.0091	2.8990	0.0790	1.290	0.300
32459-02E	5.5	1.19E-14	0.24	0.6939	0.0020	1.1850	0.0080	2.5540	0.0650	0.650	0.250
32459-02F	6.0	1.59E-14	0.32	0.6873	0.0020	1.2127	0.0078	2.3930	0.0570	0.250	0.190
32459-02G	6.5	1.98E-14	0.40	0.6893	0.0019	1.1761	0.0077	2.2650	0.0400	0.280	0.150
32459-02H	7.0	2.57E-14	0.52	0.6846	0.0017	1.2044	0.0049	2.1960	0.0370	0.080	0.120
32459-02I	7.5	3.47E-14	0.70	0.6834	0.0015	1.1985	0.0052	2.0150	0.0270	0.167	0.095
32459-02J	8.0	3.85E-14	0.78	0.6809	0.0015	1.2116	0.0047	1.9770	0.0300	0.096	0.084
32459-02K	8.5	4.99E-14	1.01	0.6793	0.0014	1.2109	0.0041	1.9420	0.0240	0.000	0.064
32459-02L	9.0	6.57E-14	1.33	0.6814	0.0014	1.2227	0.0041	1.8440	0.0260	0.209	0.048
32459-02M	9.5	9.21E-14	1.87	0.6792	0.0015	1.2099	0.0043	1.8650	0.0220	0.143	0.033
32459-02N	10.0	1.32E-13	2.67	0.6805	0.0014	1.2145	0.0033	1.8860	0.0180	0.137	0.022
32459-02O	10.5	1.61E-13	3.27	0.6764	0.0014	1.2118	0.0031	1.8170	0.0160	0.090	0.019
32459-02P	11.0	1.98E-13	4.03	0.6783	0.0014	1.2250	0.0030	1.8500	0.0190	0.075	0.018
32459-02Q	11.5	4.08E-13	8.27	0.6789	0.0014	1.2105	0.0026	1.7960	0.0130	0.063	0.010
32459-02R	12.0	8.54E-13	17.30	0.6775	0.0012	1.2046	0.0025	1.7705	0.0073	0.054	0.005
32459-02S	13.0	6.50E-13	13.14	0.6803	0.0013	1.2105	0.0027	1.8080	0.0110	0.046	0.007
32459-02T	14.0	4.20E-13	8.52	0.6795	0.0012	1.2037	0.0027	1.7670	0.0100	0.040	0.010
32459-02U	16.0	4.64E-13	9.41	0.6782	0.0013	1.2057	0.0027	1.7970	0.0100	0.050	0.009
32459-02V	18.0	3.84E-13	7.79	0.6797	0.0013	1.2026	0.0027	1.8140	0.0110	0.046	0.011
32459-02W	21.0	6.70E-13	13.59	0.6784	0.0012	1.2055	0.0025	1.7600	0.0130	0.057	0.007
32459-02X	25.0	2.21E-13	4.48	0.6811	0.0013	1.2070	0.0028	1.7990	0.0130	0.052	0.017
<b>252PR-C: Mes12 (32459) J = 0.005248 ± 0.000016</b>											
32459-03A	2.0	2.48E-16	0.01	5.0600	0.1100	6.6100	0.1800	4.8000	1.8000	155.000	13.000
32459-03B	3.0	1.19E-15	0.05	1.0164	0.0089	1.2040	0.0270	2.5200	0.3400	11.400	2.200
32459-03C	4.0	4.24E-15	0.16	0.7425	0.0025	1.1580	0.0130	2.2100	0.1400	0.400	0.730
32459-03D	5.0	1.02E-14	0.38	0.6954	0.0023	1.2013	0.0096	1.9680	0.0770	0.470	0.290
32459-03E	5.5	1.06E-14	0.40	0.6855	0.0025	1.1860	0.0088	1.8110	0.0760	0.000	0.300
32459-03F	6.0	1.27E-14	0.48	0.6813	0.0020	1.1800	0.0083	1.6930	0.0340	0.000	0.250
32459-03G	6.5	1.67E-14	0.63	0.6786	0.0019	1.2084	0.0075	1.8780	0.0450	0.000	0.180
32459-03H	7.0	2.37E-14	0.89	0.6795	0.0018	1.1889	0.0063	1.8600	0.0360	0.140	0.130
32459-03I	7.5	3.35E-14	1.26	0.6824	0.0016	1.1887	0.0055	1.7810	0.0290	0.178	0.081
32459-03J	8.0	6.16E-14	2.32	0.6810	0.0014	1.2102	0.0043	1.7670	0.0210	0.164	0.042
32459-03K	8.5	1.01E-13	3.82	0.6797	0.0016	1.2188	0.0033	1.8570	0.0280	0.133	0.027
32459-03L	9.0	1.32E-13	4.97	0.6771	0.0014	1.2164	0.0032	1.8180	0.0280	0.100	0.023
32459-03M	9.5	3.08E-13	11.61	0.6790	0.0013	1.2086	0.0027	1.8260	0.0130	0.048	0.012
32459-03N	10.0	2.64E-13	9.91	0.6801	0.0014	1.2088	0.0030	1.7960	0.0190	0.043	0.013
32459-03O	11.0	2.86E-13	10.78	0.6785	0.0014	1.2034	0.0029	1.8040	0.0130	0.032	0.011
32459-03P	12.0	2.17E-13	8.20	0.6791	0.0014	1.2025	0.0029	1.7980	0.0200	0.088	0.014
32459-03Q	13.0	2.02E-13	7.60	0.6798	0.0014	1.2077	0.0030	1.8160	0.0130	0.051	0.014
32459-03R	14.0	1.52E-13	5.74	0.6818	0.0014	1.2038	0.0029	1.8370	0.0140	0.043	0.023
32459-03S	16.0	2.13E-13	8.02	0.6799	0.0013	1.2106	0.0029	1.8130	0.0160	0.040	0.018
32459-03T	18.0	2.11E-13	7.98	0.6803	0.0014	1.2078	0.0030	1.8160	0.0140	0.051	0.017

Lab ID#	Laser Power (W)	<sup>39</sup> Ar (moles)	<sup>39</sup> Ar (%) of total)	<sup>40</sup> Ar/ <sup>39</sup> Ar ± 1σ	<sup>38</sup> Ar/ <sup>39</sup> Ar (x 10 <sup>-2</sup> ) ± 1σ	<sup>37</sup> Ar/ <sup>39</sup> Ar (x 10 <sup>-2</sup> ) ± 1σ	<sup>36</sup> Ar/ <sup>39</sup> Ar (x 10 <sup>-4</sup> ) ± 1σ	Ca/K	± 1σ	<sup>40</sup> Ar (%)	<sup>40</sup> Ar/ <sup>39</sup> ArK ± 1σ	Age (Ma)	± 1σ excluding error on J	± 1σ including error on J	Omitted because				
32459-03U	21.0	8.90E-14	3.36	0.6823	0.0015	1.2040	0.0035	1.7510	0.0210	0.130	0.038	0.03432	0.00041	99.65	0.6791	0.0019	6.419	0.018	0.026
32459-03V	24.0	3.03E-13	11.42	0.6796	0.0013	1.2028	0.0026	1.7900	0.0130	0.022	0.013	0.03508	0.00026	100.12	0.6797	0.0014	6.424	0.013	0.023
<b>Single crystal total fusions - BGC</b>																			
<b>252A: Mes1 (32474) J = 0.0051986 ± 0.0000100</b>																			
32474-01Bcomb	5.0	1.47E-13		0.7401	0.0018	1.2134	0.0049	0.9400	0.0150	0.004	0.038	0.01842	0.00028	100.08	0.7400	0.0021	6.927	0.020	0.024
32474-02Bcomb	5.0	2.00E-13		0.7415	0.0018	1.2149	0.0048	1.7020	0.0150	0.109	0.026	0.03336	0.00029	99.74	0.7389	0.0020	6.916	0.019	0.023
32474-03Bcomb	5.0	2.20E-13		0.7401	0.0018	1.2124	0.0042	0.9060	0.0120	0.128	0.025	0.01775	0.00024	99.58	0.7363	0.0020	6.893	0.019	0.023
32474-04Bcomb	5.0	2.00E-13		0.7393	0.0018	1.2120	0.0042	0.8700	0.0120	0.103	0.025	0.01706	0.00023	99.68	0.7362	0.0020	6.892	0.018	0.023
32474-05Bcomb	5.0	1.62E-13		0.7421	0.0019	1.2045	0.0050	0.8730	0.0110	0.120	0.034	0.01711	0.00021	99.61	0.7385	0.0022	6.913	0.021	0.025
32474-06	5.0	2.14E-13		0.7420	0.0019	1.2016	0.0036	0.8104	0.0065	0.084	0.015	0.01588	0.00013	99.75	0.7394	0.0020	6.922	0.018	0.023
32474-07	5.0	2.71E-13		0.7367	0.0018	1.2111	0.0034	0.8763	0.0083	0.039	0.012	0.01718	0.00016	99.94	0.7355	0.0018	6.885	0.017	0.021
32474-08	5.0	1.63E-13		0.7384	0.0019	1.2213	0.0039	0.8746	0.0076	0.059	0.019	0.01714	0.00015	99.86	0.7366	0.0019	6.895	0.018	0.022
<b>252A: Mes1 (32480) J = 0.0051660 ± 0.0000100</b>																			
32480-01Bcomb	5.0	1.88E-13		0.7442	0.0018	1.2110	0.0041	1.1710	0.0120	0.095	0.026	0.02295	0.00023	99.74	0.7415	0.0020	6.898	0.018	0.023
32480-02Bcomb	5.0	2.40E-13		0.7426	0.0018	1.2067	0.0037	0.9300	0.0110	0.108	0.023	0.01822	0.00021	99.67	0.7394	0.0019	6.878	0.018	0.022
32480-03Bcomb	5.0	1.34E-13		0.7405	0.0018	1.2090	0.0050	0.8632	0.0097	0.000	0.035	0.01692	0.00019	100.17	0.7410	0.0021	6.893	0.020	0.024
32480-04	5.0	1.84E-13		0.7457	0.0019	1.2101	0.0036	0.8844	0.0097	0.128	0.018	0.01733	0.00019	99.58	0.7419	0.0020	6.901	0.019	0.023
32480-05	5.0	2.13E-13		0.7451	0.0023	1.2134	0.0043	1.2360	0.0110	0.175	0.016	0.02423	0.00022	99.43	0.7401	0.0023	6.885	0.022	0.026
32480-06	5.0	1.17E-13		0.7444	0.0019	1.2253	0.0044	1.0269	0.0075	0.111	0.024	0.02013	0.00015	99.67	0.7412	0.0021	6.895	0.019	0.024
32480-07	5.0	1.84E-13		0.7438	0.0019	1.2082	0.0042	0.8470	0.0110	0.122	0.017	0.01660	0.00021	99.60	0.7401	0.0020	6.885	0.019	0.023
32480-08	5.0	2.18E-13		0.7432	0.0017	1.2161	0.0034	0.8881	0.0051	0.164	0.015	0.01741	0.00010	99.44	0.7383	0.0018	6.868	0.017	0.021
<b>252A: Mes1 (32486) J = 0.0051876 ± 0.0000100</b>																			
32486-02	5.0	2.74E-13		0.7389	0.0017	1.2173	0.0035	1.1196	0.0077	0.101	0.012	0.02194	0.00015	99.71	0.7361	0.0017	6.876	0.016	0.021
32486-03Bcomb	5.0	3.02E-13		0.7410	0.0018	1.2152	0.0039	0.9182	0.0089	0.102	0.019	0.01800	0.00017	99.69	0.7379	0.0019	6.893	0.018	0.022
32486-04Bcomb	5.0	2.54E-13		0.7444	0.0019	1.2135	0.0041	1.0610	0.0120	0.192	0.022	0.02079	0.00023	99.35	0.7389	0.0021	6.902	0.019	0.023
32486-05	5.0	1.85E-13		0.7415	0.0018	1.2093	0.0042	0.8046	0.0080	0.080	0.016	0.01577	0.00016	99.76	0.7390	0.0019	6.903	0.018	0.022
32486-06	5.0	1.98E-13		0.7449	0.0019	1.2075	0.0037	0.9010	0.0110	0.193	0.016	0.01766	0.00021	99.33	0.7392	0.0020	6.905	0.018	0.023
32486-08	5.0	1.29E-13		0.7400	0.0019	1.2111	0.0040	0.8856	0.0086	0.001	0.022	0.01736	0.00017	100.09	0.7399	0.0020	6.911	0.019	0.023
32486-07	5.0	1.82E-13		0.7399	0.0018	1.2126	0.0043	0.8597	0.0078	0.000	0.018	0.01685	0.00015	101.89	0.7531	0.0018	7.035	0.017	0.022
<b>&gt;1.5 nMADs from median age</b>																			
<b>252A: Mes4 (32470) J = 0.0052021 ± 0.0000100</b>																			
32470-01Bcomb	5.0	2.07E-13		0.7252	0.0020	1.2188	0.0051	1.8430	0.0200	0.185	0.030	0.03612	0.00039	99.44	0.7205	0.0022	6.749	0.021	0.025
32470-02Bcomb	5.0	2.23E-13		0.7306	0.0019	1.2245	0.0046	1.9150	0.0160	0.264	0.025	0.03754	0.00032	99.14	0.7235	0.0021	6.778	0.020	0.024
32470-03Bcomb	5.0	2.50E-13		0.7231	0.0018	1.2134	0.0043	1.8330	0.0150	0.082	0.021	0.03592	0.00029	99.86	0.7214	0.0019	6.758	0.018	0.022
32470-04Bcomb	5.0	2.20E-13		0.7211	0.0017	1.2146	0.0048	1.7520	0.0160	0.086	0.025	0.03433	0.00031	99.84	0.7192	0.0019	6.737	0.017	0.022
32470-05Bcomb	5.0	1.77E-13		0.7225	0.0018	1.2119	0.0048	1.7600	0.0160	0.046	0.029	0.03450	0.00031	100.00	0.7218	0.0020	6.761	0.019	0.023
32470-06	5.0	2.74E-13		0.7207	0.0016	1.2130	0.0034	1.6998	0.0097	0.109	0.010	0.03332	0.00019	99.74	0.7181	0.0017	6.726	0.016	0.020
32470-07	5.0	2.18E-13		0.7266	0.0017	1.2233	0.0035	1.7060	0.0120	0.157	0.017	0.03343	0.00023	99.54	0.7226	0.0018	6.769	0.017	0.021
32470-08	5.0	2.18E-13		0.7241	0.0018	1.2180	0.0047	1.7155	0.0092	0.084	0.013	0.03362	0.00018	99.84	0.7223	0.0019	6.766	0.018	0.022
<b>252A: Mes4 (32476) J = 0.0051805 ± 0.0000100</b>																			
32476-01Bcomb	5.0	2.31E-13		0.7256	0.0018	1.2059	0.0042	1.7160	0.0150	0.071	0.025	0.03364	0.00029	99.89	0.7241	0.0020	6.755	0.018	0.023
32476-02Bcomb	5.0	2.41E-13		0.7292	0.0018	1.2125	0.0043	1.8380	0.0150	0.128	0.022	0.03603	0.00030	99.68	0.7261	0.0019	6.774	0.018	0.022
32476-03Bcomb	5.0	1.92E-13		0.7265	0.0018	1.2145	0.0042	1.7180	0.0160	0.135	0.029	0.03367	0.00031	99.63	0.7231	0.0020	6.745	0.019	0.023
32476-04Bcomb	5.0	2.20E-13		0.7274	0.0017	1.2115	0.0035	1.6770	0.0110	0.126	0.024	0.03286	0.00022	99.67	0.7243	0.0018	6.756	0.017	0.021
32476-05	5.0	3.01E-13		0.7233	0.0017	1.2108	0.0035	1.6720	0.0110	0.090	0.011	0.03277	0.00022	99.81	0.7213	0.0017	6.728	0.016	0.020
32476-06	5.0	2.46E-13		0.7263	0.0017	1.2136	0.0035	1.7280	0.0110	0.117	0.012	0.03386	0.00022	99.71	0.7235	0.0017	6.749	0.016	0.021
32476-07	5.0	2.79E-13		0.7229	0.0018	1.2093	0.0033	1.7300	0.0120	0.092	0.011	0.03390	0.00023	99.81	0.7208	0.0018	6.724	0.017	0.021
32476-08	5.0	2.00E-13		0.7268	0.0017	1.2088	0.0036	1.6890	0.0130	0.146	0.016	0.03310	0.00025	99.59	0.7231	0.0017	6.746	0.016	0.021
<b>252A: Mes4 (32482) J = 0.0051695 ± 0.0000100</b>																			
32482-01Bcomb	5.0	2.64E-13		0.7274	0.0020	1.2112	0.0039	1.7780	0.0150	0.110	0.021	0.03485	0.00029	99.74	0.7248	0.0021	6.747	0.019	0.023
32482-02Bcomb	5.0	2.89E-13		0.7253	0.0017	1.2014	0.0042	1.7560	0.0150</										

Lab ID#	Laser Power (W)	<sup>39</sup> Ar (moles)	<sup>39</sup> Ar (% of total)	<sup>40</sup> Ar/ <sup>39</sup> Ar ± 1σ	<sup>38</sup> Ar/ <sup>39</sup> Ar (× 10 <sup>-2</sup> ) ± 1σ	<sup>37</sup> Ar/ <sup>39</sup> Ar (× 10 <sup>-4</sup> ) ± 1σ	<sup>36</sup> Ar/ <sup>39</sup> Ar (× 10 <sup>-4</sup> ) ± 1σ	Ca/K	<sup>40</sup> Ar (%) ± 1σ	<sup>40</sup> Ar/ <sup>39</sup> Ar ± 1σ	Age (Ma)	± 1σ excluding error on J	± 1σ including error on J	Omitted because				
22009-04	5.0	1.21E-13	0.9947	0.0020	1.2030	0.0034	1.7020	0.0210	0.225	0.011	0.03336	0.00042	99.46	0.9886	0.0021	6.765	0.014	0.020
22009-05	5.0	1.57E-13	0.9938	0.0021	1.2015	0.0033	1.5320	0.0140	0.275	0.009	0.03003	0.00027	99.30	0.9861	0.0021	6.747	0.014	0.020
22009-06	5.0	1.24E-13	1.0084	0.0022	1.1976	0.0047	1.5380	0.0160	0.823	0.013	0.03014	0.00032	97.70	0.9845	0.0023	6.736	0.016	0.021
22009-07	5.0	7.09E-14	1.0083	0.0025	1.1920	0.0057	1.5620	0.0230	0.662	0.020	0.03061	0.00045	98.18	0.9892	0.0026	6.768	0.018	0.023
22009-08	5.0	1.28E-13	1.0024	0.0021	1.2123	0.0036	1.6120	0.0270	0.549	0.011	0.03160	0.00053	98.51	0.9868	0.0021	6.752	0.015	0.020
22009-13	5.0	1.06E-13	1.0038	0.0024	1.2147	0.0042	1.5970	0.0260	0.721	0.014	0.03130	0.00051	98.00	0.9830	0.0025	6.727	0.017	0.022
22009-09	5.0	4.72E-14	1.0265	0.0021	1.2032	0.0060	1.5270	0.0230	1.372	0.027	0.02993	0.00045	96.16	0.9864	0.0024	6.750	0.016	0.021 %40Ar* <97
22009-10	5.0	8.11E-15	7.7240	0.0190	1.5990	0.0150	1.7700	0.1300	225.430	0.760	0.03460	0.00260	13.77	1.0630	0.0480	7.270	0.330	0.326 %40Ar* <97
22009-11	5.0	1.13E-13	1.0299	0.0026	1.2050	0.0046	1.5480	0.0310	1.400	0.016	0.03034	0.00060	96.10	0.9890	0.0027	6.767	0.018	0.023 %40Ar* <97
22009-12	5.0	1.11E-13	1.0221	0.0022	1.2082	0.0038	1.5140	0.0240	1.160	0.015	0.02968	0.00046	96.76	0.9883	0.0024	6.762	0.016	0.021 %40Ar* <97
<b>269B: Mes4 (2029) J = 0.0037952 ± 0.0000080</b>																		
22029B-01	5.0	1.72E-13	0.9928	0.0025	1.1998	0.0032	1.7070	0.0120	0.276	0.015	0.03345	0.00024	99.31	0.9852	0.0026	6.733	0.018	0.023
22029B-02	5.0	1.56E-13	0.9970	0.0024	1.2061	0.0034	1.6820	0.0130	0.361	0.018	0.03296	0.00026	99.06	0.9869	0.0025	6.745	0.017	0.022
22029B-03	5.0	1.47E-13	0.9942	0.0024	1.2105	0.0039	1.7160	0.0100	0.221	0.018	0.03364	0.00020	99.48	0.9883	0.0025	6.754	0.017	0.022
22029B-04	5.0	1.66E-13	0.9946	0.0025	1.1988	0.0039	1.6970	0.0140	0.182	0.015	0.03326	0.00027	99.59	0.9898	0.0025	6.764	0.017	0.022
22029B-05	5.0	2.12E-13	0.9924	0.0023	1.2034	0.0034	1.6468	0.0086	0.211	0.013	0.03228	0.00017	99.50	0.9868	0.0024	6.744	0.016	0.022
22029B-06	5.0	2.04E-13	0.9925	0.0024	1.2053	0.0035	1.6500	0.0100	0.199	0.014	0.03234	0.00020	99.54	0.9872	0.0025	6.747	0.017	0.022
22029B-07	5.0	1.61E-13	0.9999	0.0024	1.2008	0.0038	1.6530	0.0120	0.410	0.018	0.03240	0.00023	98.92	0.9884	0.0025	6.755	0.017	0.022
22029B-08	5.0	1.42E-13	1.0015	0.0027	1.2049	0.0039	1.6860	0.0120	0.354	0.021	0.03304	0.00023	99.09	0.9917	0.0028	6.777	0.019	0.024
22029B-09	5.0	2.75E-13	0.9938	0.0023	1.2011	0.0033	1.7313	0.0097	0.278	0.012	0.03393	0.00019	99.31	0.9862	0.0024	6.740	0.016	0.022
22029B-10	5.0	1.64E-13	1.0014	0.0027	1.1960	0.0046	1.7130	0.0150	0.450	0.018	0.03358	0.00029	98.80	0.9887	0.0029	6.757	0.020	0.024
22029B-11	5.0	1.65E-13	0.9955	0.0024	1.2048	0.0036	1.6370	0.0120	0.266	0.017	0.03209	0.00023	99.34	0.9882	0.0025	6.753	0.017	0.022
<b>269C: Mes4 (2050) J = 0.0037910 ± 0.0000080</b>																		
22050-01	4.0	1.28E-13	0.9911	0.0027	1.1934	0.0040	0.1356	0.0076	0.183	0.009	0.00266	0.00015	99.46	0.9851	0.0028	6.725	0.019	0.024
22050-02	4.0	1.55E-13	0.9913	0.0026	1.1961	0.0045	0.2500	0.0130	0.104	0.008	0.00489	0.00025	99.71	0.9877	0.0026	6.742	0.018	0.023
22050-03	4.0	1.15E-13	0.9978	0.0026	1.1997	0.0046	0.2160	0.0140	0.180	0.010	0.00424	0.00027	99.48	0.9919	0.0027	6.771	0.018	0.023
22050-04	4.0	1.26E-13	0.9887	0.0027	1.1977	0.0041	0.3550	0.0220	0.064	0.010	0.00695	0.00043	99.83	0.9863	0.0028	6.733	0.019	0.024
22050-05	4.0	1.12E-13	0.9963	0.0025	1.2023	0.0040	0.1820	0.0140	0.138	0.010	0.00356	0.00028	99.60	0.9917	0.0026	6.769	0.017	0.022
22050-06	4.0	1.56E-13	0.9947	0.0025	1.2069	0.0038	0.2092	0.0086	0.288	0.008	0.00410	0.00017	99.16	0.9856	0.0026	6.728	0.018	0.023
22050-07	4.0	1.26E-13	1.0112	0.0033	1.1900	0.0045	0.2760	0.0190	0.676	0.011	0.00541	0.00037	98.04	0.9907	0.0034	6.763	0.023	0.027
22050-08	4.0	1.92E-13	0.9979	0.0023	1.2082	0.0033	0.2344	0.0094	0.264	0.007	0.00459	0.00018	99.23	0.9895	0.0023	6.755	0.016	0.021
22050-09	4.0	1.11E-13	0.9995	0.0025	1.1947	0.0048	0.1540	0.0130	0.412	0.011	0.00301	0.00025	98.79	0.9867	0.0026	6.736	0.017	0.022
22050-10	4.0	1.19E-13	1.0076	0.0026	1.1982	0.0045	0.2160	0.0110	0.513	0.011	0.00424	0.00021	98.51	0.9918	0.0027	6.771	0.018	0.023
22050-11	4.0	1.69E-13	0.9971	0.0022	1.1996	0.0039	0.2708	0.0077	0.266	0.008	0.00531	0.00015	99.23	0.9887	0.0023	6.750	0.016	0.021
22050-12	4.0	1.22E-13	0.9935	0.0025	1.2048	0.0036	0.2850	0.0180	0.202	0.010	0.00558	0.00035	99.42	0.9870	0.0026	6.738	0.018	0.023
<b>269D: Mes4 (22071) J = 0.0037904 ± 0.0000057</b>																		
22071-01	4.0	1.66E-13	0.9975	0.0035	1.2092	0.0049	0.1970	0.0100	0.272	0.008	0.00385	0.00020	99.21	0.9889	0.0036	6.749	0.024	0.026
22071-02	4.0	1.27E-13	0.9968	0.0035	1.1972	0.0047	0.1420	0.0130	0.342	0.010	0.00278	0.00025	99.00	0.9861	0.0036	6.731	0.024	0.026
22071-03	4.0	1.34E-13	0.9950	0.0035	1.1957	0.0051	0.1770	0.0130	0.141	0.009	0.00348	0.00026	99.59	0.9902	0.0035	6.759	0.024	0.026
22071-04	4.0	1.65E-13	1.0008	0.0034	1.2001	0.0047	0.2172	0.0086	0.304	0.008	0.00426	0.00017	99.12	0.9912	0.0035	6.766	0.024	0.026
22071-05	4.0	1.32E-13	0.9908	0.0035	1.2020	0.0054	0.1610	0.0110	0.086	0.008	0.00315	0.00022	99.75	0.9876	0.0035	6.741	0.024	0.026
22071-06	4.0	1.10E-13	0.9875	0.0036	1.1988	0.0051	0.2240	0.0150	0.133	0.010	0.00440	0.00030	99.62	0.9830	0.0036	6.709	0.025	0.027
22071-07	4.0	1.31E-13	0.9883	0.0036	1.1977	0.0049	0.2980	0.0180	0.083	0.008	0.00583	0.00035	99.77	0.9854	0.0036	6.726	0.025	0.027
22071-08	4.0	1.18E-13	0.9988	0.0037	1.1995	0.0048	0.3850	0.0190	0.329	0.010	0.00755	0.00037	99.06	0.9886	0.0038	6.748	0.026	0.028
22071-09	4.0	1.24E-13	0.9889	0.0036	1.2038	0.0055	0.2530	0.0140	0.118	0.008	0.00497	0.00027	99.67	0.9849	0.0036	6.722	0.024	0.026
22071-10	4.0	1.16E-13	0.9876	0.0037	1.1970	0.0049	0.1840	0.0130	0.094	0.009	0.00360	0.00025	99.73	0.9842	0.0037	6.718	0.025	0.027
22071-11	4.0	9.23E-14	0.9876	0.0036	1.2025	0.0052	0.3600	0.0240	0.101	0.011	0.00705	0.00047	99.73	0.9841	0.0036	6.717	0.024	0.026
22071-12	4.0	1.21E-13	0.9921	0.0037	1.1952	0.0053	0.2350	0.0130	0.065	0.009	0.00462	0.00026	99.82	0.9896	0.0037	6.754	0.025	0.027
22071-13	4.0	1.12E-13	0.9925	0.0036	1.2218	0.0058	0.1910	0.0120	0.100	0.009	0.00375	0.00023	99.72	0.9889	0.0036	6.750	0.025	0.026
22071-14	4.0	1.71E-13	0.9890	0.0035	1.2018	0.0048	0.3130	0.0160	0.088	0.007	0.00614	0.00032	99.76	0.9859	0.0036	6.729	0.024	0.026
22071-15	4.0	7.34E-14	0.9920	0.0035	1.2020	0.0058	0.3550	0.0190	0.144	0.014	0.006							

Lab ID#	Laser Power (W)	<sup>39</sup> Ar (moles)	<sup>39</sup> Ar (% of total)	<sup>40</sup> Ar/ <sup>39</sup> Ar ± 1σ	<sup>38</sup> Ar/ <sup>39</sup> Ar (× 10 <sup>-2</sup> ) ± 1σ	<sup>37</sup> Ar/ <sup>39</sup> Ar (× 10 <sup>-4</sup> ) ± 1σ	<sup>36</sup> Ar/ <sup>39</sup> Ar (× 10 <sup>-4</sup> ) ± 1σ	Ca/K	<sup>40</sup> Ar (%) ± 1σ	<sup>40</sup> Ar/ <sup>39</sup> Ar ± 1σ	Age (Ma)	± 1σ excluding error on J	± 1σ including error on J	Omitted because
22083B-02	4.0	5.70E-14		0.8674 0.0020	1.1906 0.0049	1.2460 0.0260	0.055 0.019	0.02442 0.00052	99.92 0.0021	0.8660 0.0021	5.918	0.015 0.019	0.019 age < 6.5 Ma	
22083B-03	4.0	4.77E-14		0.8853 0.0019	1.1830 0.0049	2.2030 0.0350	0.101 0.021	0.04319 0.00069	99.85 0.0020	0.8833 0.0020	6.036	0.014 0.019	0.019 age < 6.5 Ma	
22083B-04	4.0	5.17E-14		0.8668 0.0017	1.2010 0.0049	1.3710 0.0320	0.044 0.021	0.02686 0.00063	99.97 0.0018	0.8658 0.0018	5.917	0.012 0.017	0.017 age < 6.5 Ma	
22083B-05	4.0	6.81E-14		0.8445 0.0018	1.2113 0.0058	1.1560 0.0150	0.075 0.017	0.02266 0.00030	99.85 0.0019	0.8425 0.0019	5.758	0.013 0.018	0.018 age < 6.5 Ma	
22083B-06	4.0	7.97E-14		0.8771 0.0018	1.1984 0.0040	1.2790 0.0210	0.052 0.015	0.02506 0.00040	99.94 0.0019	0.8759 0.0019	5.986	0.013 0.018	0.018 age < 6.5 Ma	
22083B-07	4.0	5.93E-14		0.9029 0.0017	1.1948 0.0044	1.3090 0.0250	0.123 0.018	0.02565 0.00049	99.71 0.0018	0.8995 0.0018	6.147	0.012 0.018	0.018 age < 6.5 Ma	
<b>257PR-C: Mes8 (32529) J = 0.0051603 ± 0.0000100</b>														
32529-01	6.0	2.99E-13		0.7146 0.0016	1.2208 0.0032	2.0590 0.0110	0.106 0.013	0.04036 0.00022	99.79 0.0017	0.7124 0.0017	6.620	0.015 0.020		
32529-02	6.0	2.01E-13		0.7144 0.0016	1.2291 0.0031	2.0145 0.0083	0.125 0.017	0.03948 0.00016	99.71 0.0017	0.7116 0.0017	6.612	0.016 0.021		
32529-03	6.0	1.36E-13		0.7206 0.0017	1.2118 0.0035	1.8770 0.0120	0.191 0.025	0.03678 0.00024	99.42 0.0019	0.7158 0.0019	6.651	0.018 0.022		
32529-04	6.0	1.29E-13		0.7172 0.0017	1.2474 0.0035	2.1670 0.0170	0.234 0.035	0.04248 0.00034	99.27 0.0020	0.7113 0.0020	6.610	0.019 0.023		
32529-06	6.0	2.01E-13		0.7144 0.0017	1.2258 0.0033	2.0970 0.0140	0.082 0.016	0.04110 0.00027	99.89 0.0017	0.7130 0.0017	6.625	0.016 0.021		
32529-07	6.0	1.36E-13		0.7156 0.0017	1.2208 0.0035	1.9930 0.0100	0.126 0.022	0.03906 0.00020	99.70 0.0018	0.7128 0.0018	6.623	0.017 0.021		
32529-10	5.8	5.53E-14		0.7154 0.0011	1.2096 0.0028	1.9859 0.0088	0.185 0.053	0.03892 0.00017	99.47 0.0020	0.7109 0.0020	6.606	0.018 0.022		
32529-11	5.8	4.80E-14		0.7168 0.0013	1.2031 0.0036	1.9900 0.0130	0.306 0.059	0.03900 0.00025	98.97 0.0022	0.7087 0.0022	6.585	0.020 0.024		
32529-12	5.8	3.28E-14		0.7154 0.0011	1.2091 0.0035	2.0110 0.0130	0.060 0.081	0.03941 0.00026	99.98 0.0027	0.7146 0.0027	6.641	0.025 0.028		
32529-13	5.8	3.49E-14		0.7147 0.0012	1.2065 0.0032	2.1430 0.0130	0.066 0.068	0.04200 0.00026	99.97 0.0024	0.7138 0.0024	6.633	0.022 0.026		
32529-14	5.8	6.52E-14		0.7184 0.0011	1.2094 0.0024	2.0140 0.0100	0.186 0.053	0.03948 0.00020	99.47 0.0019	0.7138 0.0019	6.633	0.018 0.022		
32529-15	5.8	7.65E-14		0.7163 0.0010	1.2083 0.0026	1.9786 0.0084	0.159 0.041	0.03878 0.00017	99.57 0.0016	0.7125 0.0016	6.621	0.015 0.020		
32529-16	5.8	5.34E-14		0.7149 0.0013	1.2077 0.0030	1.9552 0.0092	0.175 0.058	0.03832 0.00018	99.50 0.0021	0.7106 0.0021	6.603	0.020 0.024		
32529-05	6.0	1.12E-13		0.7430 0.0018	1.2243 0.0036	2.0150 0.0140	0.066 0.031	0.03950 0.00028	99.95 0.0020	0.7420 0.0020	6.894	0.019 0.023	>1.5 nMADs from median age	
32529-17	5.8	5.91E-14		0.7227 0.0012	1.2076 0.0027	2.0028 0.0086	0.196 0.051	0.03926 0.00017	99.43 0.0019	0.7178 0.0019	6.670	0.018 0.022	>1.5 nMADs from median age	
<b>257PR-C: Mes9 (32533) J = 0.0051638 ± 0.0000100</b>														
32533-10	4.8	3.26E-14		0.7108 0.0010	1.2032 0.0036	1.6012 0.0068	0.324 0.083	0.03138 0.00013	98.83 0.0027	0.7018 0.0027	6.526	0.025 0.028		
32533-11	4.8	4.25E-14		0.7107 0.0011	1.2044 0.0028	1.4612 0.0048	0.127 0.067	0.02864 0.00010	99.64 0.0023	0.7074 0.0023	6.578	0.021 0.025		
32533-12	4.8	3.48E-14		0.7222 0.0010	1.1978 0.0032	1.4387 0.0053	0.547 0.078	0.02820 0.00010	97.92 0.0026	0.7065 0.0026	6.569	0.024 0.027		
32533-13	4.8	4.36E-14		0.7091 0.0011	1.2009 0.0029	1.5103 0.0037	0.118 0.072	0.02960 0.00007	99.68 0.0024	0.7061 0.0024	6.566	0.022 0.026		
32533-14	4.8	7.12E-14		0.7117 0.0011	1.2021 0.0027	1.5079 0.0035	0.342 0.050	0.02955 0.00007	98.75 0.0019	0.7021 0.0019	6.529	0.017 0.021		
32533-15	4.8	5.44E-14		0.7081 0.0011	1.1986 0.0031	1.5972 0.0049	0.232 0.064	0.03131 0.00010	99.21 0.0022	0.7018 0.0022	6.526	0.020 0.024		
32533-20	5.8	4.40E-14		0.7098 0.0011	1.2139 0.0032	1.6412 0.0094	0.078 0.050	0.03217 0.00018	99.87 0.0018	0.7081 0.0018	6.585	0.017 0.021		
32533-22	5.8	5.85E-14		0.7083 0.0011	1.2021 0.0026	1.4922 0.0082	0.225 0.045	0.02925 0.00016	99.24 0.0022	0.7022 0.0017	6.530	0.016 0.020		
32533-25	5.8	7.71E-14		0.7086 0.0011	1.2072 0.0028	1.4857 0.0057	0.128 0.042	0.02912 0.00011	99.64 0.0016	0.7053 0.0016	6.559	0.015 0.020		
32533-27	5.8	4.55E-14		0.7186 0.0011	1.1997 0.0034	1.3909 0.0085	0.373 0.055	0.02726 0.00017	98.63 0.0020	0.7081 0.0020	6.584	0.019 0.023		
32533-28	5.8	4.22E-14		0.7103 0.0012	1.2081 0.0034	1.4994 0.0082	0.271 0.060	0.02939 0.00016	99.05 0.0021	0.7029 0.0021	6.536	0.020 0.024		
32533-29	5.8	3.47E-14		0.7127 0.0013	1.2022 0.0034	1.4690 0.0120	0.426 0.077	0.02879 0.00023	98.40 0.0026	0.7006 0.0026	6.515	0.024 0.027		
32533-23	5.8	1.69E-15		0.7784 0.0031	1.1820 0.0150	1.4640 0.0880	0.470 0.980	0.02870 0.00170	98.40 0.0270	0.7650 0.0290	7.110	0.270 0.271	>1.5 nMADs from median age	
32533-26	5.8	5.72E-16		0.9024 0.0065	1.2110 0.0290	3.0200 0.2400	0.500 2.800	0.05920 0.00470	98.60 0.0840	0.8890 0.0840	8.260	0.780 0.777	age > 7.2 Ma	
32533-21	5.8	1.61E-15		0.7732 0.0030	1.2290 0.0160	2.0900 0.0980	1.500 1.000	0.04100 0.00190	94.60 0.0310	0.7310 0.0310	6.790	0.290 0.291	%40Ar* <97	
32533-24	5.8	7.02E-15		0.7529 0.0020	1.2379 0.0076	1.7650 0.0280	1.290 0.270	0.03459 0.00054	95.10 0.0082	0.7156 0.0082	6.655	0.076 0.077	%40Ar* <97	
<b>257PR-C: Mes11 (32531) J = 0.0051638 ± 0.0000100</b>														
32531-07	6.0	3.95E-14		0.7087 0.0018	1.2431 0.0053	2.0740 0.0190	0.190 0.073	0.04064 0.00037	99.44 0.0028	0.7040 0.0028	6.546	0.026 0.029		
32531-22	5.8	1.51E-14		0.7102 0.0014	1.1844 0.0045	1.8740 0.0200	0.490 0.140	0.03673 0.00039	98.18 0.0044	0.6965 0.0044	6.477	0.041 0.043		
32531-23	5.8	8.60E-15		0.7128 0.0018	1.2261 0.0060	1.9680 0.0320	0.690 0.230	0.03857 0.00062	97.38 0.0070	0.6934 0.0070	6.448	0.065 0.066		
32531-28	5.8	1.39E-14		0.7038 0.0014	1.2013 0.0047	1.9650 0.0200	0.430 0.150	0.03851 0.00038	98.42 0.0047	0.6920 0.0047	6.435	0.043 0.045		
32531-33	5.8	1.25E-14		0.7109 0.0017	1.1959 0.0069	1.8660 0.0190	0.000 0.170	0.03657 0.00036	100.26 0.0052	0.7120 0.0052	6.621	0.048 0.050		
32531-43	5.8	7.27E-15		0.7148 0.0022	1.2092 0.0072	2.0410 0.0300	0.350 0.250	0.04000 0.00058	98.80 0.0077	0.7055 0.0077	6.561	0.071 0.072		
32531-44	5.8	1.07E-14		0.7039 0.0016	1.2102 0.0048	1.9390 0.0210	0.410 0.170	0.03801 0.00042	98.49 0.0054	0.6925 0.0054	6.440	0.050 0.052		
32531-48	5.8	8.66E-15		0.7047 0.0018	1.1868 0.0066	1.9890 0.0340	0.000 0.210	0.03899 0.00067	100.67 0.0066	0.7088 0.0066	6.591	0.061 0.063		
32531-50	5.8	8.85E-15		0.7055 0.0018	1.1871 0.0052	1.8930 0.0270	0.160 0.210	0.03710 0.00053	99.54 0.0165	0.7016 0.0065	6.524	0.061 0.062		
32531-52	5.8	8.13E-15		0.7034 0.0018	1.1947 0.0056	1.9220 0.0290	0.020 0.230	0.03767 0.00057	100.20 0.0071	0.7038 0.0071	6.545	0.066 0.067		
32531-53	5.8	6.70E-15		0.7112 0.0020	1.1989 0.0061	2.0600 0.0270	0.430 0.260	0.04038 0.00053	98.50 0.0079	0.6995 0.0079	6.505	0.073 0.074		
32531-54	5.8	8.86E-15		0.7050 0.0015	1.2036 0.0050	1.9060 0.0260	0.140 0.200	0.03735 0.00052	99.65 0.0163	0.7018 0.0063	6.526	0.058 0.060		
32531-55	5.8	8.59E-15		0.7062 0.0018	1.2118 0.0064	1.9040 0.0240	0.560 0.210	0.03732 0.00047	97.89 0.0065	0.6906 0.0065	6.422	0.060 0.061		
32531-56	6.0	1.95E-14		0.7132 0.0										

Lab ID#	Laser Power (W)	<sup>39</sup> Ar (moles)	<sup>39</sup> Ar (% of total)	<sup>40</sup> Ar/ <sup>39</sup> Ar ± 1σ	<sup>38</sup> Ar/ <sup>39</sup> Ar (× 10 <sup>-2</sup> ) ± 1σ	<sup>37</sup> Ar/ <sup>39</sup> Ar (× 10 <sup>-4</sup> ) ± 1σ	<sup>36</sup> Ar/ <sup>39</sup> Ar (× 10 <sup>-4</sup> ) ± 1σ	Ca/K	<sup>40</sup> Ar (%) ± 1σ	<sup>40</sup> Ar/ <sup>39</sup> ArK ± 1σ	Age (Ma)	± 1σ excluding error on J	± 1σ including error on J	Omitted because
32531-41	5.8	6.75E-15		0.7191 0.0020	1.2153 0.0059	2.0370 0.0300	0.820 0.270	0.03993 0.00059	96.90 0.0082	0.6958 0.0082	6.470	0.076	0.077	%40Ar* <97
32531-45	5.8	5.19E-15		0.7165 0.0022	1.1989 0.0076	1.8240 0.0410	1.700 0.340	0.03575 0.00081	93.20 0.0100	0.6670 0.0100	6.203	0.097	0.098	%40Ar* <97
32531-47	5.8	4.00E-15		0.7120 0.0023	1.1888 0.0095	2.1570 0.0470	1.000 0.450	0.04227 0.00093	96.10 0.0140	0.6830 0.0140	6.360	0.130	0.128	%40Ar* <97
32531-51	5.8	3.91E-16		0.8710 0.0100	1.2640 0.0370	443.6000 2.8000	22.500 3.800	8.69500 0.05400	64.00 0.1100	0.5500 0.1100	5.200	1.100	1.062	%40Ar* <97
<b>252A: Mes12 (32472) J = 0.005209 ± 0.0000100</b>														
32472-01Bcomb	5.0	3.46E-13		0.6858 0.0015	1.2030 0.0033	1.7520 0.0100	0.096 0.017	0.03434 0.00020	99.78 0.0016	0.6836 0.0016	6.405	0.015	0.019	
32472-02Bcomb	5.0	2.29E-13		0.6891 0.0017	1.2182 0.0040	1.4400 0.0130	0.207 0.023	0.02823 0.00026	99.27 0.0018	0.6834 0.0018	6.403	0.017	0.021	
32472-03Bcomb	5.0	2.89E-13		0.6857 0.0018	1.2172 0.0038	1.8660 0.0110	0.084 0.020	0.03657 0.00022	99.85 0.0019	0.6840 0.0019	6.409	0.018	0.022	
32472-04Bcomb	5.0	3.58E-13		0.6867 0.0017	1.2125 0.0037	2.0250 0.0130	0.082 0.016	0.03970 0.00026	99.88 0.0018	0.6851 0.0018	6.419	0.016	0.021	
32472-05Bcomb	5.0	3.22E-13		0.6889 0.0017	1.2084 0.0038	2.0310 0.0130	0.112 0.017	0.03981 0.00026	99.75 0.0018	0.6864 0.0018	6.431	0.016	0.021	
32472-06	5.0	2.74E-13		0.6876 0.0016	1.2155 0.0032	1.7860 0.0110	0.221 0.010	0.03500 0.00021	99.25 0.0016	0.6818 0.0016	6.388	0.015	0.020	
32472-07	5.0	2.81E-13		0.6865 0.0016	1.2091 0.0035	1.8160 0.0130	0.103 0.012	0.03560 0.00026	99.76 0.0017	0.6841 0.0017	6.410	0.016	0.020	
32472-08	5.0	2.57E-13		0.6857 0.0016	1.2107 0.0038	2.1420 0.0160	0.130 0.012	0.04199 0.00032	99.68 0.0017	0.6828 0.0017	6.398	0.016	0.020	
<b>252A: Mes12 (32478) J = 0.0051716 ± 0.0000100</b>														
32478-01Bcomb	5.0	2.23E-13		0.6905 0.0018	1.2128 0.0050	2.0730 0.0200	0.151 0.025	0.04064 0.00039	99.59 0.0020	0.6870 0.0020	6.398	0.019	0.022	
32478-02Bcomb	5.0	2.66E-13		0.6949 0.0017	1.2197 0.0044	2.1820 0.0160	0.331 0.023	0.04276 0.00031	98.84 0.0019	0.6861 0.0019	6.390	0.018	0.022	
32478-03Bcomb	5.0	2.61E-13		0.6902 0.0018	1.2122 0.0040	1.9230 0.0170	0.117 0.022	0.03769 0.00033	99.72 0.0019	0.6876 0.0019	6.403	0.018	0.022	
32478-04Bcomb	5.0	2.70E-13		0.6914 0.0017	1.2189 0.0043	2.1700 0.0160	0.187 0.020	0.04253 0.00032	99.44 0.0019	0.6868 0.0019	6.397	0.017	0.021	
32478-05	5.0	3.02E-13		0.6885 0.0016	1.2118 0.0035	1.8380 0.0130	0.097 0.010	0.03602 0.00025	99.79 0.0017	0.6864 0.0017	6.393	0.016	0.020	
32478-06	5.0	2.48E-13		0.6901 0.0016	1.2045 0.0032	1.8210 0.0130	0.130 0.012	0.03570 0.00025	99.65 0.0017	0.6870 0.0017	6.398	0.015	0.020	
32478-07	5.0	2.18E-13		0.6909 0.0016	1.2056 0.0040	1.8166 0.0097	0.166 0.014	0.03561 0.00019	99.50 0.0017	0.6867 0.0017	6.396	0.016	0.020	
32478-08	5.0	2.82E-13		0.6949 0.0016	1.2189 0.0032	1.9010 0.0110	0.243 0.015	0.03726 0.00021	99.18 0.0017	0.6885 0.0017	6.412	0.016	>1.5 nMADs from median age	
<b>252A: Mes12 (32484) J = 0.0051777 ± 0.0000100</b>														
32484-02Bcomb	5.0	3.02E-13		0.6900 0.0017	1.2164 0.0039	2.0040 0.0140	0.110 0.020	0.03928 0.00027	99.75 0.0019	0.6876 0.0019	6.411	0.017	0.021	
32484-03Bcomb	5.0	3.20E-13		0.6886 0.0018	1.2167 0.0039	2.0360 0.0180	0.050 0.018	0.03991 0.00036	100.02 0.0020	0.6880 0.0019	6.415	0.017	0.021	
32484-04Bcomb	5.0	2.00E-13		0.6968 0.0021	1.2286 0.0049	2.1470 0.0190	0.365 0.028	0.04208 0.00037	98.69 0.0020	0.6870 0.0023	6.406	0.022	0.025	
32484-05	5.0	2.34E-13		0.6896 0.0016	1.2145 0.0034	1.8130 0.0100	0.146 0.014	0.03553 0.00020	99.58 0.0017	0.6859 0.0017	6.396	0.016	0.020	
32484-06	5.0	3.44E-13		0.6899 0.0015	1.2096 0.0033	1.8530 0.0120	0.107 0.009	0.03632 0.00023	99.75 0.0016	0.6875 0.0016	6.411	0.014	0.019	
32484-08	5.0	2.19E-13		0.6911 0.0017	1.2166 0.0038	1.9040 0.0130	0.175 0.014	0.03732 0.00026	99.47 0.0017	0.6867 0.0017	6.403	0.016	0.020	
32484-09Bcomb	5.0	2.07E-13		0.6925 0.0018	1.2125 0.0044	1.8130 0.0140	0.126 0.027	0.03553 0.00028	99.67 0.0020	0.6895 0.0020	6.429	0.018	0.022	
32484-07	5.0	2.27E-13		0.6883 0.0016	1.2166 0.0034	2.1500 0.0100	0.000 0.014	0.04214 0.00020	100.86 0.0017	0.6935 0.0017	6.466	0.015	>1.5 nMADs from median age	
<b>257PR-C: Mes14 (32523) J = 0.0051380 ± 0.0000100</b>														
32523-01	5.0	1.55E-13		0.6919 0.0016	1.2137 0.0032	2.1300 0.0100	0.242 0.018	0.04174 0.00020	99.21 0.0017	0.6857 0.0017	6.345	0.016	0.020	
32523-02XX	6.0	2.71E-13		0.6900 0.0015	1.2178 0.0031	2.2150 0.0120	0.133 0.012	0.04342 0.00023	99.68 0.0016	0.6871 0.0016	6.358	0.015	0.019	
32523-04X	6.0	1.60E-13		0.6921 0.0017	1.2175 0.0035	2.7040 0.0150	0.216 0.021	0.05300 0.00029	99.38 0.0018	0.6871 0.0018	6.358	0.017	0.021	
32523-05	6.0	1.42E-13		0.6886 0.0016	1.2217 0.0036	2.4363 0.0096	0.119 0.020	0.04775 0.00019	99.77 0.0017	0.6863 0.0017	6.350	0.016	0.020	
32523-06	6.0	1.23E-13		0.6900 0.0017	1.2117 0.0040	2.2800 0.0120	0.091 0.023	0.04469 0.00024	99.87 0.0018	0.6884 0.0018	6.370	0.017	0.021	
32523-07	6.0	1.86E-13		0.6907 0.0017	1.2160 0.0032	1.9720 0.0120	0.148 0.016	0.03864 0.00023	99.59 0.0017	0.6871 0.0017	6.358	0.016	0.020	
32523-11	5.7	9.17E-14		0.6930 0.0010	1.1956 0.0021	2.0855 0.0056	0.317 0.041	0.04088 0.00011	98.89 0.0016	0.6846 0.0016	6.334	0.015	0.019	
32523-12	5.7	6.59E-14		0.6948 0.0011	1.1999 0.0029	2.7061 0.0070	0.256 0.048	0.05304 0.00014	99.22 0.0018	0.6887 0.0018	6.373	0.017	0.021	
32523-14	5.7	8.58E-14		0.6911 0.0010	1.2043 0.0025	2.0539 0.0065	0.170 0.040	0.04026 0.00013	99.51 0.0016	0.6870 0.0016	6.356	0.015	0.019	
32523-15	5.7	6.69E-14		0.6933 0.0012	1.2070 0.0025	2.2305 0.0054	0.213 0.049	0.04372 0.00011	99.35 0.0019	0.6881 0.0019	6.367	0.018	0.022	
32523-16	5.7	8.58E-14		0.6905 0.0011	1.2037 0.0024	2.2530 0.0071	0.188 0.040	0.04416 0.00014	99.45 0.0016	0.6860 0.0016	6.348	0.015	0.019	
32523-10	5.6	8.15E-15		0.7011 0.0019	1.2027 0.0062	1.8860 0.0120	0.220 0.260	0.03696 0.00024	99.30 0.0020	0.6955 0.0080	6.436	0.074	0.075	>1.5 nMADs from median age
32523-13	5.7	6.87E-14		0.6893 0.0011	1.1954 0.0028	2.1301 0.0052	0.292 0.053	0.04175 0.00010	98.99 0.0020	0.6816 0.0020	6.307	0.018	0.022	>1.5 nMADs from median age
32523-03	5.0	1.74E-13		1.0974 0.0025	1.2309 0.0032	1.9404 0.0071	0.288 0.020	0.03803 0.00014	99.37 0.0026	1.0897 0.0026	10.073	0.024	0.031	age > 7. Ma
<b>257PR-C: Ifo3 (32535) J = 0.0051604 ± 0.0000100</b>														
32535-01	0.6	7.74E-14		0.6770 0.0010	1.1993 0.0027	1.9416 0.0053	0.128 0.042	0.03805 0.00010	99.67 0.0016	0.6741 0.0016	6.265	0.015	0.019	
32535-02	0.6	6.17E-14		0.6805 0.0011	1.2047 0.0026	3.6610 0.0091	0.172 0.052	0.07175 0.00018	99.68 0.0016	0.6776 0.0019	6.297	0.018	0.021	
32535-03	0.6	5.75E-14		0.6766 0.0011	1.2037 0.0031	2.0046 0.0068	0.154 0.046	0.03929 0.00013	99.57 0.0018	0.6730 0.0018	6.254	0.016	0.020	
32535-04	0.6	8.78E-14		0.6780 0.0010	1.1988 0.0026	1.9811 0.0051	0.136 0.036	0.03883 0.00010	99.64 0.0016	0.6748 0.0015	6.272	0.014	0.018	
32535-05	0.6	3.05E-14		0.6795 0.0010	1.2003 0.0036	1.8749 0.0076	0.000 0.085	0.03675 0.00015	100.33 0.0015	0.6810 0.0027	6.329	0.025	0.028	
32535-06	0.6	5.65E-14		0.6832 0.0011	1.1973 0.0030	2.0028 0.0053	0.220 0.049	0.03926 0.00010	99.29 0.0018					

Lab ID#	Laser Power (W)	<sup>39</sup> Ar (moles)	<sup>39</sup> Ar (% of total)	<sup>40</sup> Ar/ <sup>39</sup> Ar ± 1σ	<sup>38</sup> Ar/ <sup>39</sup> Ar ± 1σ (× 10 <sup>-2</sup> )	<sup>37</sup> Ar/ <sup>39</sup> Ar ± 1σ (× 10 <sup>-2</sup> )	<sup>36</sup> Ar/ <sup>39</sup> Ar ± 1σ (× 10 <sup>-4</sup> )	Ca/K	± 1σ	<sup>40</sup> Ar (%)	<sup>40</sup> Ar/ <sup>39</sup> ArK ± 1σ	Age (Ma)	± 1σ excluding error on J	± 1σ including error on J	Omitted because			
<b>257PR-C: Ifo4 (32537) J = 0.0051544 ± 0.0000100</b>																		
32537-01	5.8	1.23E-13	0.6774	0.0009	1.1942	0.0023	1.7045	0.0043	0.118	0.030	0.03341	0.00008	99.69	0.6746	0.0013	6.262	0.012	0.017
32537-02	5.8	8.51E-14	0.6781	0.0010	1.2005	0.0025	1.6353	0.0044	0.198	0.038	0.03205	0.00009	99.33	0.6729	0.0015	6.246	0.014	0.018
32537-03	5.8	4.76E-14	0.6836	0.0010	1.2047	0.0029	2.0744	0.0073	0.517	0.057	0.04066	0.00014	98.01	0.6693	0.0020	6.213	0.019	0.022
32537-04	5.8	9.01E-14	0.6765	0.0010	1.2036	0.0024	1.7204	0.0051	0.162	0.034	0.03372	0.00010	99.50	0.6724	0.0015	6.242	0.014	0.018
32537-05	5.8	9.18E-14	0.6878	0.0010	1.2044	0.0026	1.7393	0.0050	0.499	0.038	0.03409	0.00010	98.06	0.6738	0.0015	6.254	0.014	0.018
32537-06	5.8	7.96E-14	0.6766	0.0010	1.2027	0.0022	1.7340	0.0047	0.157	0.039	0.03399	0.00009	99.52	0.6726	0.0015	6.244	0.014	0.019
32537-07	5.8	4.27E-14	0.6769	0.0011	1.2189	0.0030	1.8216	0.0073	0.108	0.060	0.03570	0.00014	99.75	0.6745	0.0021	6.261	0.019	0.023
32537-08	5.8	5.39E-14	0.6789	0.0011	1.2065	0.0029	1.6386	0.0055	0.318	0.052	0.03212	0.00011	98.81	0.6701	0.0019	6.220	0.018	0.021
32537-09	5.8	1.22E-13	0.6763	0.0010	1.1948	0.0025	1.7254	0.0049	0.178	0.033	0.03382	0.00010	99.43	0.6717	0.0014	6.235	0.013	0.018
32537-10	5.8	6.19E-14	0.6757	0.0011	1.1996	0.0026	1.7786	0.0055	0.218	0.049	0.03486	0.00011	99.26	0.6700	0.0019	6.220	0.017	0.021
32537-21	5.8	4.39E-14	0.6754	0.0011	1.1959	0.0036	1.9783	0.0098	0.288	0.060	0.03877	0.00019	98.98	0.6678	0.0021	6.199	0.019	0.023
32537-25	5.8	5.36E-14	0.6736	0.0012	1.1928	0.0028	1.6918	0.0086	0.219	0.052	0.03316	0.00017	99.25	0.6678	0.0019	6.199	0.018	0.022
32537-26	5.8	3.04E-14	0.6766	0.0011	1.1902	0.0034	1.6350	0.0120	0.092	0.078	0.03204	0.00024	99.80	0.6746	0.0026	6.262	0.024	0.027
32537-20	5.8	2.91E-15	0.8303	0.0023	1.2220	0.0110	1.9260	0.0470	5.450	0.580	0.03775	0.00093	80.80	0.6700	0.0170	6.220	0.160	0.161 %40Ar* <97
32537-22	5.8	1.33E-14	0.6910	0.0014	1.2090	0.0056	1.8670	0.0210	1.150	0.170	0.03659	0.00041	95.29	0.6578	0.0052	6.107	0.048	0.049 %40Ar* <97
32537-23	5.8	6.46E-15	0.7269	0.0022	1.2048	0.0060	2.2610	0.0370	2.520	0.300	0.04431	0.00072	90.00	0.6535	0.0091	6.066	0.085	0.086 %40Ar* <97
32537-24	5.8	2.17E-14	0.6991	0.0012	1.2131	0.0045	1.7880	0.0150	0.760	0.110	0.03505	0.00030	96.99	0.6774	0.0035	6.288	0.032	0.034 %40Ar* <97
<b>257PR-C: Ifo5 (32539) J = 0.0051475 ± 0.0000100</b>																		
32539-02	5.8	7.32E-14	0.6751	0.0011	1.1928	0.0026	1.6908	0.0055	0.108	0.045	0.03314	0.00011	99.73	0.6726	0.0017	6.235	0.016	0.020
32539-03	5.8	1.04E-13	0.6770	0.0010	1.1958	0.0025	1.6529	0.0036	0.187	0.036	0.03240	0.00007	99.38	0.6721	0.0015	6.231	0.014	0.018
32539-04	5.8	5.02E-14	0.6767	0.0012	1.2035	0.0026	1.6410	0.0071	0.166	0.058	0.03216	0.00014	99.47	0.6724	0.0021	6.234	0.019	0.023
32539-05	5.8	6.49E-14	0.6749	0.0010	1.1988	0.0025	1.7376	0.0048	0.167	0.046	0.03406	0.00009	99.48	0.6706	0.0017	6.217	0.016	0.020
32539-06	5.8	6.22E-14	0.6783	0.0010	1.1999	0.0027	1.6239	0.0061	0.109	0.048	0.03183	0.00012	99.72	0.6757	0.0018	6.264	0.017	0.021
32539-07	5.8	5.69E-14	0.6775	0.0010	1.1967	0.0029	1.5722	0.0074	0.148	0.054	0.03082	0.00014	99.54	0.6737	0.0019	6.245	0.018	0.022
32539-08	5.8	6.99E-14	0.6781	0.0010	1.1976	0.0028	1.6207	0.0054	0.148	0.045	0.03177	0.00011	99.55	0.6743	0.0017	6.251	0.016	0.020
32539-09	5.8	5.90E-14	0.6774	0.0012	1.2027	0.0029	1.4930	0.0052	0.118	0.051	0.02926	0.00010	99.67	0.6744	0.0019	6.252	0.018	0.022
32539-10	5.8	5.40E-14	0.6739	0.0012	1.1901	0.0031	1.5762	0.0057	0.122	0.058	0.03089	0.00011	99.66	0.6709	0.0021	6.219	0.020	0.023
32539-20	5.8	4.91E-14	0.6770	0.0011	1.1933	0.0028	1.6292	0.0095	0.040	0.054	0.03193	0.00019	100.03	0.6764	0.0020	6.271	0.018	0.022
32539-21	5.8	1.74E-14	0.6816	0.0013	1.2034	0.0044	1.7100	0.0200	0.330	0.130	0.03352	0.00040	98.77	0.6725	0.0040	6.234	0.037	0.039
32539-24	5.8	5.25E-14	0.6800	0.0011	1.2007	0.0028	1.5385	0.0086	0.239	0.054	0.03015	0.00017	99.15	0.6735	0.0020	6.243	0.018	0.022
32539-25	5.8	3.25E-14	0.6772	0.0012	1.1997	0.0032	1.9070	0.0140	0.225	0.078	0.03737	0.00027	99.25	0.6714	0.0026	6.224	0.024	0.027
32539-01	5.8	6.59E-14	0.6769	0.0010	1.1946	0.0026	1.5442	0.0058	0.373	0.048	0.03027	0.00011	98.56	0.6664	0.0018	6.178	0.016	0.020 >1.5 nMADs from median age
32539-22	5.8	2.93E-15	0.6994	0.0022	1.2083	0.0100	4.1700	0.0740	2.100	0.630	0.08170	0.00140	91.60	0.6400	0.0190	5.930	0.180	0.176 %40Ar* <97
32539-23	5.8	8.88E-16	0.7358	0.0049	1.2150	0.0200	5.5500	0.2000	5.800	2.000	0.10890	0.00400	77.50	0.5690	0.0590	5.280	0.540	0.543 %40Ar* <97
32539-26	5.8	3.51E-14	0.7279	0.0011	1.2373	0.0035	1.7090	0.0110	1.628	0.076	0.03349	0.00022	93.58	0.6805	0.0025	6.308	0.024	0.027 %40Ar* <97

#### Single crystal total fusions - VU

Lab ID#	Laser Power (W)	<sup>39</sup> Ar (moles)	<sup>40</sup> Ar/ <sup>39</sup> Ar ± 1σ	<sup>38</sup> Ar/ <sup>39</sup> Ar ± 1σ	<sup>37</sup> Ar/ <sup>39</sup> Ar ± 1σ	<sup>36</sup> Ar/ <sup>39</sup> Ar ± 1σ	Ca/K	± 1σ	<sup>40</sup> Ar (%)	<sup>40</sup> Ar/ <sup>39</sup> ArK ± 1σ	Age (Ma)	± 1σ excluding error on J	± 1σ including error on J	Omitted because				
<b>VU37: Mes1 (01M0165) J = 0.001849 ± 0.000005 (TCR)</b>																		
01M0165A	20.0	9.51E-14	2.0729	0.0022	0.01208	0.00004	0.0122	0.0011	0.0000173	0.0000060	0.02838	0.00284	99.76	2.0679	0.0028	6.885	0.009	0.021
01M0165B	20.0	7.74E-14	2.0971	0.0024	0.01209	0.00004	0.0124	0.0019	0.0000731	0.0000087	0.02874	0.00457	98.97	2.0756	0.0035	6.910	0.012	0.023
01M0165D	20.0	8.87E-14	2.0829	0.0023	0.01206	0.00003	0.0096	0.0018	0.0000296	0.0000052	0.02226	0.00442	99.57	2.0707	0.0027	6.894	0.009	0.021
01M0165E	20.0	8.69E-14	2.0846	0.0023	0.01222	0.00004	0.0105	0.0015	0.0000448	0.0000053	0.02454	0.00360	99.36	2.0680	0.0028	6.885	0.009	0.021
01M0165F	20.0	1.08E-13	2.0811	0.0023	0.01215	0.00003	0.0114	0.0011	0.0000231	0.0000042	0.02660	0.00298	99.67	2.0709	0.0026	6.895	0.009	0.021
01M0165H	20.0	5.75E-14	2.1170	0.0023	0.01223	0.00004	0.0105	0.0018	0.0001366	0.0000090	0.02431	0.00437	98.09	2.0676	0.0035	6.884	0.012	0.022
01M0165I	20.0	7.98E-14	2.0882	0.0022	0.01216	0.00005	0.0075	0.0013	0.0000383	0.0000038	0.01755	0.00310	99.44	2.0676	0.0024	6.884	0.008	0.021
01M0165J	20.0	7.05E-14	2.1007	0.0025	0.01212	0.00004	0.0099	0.0014	0.0000232	0.0000071	0.02306	0.00355	99.67	2.0757	0.0032	6.911	0.011	0.022
<b>VU37: Mes4 (00M0170, 01M0191) J = 0.001449 ± 0.000003 (TCR)</b>																		
00M0170Brecomb	20.0	7.58E-15	2.5902	0.0041	0.01211	0.00014	0.0167	0.000										

Lab ID#	Laser Power (W)	<sup>39</sup> Ar (moles)	<sup>40</sup> Ar/ <sup>39</sup> Ar ± 1σ	<sup>38</sup> Ar/ <sup>39</sup> Ar ± 1σ	<sup>37</sup> Ar/ <sup>39</sup> Ar ± 1σ	<sup>36</sup> Ar/ <sup>39</sup> Ar ± 1σ	Ca/K	± 1σ	<sup>40</sup> Ar (%)	<sup>40</sup> Ar/ <sup>39</sup> Ar <sub>K</sub> ± 1σ	Age (Ma)	± 1σ	± 1σ	± 1σ	Omitted because				
<b>VU42: Mes4 (A3) J = 0.001869 ± 0.000005</b>																			
01M0379K	20.0	3.05E-14	2.0643	0.0059	0.01217	0.00010	0.0168	0.0002	0.0000621	0.0000172	0.03906	0.00186	99.13	2.0464	0.0078	7.005	0.027	0.029	>1.5 nMADs from median age
<b>VU37 Mes6 (01m0171) J = 0.001563 ± 0.000004 (TCR)</b>																			
01M0171B	20.0	9.90E-15	2.4099	0.0026	0.01220	0.00009	0.0386	0.0070	0.0001010	0.0000459	0.08978	0.01691	98.85	2.3822	0.0138	6.705	0.039	0.042	
01M0171D	20.0	6.85E-15	2.4296	0.0030	0.01226	0.00011	0.0076	0.0109	0.0002036	0.0000586	0.01779	0.02532	97.51	2.3691	0.0176	6.668	0.049	0.052	
01M0171G	20.0	4.34E-15	2.4509	0.0033	0.01204	0.00016	0.0205	0.0229	0.0003674	0.0000964	0.04775	0.05339	95.60	2.3326	0.0286	6.565	0.080	0.082	
01M0171I	20.0	2.97E-15	2.5016	0.0032	0.01180	0.00026	0.0035	0.0257	0.0006631	0.0001301	0.00814	0.05984	92.14	2.2799	0.0382	6.417	0.107	0.108	
01M0171K	20.0	3.23E-15	2.5420	0.0036	0.01212	0.00019	-0.0276	0.0259	0.0003718	0.0001147	---	---	95.64	2.4048	0.0338	6.768	0.095	0.096	
01M0171N	20.0	1.30E-14	2.5385	0.0033	0.01230	0.00007	0.0223	0.0058	0.0004631	0.0000262	0.05194	0.01372	94.64	2.3763	0.0083	6.688	0.023	0.028	
<b>VU37: Mes8 (01M0192) J = 0.001460 ± 0.000003 (TCR)</b>																			
01M0192A	20.0	8.11E-15	2.6052	0.0031	0.01254	0.00014	0.0081	0.0101	0.0002323	0.0000365	0.01879	0.02356	97.36	2.5363	0.0112	6.668	0.030	0.033	
01M0192B	20.0	3.48E-15	2.5635	0.0037	0.01292	0.00018	0.0049	0.0293	0.000433	0.0000615	0.01138	0.06816	99.48	2.5503	0.0187	6.705	0.049	0.051	
01M0192D	20.0	4.91E-15	2.5463	0.0035	0.01277	0.00010	0.0045	0.0191	0.000148	0.0000636	0.01044	0.04433	99.81	2.5693	0.0194	6.755	0.051	0.053	
01M0192E	20.0	5.46E-15	2.5639	0.0045	0.01271	0.00015	0.0000	0.0162	0.0001743	0.0000527	---	---	97.96	2.5391	0.0164	6.675	0.043	0.046	
01M0192F	20.0	1.30E-14	2.5928	0.0029	0.01244	0.00010	0.0106	0.0105	0.0003486	0.0000205	0.02469	0.02447	96.02	2.5238	0.0068	6.635	0.018	0.024	
01M0192G	20.0	2.00E-14	2.3491	0.0029	0.01252	0.00008	0.0393	0.0063	0.0003812	0.000095	0.09134	0.01542	95.30	2.2693	0.0041	5.967	0.011	0.017	>1.5 nMADs from median age
<b>VU42: Mes8 (A4) J = 0.001870 ± 0.000004</b>																			
02M0268B	20.0	1.66E-14	2.1072	0.0058	0.01217	0.00009	0.0204	0.0003	0.0005190	0.0000641	0.04733	0.00102	92.76	1.9546	0.0197	6.582	0.066	0.068	
02M0268C	20.0	1.63E-14	1.9936	0.0053	0.01223	0.00009	0.0198	0.0003	0.0001103	0.0000459	0.04610	0.0105	98.40	1.9617	0.0145	6.606	0.049	0.051	
02M0268D	20.0	3.25E-14	2.0201	0.0054	0.01233	0.00008	0.0201	0.0002	0.0002246	0.0000267	0.04683	0.0089	96.75	1.9545	0.0095	6.582	0.032	0.035	
02M0268F	20.0	2.58E-14	2.0302	0.0054	0.01216	0.00007	0.0202	0.0003	0.0002830	0.0000244	0.04706	0.00100	95.92	1.9473	0.0089	6.558	0.030	0.034	
02M0268G	20.0	2.43E-14	2.0392	0.0053	0.01221	0.00009	0.0199	0.0002	0.0002825	0.0000358	0.04640	0.00085	95.94	1.9565	0.0118	6.588	0.040	0.043	
02M0268H	20.0	1.49E-14	1.9530	0.0055	0.01219	0.00010	0.0195	0.0003	0.0000661	0.0000418	0.04528	0.0102	99.94	1.9519	0.0135	6.573	0.045	0.048	
02M0268J	20.0	1.60E-14	1.9801	0.0052	0.01213	0.00008	0.0196	0.0003	0.0001022	0.0000512	0.04555	0.00097	98.51	1.9507	0.0160	6.569	0.054	0.056	
02M0268K	20.0	2.36E-14	2.0624	0.0054	0.01229	0.00008	0.0203	0.0002	0.0003523	0.0000336	0.04731	0.00092	94.99	1.9591	0.0112	6.597	0.038	0.041	
02M0268N	20.0	2.75E-14	2.0077	0.0054	0.01218	0.00008	0.0199	0.0002	0.0001643	0.0000268	0.04639	0.00091	97.62	1.9598	0.0095	6.600	0.032	0.036	
02M1267Lrecomb	20.0	1.02E-14	1.9979	0.0029	0.0122	0.0001	0.0185	0.0007	0.0000984	0.0001064	0.04314	98.57	1.9694	0.0316	6.632	0.106	0.107		
<b>VU37: Mes9 (B3: 00M0239, 00M0245, 00M0246) J = 0.001853 ± 0.000005 (TCR)</b>																			
00M0246recomb	20.0	6.25E-14	1.9914	0.0043	0.01212	0.00007	0.0153	0.0002	0.0001088	0.0000060	0.03544	97.59	1.9596	0.0047	6.539	0.016	0.024		
00M0245recomb	20.0	1.93E-14	2.0270	0.0059	0.01223	0.00012	0.0155	0.0003	0.0002449	0.0000103	0.03604	96.44	1.9550	0.0067	6.524	0.022	0.029		
00M0239recomb	20.0	2.86E-14	2.0662	0.0052	0.01217	0.00008	0.0156	0.0002	0.0003546	0.0000105	0.03638	94.94	1.9617	0.0061	6.546	0.020	0.028		
<b>VU37: Mes9 (01M0167) J = 0.001861 ± 0.000006 (TCR)</b>																			
01M0167A	20.0	1.14E-13	1.9580	0.0022	0.01206	0.00004	0.0174	0.0007	0.0000370	0.0000049	0.04057	0.00262	99.47	1.9476	0.0026	6.527	0.009	0.021	
01M0167C	20.0	5.84E-14	1.9677	0.0020	0.01206	0.00003	0.0184	0.0009	0.0000437	0.0000086	0.04291	0.00301	99.37	1.9522	0.0033	6.542	0.011	0.022	
01M0167D	20.0	1.03E-13	1.9650	0.0020	0.01209	0.00004	0.0167	0.0006	0.0000365	0.0000054	0.03884	0.00246	99.47	1.9516	0.0026	6.540	0.009	0.021	
01M0167E	20.0	3.74E-14	1.9659	0.0024	0.01194	0.00005	0.0245	0.0002	0.0000511	0.0000124	0.05689	0.00664	99.29	1.9487	0.0044	6.531	0.015	0.024	
01M0167G	20.0	3.11E-14	1.9874	0.0021	0.01211	0.00003	0.0172	0.0024	0.0000762	0.0000123	0.04001	0.00589	98.89	1.9527	0.0042	6.544	0.014	0.024	
<b>VU42: Mes9 (A5) J = 0.001871 ± 0.000004</b>																			
02M0270A	20.0	3.64E-14	1.9434	0.0052	0.01215	0.00008	0.0151	0.0001	0.0000516	0.0000182	0.03518	0.00065	99.23	1.9285	0.0075	6.498	0.025	0.029	
02M0270B	20.0	1.68E-14	2.0484	0.0056	0.01253	0.00010	0.0149	0.0002	0.0003694	0.0000463	0.03458	0.00073	94.69	1.9395	0.0147	6.535	0.049	0.052	
02M0270D	20.0	2.84E-14	2.0453	0.0055	0.01216	0.00009	0.0154	0.0002	0.0004126	0.0000197	0.03586	0.00070	94.06	1.9238	0.0078	6.482	0.026	0.030	
02M0270E	20.0	2.00E-14	2.0344	0.0061	0.01213	0.00009	0.0145	0.0002	0.0003493	0.0000275	0.03375	0.00076	94.94	1.9314	0.0100	6.508	0.034	0.037	
02M0270F	20.0	3.35E-14	1.9487	0.0052	0.01214	0.00008	0.0154	0.0002	0.0000750	0.0000264	0.03592	0.00075	98.88	1.9269	0.0094	6.492	0.031	0.035	
02M0270H	20.0	2.31E-14	2.0070	0.0053	0.01227	0.00008	0.0154	0.0002	0.0002323	0.0000408	0.03588	0.00079	96.60	1.9387	0.0131	6.532	0.044	0.047	
02M0270J	20.0	2.53E-14	1.9414	0.0051	0.01220	0.00008	0.0154	0.0003	0.0003000	0.0000252	0.03574	0.00082	99.56	1.9329	0.0090	6.513	0.030	0.034	
02M0270L	20.0	3.44E-14	1.9755	0.0052	0.01217	0.00009	0.0137	0.0002	0.0001462	0.0000233	0.03195	0.00068	97.82	1.9325	0.0086	6.511	0.029	0.033	
02M0270M	20.0	1.30E-14	1.9530	0.0053	0.01223	0.00011	0.0157	0.0003	0.0001208	0.0000528	0.03654	0.00095	98.19	1.9177	0.0164	6.462	0.055	0.057	
02M0270I	20.0	1.65E-14	2.0715	0.0055	0.01230	0.00010	0.0155	0.0003	0.0003717	0.0000345	0.03608	0.00097	94.71	1.9620	0.0114	6.611	0.038	0.041	>1.5 nMADs from median age
<b>VU42: Mes10 (A7) J = 0.001873 ± 0.000004</b>																			
02M0272B	20.0	2.15E-14																	

Lab ID#	Laser Power (W)	<sup>39</sup> Ar (moles)	<sup>40</sup> Ar/ <sup>39</sup> Ar ± 1σ	<sup>39</sup> Ar/ <sup>39</sup> Ar ± 1σ	<sup>37</sup> Ar/ <sup>39</sup> Ar ± 1σ	<sup>36</sup> Ar/ <sup>39</sup> Ar ± 1σ	Ca/K	± 1σ	<sup>40</sup> Ar (%)	<sup>40</sup> Ar/ <sup>39</sup> Ar ± 1σ	Age (Ma)	± 1σ excluding error on J	± 1σ including error on J	Omitted because				
02M0272H	20.0	1.18E-14	2.0201	0.0054	0.01233	0.00012	0.0180	0.0003	0.0000650	0.0000720	0.04184	0.00094	99.08	2.0015	0.0219	6.750	0.074	0.075 >1.5 nMADs from median age
02M0272J	20.0	3.12E-14	2.0619	0.0056	0.01213	0.00009	0.0088	0.0001	0.0000390	0.0000162	0.02057	0.00046	99.43	2.0502	0.0073	6.914	0.025	0.029 >1.5 nMADs from median age
02M0272L	20.0	1.71E-14	2.2761	0.0062	0.01259	0.00011	0.0347	0.0004	0.0008464	0.0000625	0.08077	0.00155	89.09	2.0278	0.0193	6.839	0.065	0.067 >1.5 nMADs from median age
<b>VU37: Mes11 (00m0160) J = 0.001641 ± 0.000004 (TCR)</b>																		
00M0160A	20.0	1.17E-14	2.2452	0.0039	0.01230	0.00008	0.0884	0.0005	0.0001919	0.000065	0.20561	0.00332	97.74	2.1946	0.0043	6.485	0.013	0.020
00M0160D	20.0	8.78E-15	2.2926	0.0039	0.01202	0.00006	0.0553	0.0004	0.0003270	0.0000180	0.12875	0.00215	95.93	2.1994	0.0065	6.499	0.019	0.025
00M0160E	20.0	1.73E-14	2.2187	0.0038	0.01210	0.00009	0.0553	0.0004	0.000685	0.0000074	0.12859	0.00215	99.24	2.2020	0.0043	6.507	0.013	0.020
00M0160F	20.0	9.42E-15	2.2412	0.0041	0.01219	0.00012	0.2290	0.0014	0.0001996	0.000066	0.53309	0.00872	98.12	2.1995	0.0045	6.500	0.013	0.020
00M0160B	20.0	5.08E-15	2.2942	0.0042	0.01220	0.00014	0.5126	0.0033	0.0004838	0.0000160	1.19318	0.01972	95.47	2.1910	0.0063	6.475	0.018	0.024 Ca/K >1
<b>VU37: Mes12 (00M0172,00M0248,01M0168) J = 0.001723 ± 0.000004</b>																		
00M0172A	20.0	6.65E-14	2.1060	0.0035	0.01215	0.00006	0.0170	0.0001	0.0001322	0.0000040	0.03964	0.00069	98.16	2.0674	0.0036	6.415	0.011	0.020
00M0172D	20.0	5.67E-14	2.1469	0.0036	0.01198	0.00005	0.0179	0.0002	0.0001958	0.0000059	0.04159	0.00076	97.33	2.0689	0.0039	6.420	0.012	0.020
00M0248D	20.0	1.04E-14	2.1019	0.0070	0.01215	0.00011	0.0175	0.0005	0.0000210	0.0000153	0.04081	0.00158	99.73	2.0658	0.0082	6.410	0.025	0.030
01M0168A	20.0	1.12E-13	2.0970	0.0023	0.01209	0.00003	0.0224	0.0007	0.0001171	0.0000046	0.05206	0.00305	98.39	2.0633	0.0026	6.402	0.008	0.018
01M0168D	20.0	1.63E-13	2.0902	0.0022	0.01211	0.00004	0.0188	0.0006	0.0001029	0.0000028	0.04384	0.00258	98.57	2.0605	0.0024	6.393	0.007	0.018
01M0168E	20.0	7.96E-14	2.1049	0.0026	0.01198	0.00005	0.0231	0.0010	0.0000499	0.0000061	0.05364	0.00358	99.34	2.0608	0.0031	6.394	0.010	0.019
01M0168B	20.0	7.42E-14	2.1397	0.0023	0.01217	0.00005	0.0226	0.0013	0.0002363	0.000081	0.05250	0.00395	96.78	2.0503	0.0032	6.362	0.010	0.019 >1.5 nMADs from median age
00M0248E	20.0	2.74E-14	2.6949	0.0185	0.01290	0.00016	0.0134	0.0003	0.0004205	0.0000189	0.03122	0.00102	95.39	2.5335	0.0184	7.858	0.057	0.060 age > 7.2 Ma
<b>VU42: Mes12 (A8) J = 0.001874 ± 0.000004</b>																		
02M0273A	20.0	3.12E-14	1.9333	0.0052	0.01229	0.00008	0.0187	0.0002	0.0000882	0.0000194	0.04347	0.00081	98.68	1.9078	0.0077	6.439	0.026	0.030
02M0273B	20.0	2.58E-14	2.0217	0.0053	0.01243	0.00008	0.0193	0.0002	0.0004071	0.0000266	0.04488	0.00089	94.08	1.9021	0.0093	6.419	0.031	0.034
02M0273D	20.0	3.23E-14	2.0168	0.0053	0.01232	0.00008	0.0134	0.0002	0.0004106	0.0000348	0.03127	0.00066	93.99	1.8957	0.0114	6.398	0.039	0.041
02M0273E	20.0	2.31E-14	2.0612	0.0054	0.01233	0.00009	0.0182	0.0003	0.0005397	0.0000352	0.04231	0.00102	92.29	1.9023	0.0115	6.420	0.039	0.041
02M0273F	20.0	2.43E-14	2.1041	0.0058	0.01262	0.00008	0.0191	0.0003	0.0006833	0.0000411	0.04451	0.00096	90.43	1.9028	0.0132	6.422	0.045	0.047
02M0273H	20.0	3.38E-14	2.0181	0.0053	0.01231	0.00008	0.0172	0.0002	0.0003797	0.0000265	0.04000	0.00080	94.46	1.9064	0.0093	6.434	0.031	0.034
02M0273I	20.0	4.90E-14	1.9324	0.0051	0.01233	0.00008	0.0211	0.0002	0.0000963	0.0000180	0.04903	0.00090	98.57	1.9047	0.0074	6.428	0.025	0.029
02M0273J	20.0	3.62E-14	1.9488	0.0052	0.01219	0.00007	0.0192	0.0002	0.0001429	0.0000183	0.04465	0.00084	97.87	1.9072	0.0074	6.437	0.025	0.029
02M0273M	20.0	2.62E-14	1.9128	0.0052	0.01221	0.00008	0.0181	0.0002	0.0006060	0.0000238	0.04206	0.00085	99.10	1.8957	0.0087	6.398	0.029	0.033
02M0273L	20.0	3.57E-14	1.9329	0.0051	0.01226	0.00008	0.0179	0.0002	0.0001749	0.0000267	0.04159	0.00077	97.35	1.8817	0.0093	6.351	0.031	0.034 >1.5 nMADs from median age
<b>VU37: Mes14 (01M0166) J = 0.001636 ± 0.000004 (TCR)</b>																		
01M0166A	20.0	1.85E-14	2.1587	0.0023	0.01221	0.00012	0.0081	0.0054	0.0000206	0.0000174	0.01891	0.01270	99.71	2.1524	0.0057	6.342	0.017	0.023
01M0166B	20.0	6.15E-14	2.1442	0.0023	0.01210	0.00004	0.0179	0.0011	0.0000369	0.0000058	0.04161	0.00332	99.52	2.1339	0.0029	6.287	0.008	0.017
01M0166C	20.0	2.92E-14	2.1691	0.0023	0.01218	0.00004	0.0327	0.0024	0.0000334	0.0000202	0.07602	0.00685	99.62	2.1491	0.0064	6.332	0.019	0.024
01M0166E	20.0	3.51E-14	2.1974	0.0023	0.01221	0.00005	0.0303	0.0016	0.0001581	0.0000104	0.07038	0.00511	97.94	2.1404	0.0038	6.306	0.011	0.019
01M0166F	20.0	4.12E-14	2.2088	0.0026	0.01219	0.00006	0.0332	0.0018	0.0001645	0.0000107	0.07713	0.00578	97.88	2.1501	0.0040	6.335	0.012	0.019
01M0166G	20.0	2.80E-14	2.1779	0.0024	0.01226	0.00006	0.0437	0.0030	0.0000374	0.0000122	0.10156	0.00865	99.61	2.1442	0.0043	6.318	0.013	0.020
01M0166I	20.0	2.62E-14	2.1950	0.0026	0.01218	0.00007	0.0172	0.0036	0.0000493	0.0000180	0.04003	0.00865	99.36	2.1556	0.0059	6.351	0.017	0.023
01M0166J	20.0	1.47E-14	2.3416	0.0025	0.01223	0.00007	0.0065	0.0049	0.0000248	0.0000268	0.01508	0.01137	99.67	2.1641	0.0077	6.376	0.023	0.027
<b>VU42: Mes14 (A9) J = 0.001874 ± 0.000004</b>																		
02M0275A	20.0	1.08E-14	1.8803	0.0051	0.01225	0.00010	0.0173	0.0005	0.0000170	0.0000676	0.04023	0.00133	99.76	1.8757	0.0206	6.330	0.069	0.071
02M0275C	20.0	2.29E-14	1.9321	0.0052	0.01212	0.00008	0.0204	0.0003	0.0001996	0.0000305	0.04739	0.00100	96.98	1.8739	0.0103	6.324	0.035	0.037
02M0275D	20.0	9.65E-15	1.8716	0.0051	0.01219	0.00010	0.0190	0.0003	0.000054	0.0000657	0.04423	0.00096	99.95	1.8707	0.0201	6.313	0.068	0.069
02M0275E	20.0	1.80E-14	1.9081	0.0051	0.01226	0.00009	0.0172	0.0002	0.0001132	0.0000241	0.03994	0.00805	98.27	1.8751	0.0087	6.328	0.029	0.032
02M0275G	20.0	1.90E-14	1.9311	0.0051	0.01215	0.00008	0.0216	0.0003	0.0003001	0.0000383	0.05019	0.0107	95.45	1.8433	0.0123	6.221	0.042	0.044
02M0275I	20.0	3.31E-14	1.9628	0.0054	0.01225	0.00008	0.0220	0.0002	0.0003583	0.0000198	0.05111	0.00996	94.65	1.8578	0.0078	6.270	0.026	0.030
02M0275K	20.0	3.15E-14	1.9576	0.0053	0.01226	0.00008	0.0215	0.0002	0.0003267	0.0000171	0.04992	0.00998	95.11	1.8619	0.0071	6.284	0.024	0.028
02M0275L	20.0	1.90E-14	2.0124	0.0054	0.01220	0.00008	0.0190	0.0003	0.0004665	0.0000437	0.04411	0.00102	93.18	1.8752	0.0138	6.329	0.047	0.049
02M0275M	20.0	1.87E-14	2.0900	0.0056	0.01218	0.00008	0.0235	0.0003	0.0007781	0.0000401	0.05470	0.00111	89.04	1.8611	0.0128	6.281	0.043	0.045
02M0275H	20.0	1.56E-14	1.8966	0.0051	0.01215	0.00008	0.0201	0.0004	0.0002204	0.0000407	0.04680	0.00120	96.60	1.8322	0.0130	6.184	0.044	0.

Lab ID#	Laser Power (W)	<sup>39</sup> Ar (moles)	<sup>40</sup> Ar/ <sup>39</sup> Ar ± 1σ	<sup>38</sup> Ar/ <sup>39</sup> Ar ± 1σ	<sup>37</sup> Ar/ <sup>39</sup> Ar ± 1σ	<sup>36</sup> Ar/ <sup>39</sup> Ar ± 1σ	Ca/K	± 1σ	<sup>40</sup> Ar (%)	<sup>40</sup> Ar/ <sup>39</sup> ArK ± 1σ	Age (Ma)	± 1σ excluding error on J	± 1σ including error on J	Omitted because				
02M0279H	20.0	3.40E-14	1.8836	0.0051	0.01225	0.00008	0.0184	0.0003	0.0001113	0.0000194	0.04275	0.00091	98.28	1.8513	0.0076	6.251	0.026	0.029
02M0279I	20.0	1.85E-14	1.9697	0.0063	0.01226	0.00008	0.0182	0.0003	0.0003927	0.0000324	0.04233	0.00099	94.14	1.8542	0.0113	6.261	0.038	0.040
02M0279K	20.0	2.42E-14	1.9307	0.0052	0.01222	0.00010	0.0188	0.0002	0.0002789	0.0000380	0.04374	0.00090	95.76	1.8489	0.0123	6.243	0.041	0.044
02M0279L	20.0	1.96E-14	1.8694	0.0051	0.01231	0.00010	0.0178	0.0003	0.0000857	0.0000372	0.04128	0.00094	98.67	1.8446	0.0121	6.229	0.041	0.043
02M0279M	20.0	1.59E-14	1.9172	0.0053	0.01239	0.00010	0.0172	0.0002	0.0002329	0.0000391	0.04009	0.00083	96.44	1.8488	0.0127	6.243	0.043	0.045
<b>VU37: Mes17 (00M0237,00M0238) J = 0.001736 ± 0.000004 (TCR)</b>																		
00M0237B	20.0	3.09E-14	2.0209	0.0068	0.01212	0.00011	0.0168	0.0003	0.0001149	0.0000104	0.03899	0.00115	98.34	1.9875	0.0075	6.214	0.023	0.028
00M0237D	20.0	3.17E-14	2.1454	0.0075	0.01213	0.00019	0.0230	0.0005	0.0005215	0.0000343	0.05346	0.00168	92.86	1.9923	0.0126	6.229	0.039	0.042
00M0238recomb	20.0	3.64E-14	2.0570	0.0064	0.01211	0.00010	0.0155	0.0003	0.0002017	0.0000083	0.03596	0.00168	97.06	1.9977	0.0068	6.246	0.021	0.026
<b>VU37: Mes17 (00M0236) J = 0.001747 ± 0.000004 (TCR)</b>																		
00M0236recomb	20.0	5.94E-14	2.0733	0.0067	0.01209	0.00009	0.0147	0.0002	0.0003414	0.0000055	0.03414	0.00168	95.14	1.9727	0.0069	6.207	0.022	0.027
<b>VU42: Mes17 (A13) J = 0.001875 ± 0.000004</b>																		
02M0280A	20.0	4.14E-14	1.9374	0.0060	0.01245	0.00008	0.0159	0.0002	0.0002828	0.0000221	0.03689	0.00072	95.71	1.8542	0.0087	6.261	0.029	0.032
02M0280B	20.0	4.56E-14	1.9117	0.0054	0.01227	0.00007	0.0173	0.0002	0.0001932	0.0000199	0.04027	0.00081	97.04	1.8551	0.0079	6.264	0.027	0.030
02M0280C	20.0	3.47E-14	1.9148	0.0056	0.01227	0.00008	0.0181	0.0003	0.0002421	0.0000211	0.04204	0.00093	96.31	1.8441	0.0082	6.227	0.028	0.031
02M0280E	20.0	2.44E-14	1.9154	0.0053	0.01210	0.00008	0.0162	0.0002	0.0002513	0.0000322	0.03768	0.00076	96.14	1.8416	0.0108	6.219	0.036	0.039
02M0280F	20.0	1.76E-14	1.9966	0.0057	0.01241	0.00010	0.0173	0.0002	0.0004788	0.0000352	0.04032	0.00079	92.94	1.8556	0.0117	6.266	0.039	0.042
02M0280G	20.0	2.60E-14	1.9438	0.0059	0.01216	0.00008	0.0148	0.0002	0.0003252	0.0000385	0.03450	0.00077	95.07	1.8480	0.0127	6.240	0.043	0.045
02M0280I	20.0	3.21E-14	1.8807	0.0050	0.01219	0.00008	0.0168	0.0002	0.0001046	0.0000280	0.03919	0.00076	98.38	1.8503	0.0096	6.248	0.032	0.035
02M0280J	20.0	2.54E-14	1.9358	0.0052	0.01217	0.00009	0.0180	0.0002	0.0002629	0.0000316	0.04193	0.00085	96.01	1.8587	0.0106	6.276	0.036	0.038
02M0280K	20.0	2.46E-14	1.8500	0.0049	0.01211	0.00009	0.0164	0.0002	0.0000444	0.0000266	0.03804	0.00077	99.95	1.8491	0.0093	6.244	0.031	0.034
02M0280M	20.0	2.79E-14	1.8748	0.0053	0.01219	0.00008	0.0169	0.0003	0.0001039	0.0000235	0.03919	0.00087	98.39	1.8446	0.0087	6.229	0.029	0.032
<b>VU42: Mes18 (A15) J = 0.001874 ± 0.000004</b>																		
02M0302C	20.0	1.30E-14	1.8584	0.0021	0.01226	0.00005	0.0160	0.0002	0.0000554	0.0000444	0.03711	0.00084	99.14	1.8425	0.0133	6.218	0.045	0.047
02M0302D	20.0	2.38E-14	1.8467	0.0019	0.01220	0.00005	0.0176	0.0002	0.000049	0.0000206	0.04093	0.00095	99.95	1.8458	0.0064	6.230	0.021	0.025
02M0302E	20.0	1.32E-14	1.8581	0.0021	0.01236	0.00008	0.0153	0.0004	0.0000568	0.0000455	0.03567	0.00121	99.11	1.8416	0.0136	6.216	0.046	0.048
02M0302G	20.0	1.19E-14	1.8709	0.0021	0.01228	0.00006	0.0179	0.0003	0.0000343	0.0000421	0.04156	0.00106	99.49	1.8613	0.0126	6.282	0.042	0.045
02M0302H	20.0	1.80E-14	1.8486	0.0019	0.01226	0.00005	0.0217	0.0002	0.0000439	0.0000366	0.05050	0.00108	99.34	1.8365	0.0110	6.198	0.037	0.039
02M0302I	20.0	1.40E-14	1.8513	0.0021	0.01233	0.00005	0.0220	0.0005	0.0000526	0.0000264	0.05126	0.00160	99.21	1.8367	0.0081	6.199	0.027	0.030
02M0302K	20.0	1.98E-14	1.8637	0.0022	0.01222	0.00004	0.0166	0.0002	0.0000628	0.0000272	0.03869	0.00089	99.03	1.8456	0.0083	6.229	0.028	0.031
02MA302A	20.0	1.02E-14	1.8400	0.0013	0.01228	0.00005	0.0227	0.0006	0.0000494	0.0000469	0.05268	0.00197	99.26	1.8263	0.0139	6.164	0.047	0.049
02MA302C	20.0	9.16E-15	1.8497	0.0015	0.01224	0.00006	0.0189	0.0012	0.0000122	0.0000576	0.04387	0.00309	99.95	1.8467	0.0171	6.233	0.058	0.059
02MA302B	20.0	1.11E-14	1.8704	0.0013	0.01229	0.00006	0.0198	0.0007	0.0000054	0.0000484	0.04609	0.00201	99.84	1.8695	0.0144	6.309	0.048	>1.5 nMADs from median age
<b>VU42: Ifo1 (A17) J = 0.001873 ± 0.000004</b>																		
02M0304A	20.0	4.73E-14	1.9974	0.0021	0.01240	0.00003	0.0181	0.0001	0.0003206	0.0000220	0.04199	0.00088	95.28	1.9032	0.0068	6.420	0.023	0.027
02M0304B	20.0	1.96E-14	1.9245	0.0025	0.01244	0.00006	0.0182	0.0003	0.0000883	0.0000568	0.04228	0.00105	98.67	1.8990	0.0170	6.405	0.057	0.059
02M0304D	20.0	1.91E-14	1.9212	0.0020	0.01234	0.00006	0.0186	0.0004	0.0000923	0.0000491	0.04314	0.00133	98.61	1.8945	0.0147	6.390	0.049	0.051
02M0304E	20.0	2.98E-14	1.9329	0.0020	0.01249	0.00005	0.0193	0.0002	0.0001115	0.0000334	0.04493	0.00099	98.33	1.9007	0.0101	6.411	0.034	0.036
02M0304F	20.0	4.47E-14	1.9653	0.0024	0.01237	0.00004	0.0175	0.0001	0.0002126	0.0000230	0.04067	0.00081	96.83	1.9030	0.0072	6.419	0.024	0.028
02M0304H	20.0	3.97E-14	1.9687	0.0023	0.01241	0.00003	0.0202	0.0002	0.0002508	0.0000234	0.04704	0.00102	96.27	1.8954	0.0073	6.393	0.025	0.028
02M0304I	20.0	2.41E-14	1.9276	0.0022	0.01244	0.00005	0.0196	0.0002	0.0000949	0.0000440	0.04561	0.00097	98.58	1.9003	0.0132	6.410	0.044	0.046
02M0304M	20.0	2.30E-14	1.9428	0.0030	0.01256	0.00006	0.0194	0.0002	0.0001276	0.0000467	0.04517	0.00105	98.09	1.9058	0.0141	6.428	0.048	0.049
02M0304J	20.0	3.44E-14	1.9298	0.0020	0.01236	0.00003	0.0185	0.0002	0.0000493	0.0000285	0.04302	0.00096	99.28	1.9158	0.0087	6.462	0.029	>1.5 nMADs from median age
02M0304L	20.0	4.59E-14	1.9563	0.0023	0.01250	0.00005	0.0172	0.0001	0.0001428	0.0000238	0.04008	0.00083	97.87	1.9146	0.0074	6.458	0.025	>1.5 nMADs from median age
<b>VU42: Ifo2 (A16) J = 0.001874 ± 0.000004</b>																		
02M0303A	20.0	1.83E-14	1.9071	0.0025	0.01225	0.00006	0.0187	0.0002	0.0000228	0.0000293	0.04355	0.00092	99.68	1.9010	0.0090	6.416	0.030	0.034
02M0303B	20.0	4.46E-14	1.9213	0.0026	0.01241	0.00005	0.0185	0.0001	0.0000586	0.0000110	0.04291	0.00090	99.13	1.9046	0.0041	6.428	0.014	0.020
02M0303C	20.0	4.22E-14	1.9076	0.0025	0.01235	0.00005	0.0182	0.0001	0.0000301	0.0000164	0.04231	0.00088	99.56	1.8993	0.0054	6.410	0.018	0.023
02M0303E	20.0	2.40E-14	1.9066	0.0021	0.01254	0.00006	0.0192	0.0002	0.0000111	0.0000234	0.04469	0.00098	99.86	1.9040	0.0072	6.426	0.024	0.028
02M0303F	20.0	2.32E-14	1.9017	0.003														

Lab ID#	Laser Power (W)	<sup>39</sup> Ar (moles)	<sup>40</sup> Ar/ <sup>39</sup> Ar ± 1σ	<sup>38</sup> Ar/ <sup>39</sup> Ar ± 1σ	<sup>37</sup> Ar/ <sup>39</sup> Ar ± 1σ	<sup>36</sup> Ar/ <sup>39</sup> Ar ± 1σ	Ca/K	<sup>40</sup> Ar (%)	<sup>40</sup> Ar/ <sup>39</sup> Ar <sub>K</sub> ± 1σ	Age (Ma)	± 1σ excluding error on J	± 1σ including error on J	Omitted because					
<b>VU42: Ifo3 (A19) J = 0.001872 ± 0.000004</b>																		
02M0307B	20.0	1.92E-14	1.8746	0.0019	0.01235	0.00005	0.0200	0.0003	0.0000255	0.0000460	0.04646	0.00112	97.13	1.8678	0.0137	6.297	0.046	0.048
02M0307C	20.0	2.54E-14	1.8650	0.0026	0.01229	0.00005	0.0215	0.0001	0.0000111	0.0000200	0.04990	0.00102	98.49	1.8625	0.0065	6.279	0.022	0.025
02M0307D	20.0	2.20E-14	1.8710	0.0023	0.01238	0.00007	0.0176	0.0001	0.0000082	0.0000260	0.04085	0.00085	98.18	1.8691	0.0080	6.302	0.027	0.030
02M0307F	20.0	3.41E-14	1.9027	0.0022	0.01230	0.00005	0.0203	0.0001	0.0001177	0.0000259	0.04719	0.00099	95.70	1.8687	0.0080	6.300	0.027	0.030
02M0307G	20.0	2.49E-14	1.8961	0.0023	0.01238	0.00006	0.0211	0.0003	0.0000629	0.0000302	0.04908	0.00122	95.02	1.8783	0.0092	6.332	0.031	0.034
02M0307H	20.0	4.86E-14	1.9345	0.0025	0.01236	0.00005	0.0201	0.0001	0.0002408	0.0000150	0.04666	0.00096	95.15	1.8641	0.0051	6.284	0.017	0.022
02M0307J	20.0	2.20E-14	1.8872	0.0022	0.01237	0.00005	0.0192	0.0003	0.0001041	0.0000329	0.04474	0.00116	95.89	1.8571	0.0100	6.261	0.034	0.036
02M0307K	20.0	2.45E-14	1.9214	0.0019	0.01239	0.00005	0.0205	0.0001	0.0001459	0.0000219	0.04762	0.00097	97.45	1.8790	0.0067	6.335	0.023	0.026
02M0307L	20.0	3.69E-14	1.9141	0.0021	0.01250	0.00003	0.0196	0.0001	0.0001879	0.0000130	0.04562	0.00096	99.75	1.8593	0.0044	6.268	0.015	0.020
02M0307N	20.0	2.30E-14	1.8887	0.0020	0.01235	0.00007	0.0194	0.0002	0.0000986	0.0000274	0.04500	0.00099	99.44	1.8602	0.0084	6.272	0.028	0.031
<b>VU37: Ifo4 (01M0113/01M0193) J = 0.001807 ± 0.000005 (TCR)</b>																		
01M0193B	20.0	5.08E-14	1.9590	0.0025	0.01224	0.00006	0.0169	0.0022	0.0001206	0.0000092	0.03934	0.00558	98.20	1.9238	0.0037	6.261	0.012	0.020
01M0193C	20.0	5.62E-14	1.9527	0.0022	0.01216	0.00004	0.0173	0.0028	0.0001034	0.0000055	0.04033	0.00686	98.46	1.9226	0.0027	6.257	0.009	0.018
01M0193D	20.0	7.00E-14	1.9447	0.0026	0.01215	0.00006	0.0180	0.0025	0.0000792	0.0000059	0.04194	0.00617	98.82	1.9144	0.0031	6.230	0.010	0.019
01M0193F	20.0	5.65E-14	1.9382	0.0022	0.01215	0.00003	0.0224	0.0021	0.0000521	0.0000058	0.05204	0.00561	99.25	1.9163	0.0028	6.236	0.009	0.019
01M0113C	20.0	1.03E-13	1.9880	0.0024	0.01211	0.00004	0.0228	0.0009	0.0001960	0.0000026	0.05309	0.00323	97.13	1.9150	0.0025	6.232	0.008	0.018
01M0113E	20.0	1.43E-13	1.9566	0.0031	0.01247	0.00004	0.0188	0.0005	0.0000762	0.0000062	0.04367	0.00238	98.88	1.9186	0.0036	6.244	0.012	0.020
01M0193A	20.0	4.74E-14	1.9619	0.0023	0.01228	0.00005	0.0223	0.0026	0.0000527	0.0000092	0.05189	0.00659	99.25	1.9473	0.0035	6.337	0.012	0.020
<b>VU42: Ifo4 (A20) J = 0.001870 ± 0.000004</b>																		
02M0308A	20.0	3.08E-14	1.9050	0.0023	0.01230	0.00004	0.0179	0.0001	0.0001437	0.0000361	0.04158	0.00088	97.80	1.8631	0.0109	6.274	0.037	0.039
02M0308B	20.0	2.16E-14	1.8594	0.0028	0.01235	0.00005	0.0185	0.0004	0.0000056	0.0000543	0.04297	0.00126	99.94	1.8583	0.0163	6.259	0.055	0.056
02M0308D	20.0	4.34E-14	1.8626	0.0019	0.01233	0.00004	0.0176	0.0001	0.0000050	0.0000275	0.04103	0.00088	99.95	1.8617	0.0083	6.270	0.028	0.031
02M0308E	20.0	2.16E-14	1.9078	0.0019	0.01255	0.00004	0.0174	0.0002	0.0000793	0.0000496	0.04057	0.00093	98.80	1.8849	0.0148	6.348	0.050	0.051
02M0308F	20.0	3.81E-14	1.9027	0.0022	0.01247	0.00004	0.0182	0.0002	0.0001880	0.0000297	0.04231	0.00099	97.11	1.8477	0.0090	6.223	0.030	0.033
02M0308H	20.0	4.34E-14	1.8760	0.0020	0.01230	0.00003	0.0179	0.0002	0.0000373	0.0000212	0.04157	0.00090	99.44	1.8655	0.0066	6.283	0.022	0.026
02M0308I	20.0	3.22E-14	1.8682	0.0027	0.01237	0.00004	0.0185	0.0002	0.0000179	0.0000294	0.04304	0.00093	99.75	1.8635	0.0091	6.276	0.030	0.033
02M0308J	20.0	2.43E-14	1.8563	0.0025	0.01238	0.00005	0.0181	0.0002	0.0000197	0.0000427	0.04208	0.00096	99.72	1.8510	0.0129	6.234	0.043	0.045
02M0308L	20.0	4.58E-14	1.9175	0.0036	0.01262	0.00004	0.0175	0.0001	0.0001492	0.0000231	0.04059	0.00085	97.73	1.8739	0.0077	6.311	0.026	0.029
02M0308M	20.0	1.85E-14	1.9020	0.0028	0.01265	0.00004	0.0179	0.0002	0.0000399	0.0000561	0.04159	0.00101	99.41	1.8908	0.0168	6.368	0.056	0.058
<b>VU37: Ifo5 (01M0112) J = 0.001761 ± 0.000005 (TCR)</b>																		
01M0112A	20.0	7.48E-14	2.0776	0.0023	0.01225	0.00004	0.0218	0.0014	0.0003944	0.0000060	0.05071	0.00407	94.43	1.9619	0.0028	6.222	0.009	0.018
01M0112D	20.0	8.28E-14	1.9623	0.0021	0.01206	0.00003	0.0166	0.0008	0.0000713	0.0000051	0.03851	0.00257	98.95	1.9626	0.0026	6.224	0.008	0.018
01M0112F	20.0	8.96E-14	2.0430	0.0022	0.01218	0.00004	0.0198	0.0010	0.0003620	0.0000033	0.04615	0.00315	94.80	1.9653	0.0023	6.233	0.007	0.018
01M0112I	20.0	5.00E-14	2.0795	0.0024	0.01225	0.00005	0.0185	0.0010	0.0003695	0.0000082	0.04303	0.00318	94.78	1.9630	0.0034	6.226	0.011	0.019
01M0112K	20.0	6.82E-14	2.0688	0.0024	0.01213	0.00003	0.0210	0.0006	0.0004304	0.0000076	0.04883	0.00275	93.89	1.9633	0.0033	6.227	0.010	0.019
01M0112N	20.0	1.86E-13	2.0107	0.0022	0.01209	0.00003	0.0190	0.0004	0.0002242	0.0000032	0.04410	0.00228	96.73	1.9661	0.0023	6.235	0.007	0.018
<b>VU42: Ifo5 (A21) J = 0.001869 ± 0.000004</b>																		
02M0309A	20.0	2.00E-14	1.8696	0.0025	0.01258	0.00004	0.0166	0.0004	0.0000910	0.0000372	0.03853	0.00117	98.58	1.8431	0.0113	6.204	0.038	0.040
02M0309C	20.0	1.17E-14	1.8496	0.0020	0.01212	0.00010	0.0167	0.0005	0.0000049	0.0000780	0.03875	0.00135	99.95	1.8486	0.0231	6.223	0.078	0.079
02M0309D	20.0	8.83E-15	1.8559	0.0022	0.01219	0.00009	0.0150	0.0003	0.0000042	0.0000075	0.03499	0.00100	99.95	1.8550	0.0218	6.244	0.073	0.075
02M0309E	20.0	1.72E-14	1.8823	0.0022	0.01243	0.00007	0.0180	0.0002	0.0001394	0.0000514	0.04192	0.00094	97.84	1.8417	0.0154	6.199	0.052	0.053
02M0309G	20.0	3.37E-14	1.8449	0.0019	0.01216	0.00005	0.0167	0.0001	0.0000045	0.0000255	0.03886	0.00083	99.95	1.8441	0.0078	6.207	0.026	0.029
02M0309H	20.0	1.86E-14	1.9045	0.0022	0.01214	0.00006	0.0157	0.0003	0.0001765	0.0000406	0.03652	0.00096	97.28	1.8528	0.0122	6.236	0.041	0.043
02M0309I	20.0	3.94E-14	1.8846	0.0019	0.01213	0.00003	0.0163	0.0001	0.0001564	0.0000188	0.03789	0.00079	97.57	1.8388	0.0059	6.190	0.020	0.024
02M0309K	20.0	3.29E-14	1.8835	0.0019	0.01216	0.00004	0.0167	0.0001	0.0001523	0.0000231	0.03877	0.00082	97.63	1.8389	0.0071	6.190	0.024	0.027
02M0309L	20.0	2.88E-14	1.8722	0.0019	0.01216	0.00004	0.0172	0.0001	0.0000985	0.0000296	0.04003	0.00083	98.47	1.8436	0.0089	6.206	0.030	0.033
02M0309M	20.0	4.38E-14	1.8520	0.0025	0.01215	0.00003	0.0152	0.0002	0.0000196	0.0000353	0.03079	0.0079	99.70	1.8465	0.0061	6.215	0.021	0.024
<b>VU37: Iza1 (00M0153,01M0190) J = 0.001576 ± 0.000005 (TCR)</b>																		
01M0190A	20.0	3.99E-14	2.3828	0.0030	0.01214	0.00006	0.0200	0.0026	0.0000464	0.0000087	0.04655	0.00652	99.45	2.3699	0.0040</td			

### **Age and error equations for astronomically calibrated standard**

$$T_{FC} = \frac{1}{\lambda} \times \ln[(e^{\lambda t_{astro}} - 1) \times R_{astro}^{FC} + 1] = \frac{1}{\lambda} \times \ln[X] \quad [\text{equation 5 in (S1)}]$$

$$\sigma_{T_{FC}} = \sqrt{\left(\frac{\partial T_{FC}}{\partial \lambda}\right)^2 \times \sigma_{\lambda}^2 + \left(\frac{\partial T_{FC}}{\partial t_{astro}}\right)^2 \times \sigma_{t_{astro}}^2 + \left(\frac{\partial T_{FC}}{\partial R_{astro}^{FC}}\right)^2 \times \sigma_{R_{astro}^{FC}}^2}$$

with

$$\frac{\partial T_{FC}}{\partial \lambda} = \frac{-1}{\lambda^2} \times \ln[X] + \frac{R_{astro}^{FC} \times t_{astro} \times e^{\lambda t_{astro}}}{\lambda \times X}$$

$$\frac{\partial T_{FC}}{\partial t_{astro}} = \frac{R_{astro}^{FC} \times e^{\lambda t_{astro}}}{X}$$

$$\frac{\partial T_{FC}}{\partial R_{astro}^{FC}} = \frac{(e^{\lambda t_{astro}} - 1)}{\lambda \times X}$$

$$\lambda = (5.463 \pm 0.107) \times 10^{-10}$$

[decay constant, note that this not the value used by convention, but the value of (S9)]

$$t_{astro} = 6.500 \pm 0.005 \times 10^6 \text{ yr}$$

[astronomical age]

$$R_{astro}^{FC} = 4.3664 \pm 0.0009$$

[intercalibration factor between FCs and Melilla tephra, see caption Fig. 2]

Above values yield  $28.201 \pm 0.023$  Ma for FCs (1 sigma), or  $28.201 \pm 0.046$  Ma (2 sigma)

Note that the error increases to  $\pm 0.044$  Ma and  $\pm 0.087$  Ma for respectively an uncertainty of  $\pm 10$  kyr and  $\pm 20$  kyr in the astronomical age (all 1 sigma).

**Table S3 Published  $^{40}\text{Ar}/^{39}\text{Ar}$  data for Matuyama-Bruhnes reversal**

Dates are reported as in the original publication along with the standard, standard age, dated material and analytical methods. To allow direct comparison all data are recalculated to the astronomically calibrated FCs age of  $28.201 \pm 0.046$  Ma (this study). Not all studies report their data relative to FCs. Those data are converted to FCs ages using the following intercalibration factors:  $R^{\text{FC}}_{\text{TC}}$   $0.9889 \pm 0.0020$  (*S1*);  $R^{\text{FC}}_{\text{AC}}$   $23.646 \pm 0.068$  (*S1*);  $R^{\text{FC}}_{\text{SB-3}}$   $0.1626$  [calculated with FC 27.51 Ma and SB-3 162.9 Ma (*S10*)],  $R^{\text{FC}}_{\text{FCT-3biotite}}$   $0.9950 \pm 0.0168$  (*S11*) and  $R^{\text{FC}}_{\text{Be4-biotite}} = R^{\text{FC}}_{\text{SB-3}} \times R^{\text{SB-3}}_{\text{Be4-biotite}} = 0.1626 \times 9.8588 = 1.6031$  [with Be4-biotite 17.25 Ma relative to 162.9 SB-3 biotite (*S12*)]. Total external uncertainties at the 95% confidence level are reported for recalculated ages. For  $R^{\text{FC}}_{\text{SB-3}}$  and  $R^{\text{FC}}_{\text{Be4-biotite}}$  uncertainties are not given and are excluded in uncertainties in recalculated ages. The astronomical age for this boundary is 781 kyr (*S13*).

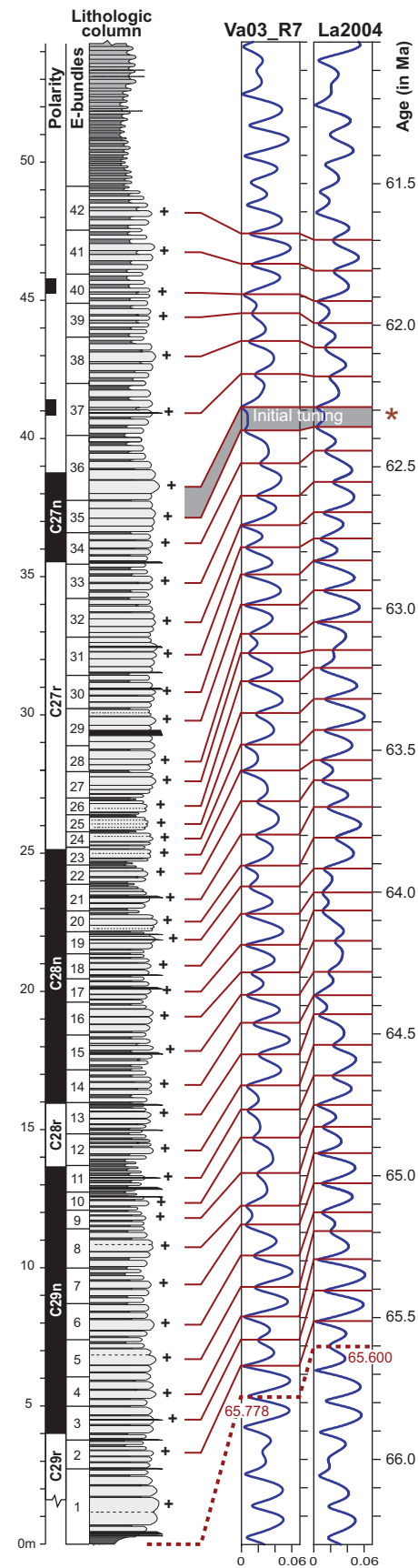
Publi-cation	Age (ka)	Material	Standard	Method*	Age relative to FCs 28.201 Ma (in ka)
<b><math>^{40}\text{Ar}/^{39}\text{Ar}</math> dating on lava flows with transitional polarity assuming to be the MB boundary</b>					
(S14)	783 $\pm$ 16	whole rock of 3 flows, Maui, Hawaii	FCT3 biotite 27.95 Ma rel. to SB3-bio 162.9	wm of 3 isochron ages	794 $\pm$ 16
(S15)	775.6 $\pm$ 2.0	whole rock and groundmass of 6 flows, Maui, Hawaii	TCs 28.34 / ACs 1.194	wm of 6 isochron ages, 20 experiments	780 $\pm$ 2
(S16)	798.4 $\pm$ 12.4	groundmass of 3 flows, La Palma	ACs 1.194	wm of 3 isochron ages, 14 experiments + isochron age La Palma flow ( <i>S17</i> )	803 $\pm$ 12
(S17)	778.7 $\pm$ 3.8	plagioclase, groundmass and whole rock of 8 flows, on Maui, Tahiti, Chili and La Palma	TCs 27.92	wm of 8 isochron ages	795 $\pm$ 4
(S18) <sup>†</sup>	791.7 $\pm$ 3.0	whole rock of 9 flows, Chili	TCs 28.34 / ACs 1.194	wm of 9 isochron ages, 22 experiments	797 $\pm$ 4
<b><math>^{40}\text{Ar}/^{39}\text{Ar}</math> dating on volcanic domes with slightly below the MB boundary (reversed polarity)</b>					
(S19)	793 $\pm$ 18	sanidine of Cerro Santa Rosa II dome, Jemez Mountains, New Mexico	FCs 27.55 / TCs 27.92 both rel. to MMhb-1 513.9	wm of 4 multigrain laser fusions	812 $\pm$ 18
(S19)	812 $\pm$ 24	sanidine of Cerro San Luis dome, Jemez Mountains, New Mexico	FCs 27.55 / TCs 27.92 both rel. to MMhb-1 513.9	wm of 9 multigrain laser fusions	831 $\pm$ 24
(S19)	794 $\pm$ 8	sanidine of Serro Seco dome, Jemez Mountains, New Mexico	FCs 27.55 / TCs 27.92 both rel. to MMhb-1 513.9	wm of multigrain 4 laser fusions	813 $\pm$ 8
(S20)	787 $\pm$ 30	sanidine of Santa Rosa II dome, Valles caldera, New Mexico	FCT-3s 27.9	isochron age of 8 single crystal laser fusions	795 $\pm$ 30
(S20)	800 $\pm$ 6	sanidine of San Luis dome, Valles caldera, New Mexico	FCT-3s 27.9	isochron age of 11 single crystal laser fusions	809 $\pm$ 6
(S20)	800 $\pm$ 14	sanidine of Seco dome, Valles caldera, New Mexico	FCT-3s 27.9	isochron age of 14 single crystal laser fusions	809 $\pm$ 14
<b><math>^{40}\text{Ar}/^{39}\text{Ar}</math> dating on volcanic layers bracketing the MB boundary</b>					
(S19)	789 $\pm$ 6	Sanidine of Oldest Toba Tuff, Sumatra (reversed polarity)	FCs 27.55 / TCs 27.92 both rel. to MMhb-1 513.9	wm of multigrain laser fusion (n=4)	808 $\pm$ 6
(S21)	> 747 $\pm$ 12	anorthoclase of airfall ash, Olorgesailie Fm, Kenya (in normal polarity interval)	FCs 27.84	isochron age of 12 single crystal anorthoclase laser fusions	> 757 $\pm$ 12
(S22)	791 $\pm$ 40	biotite of ash-D ODP site 758 (ash D = 5 cm below MBB)	FCT-3 biotite 27.99	wm of 4 multigrain laser fusions: $800 \pm 20$ ka for ash-D. Age for MB by linear interpolation of sedimentation rate	801 $\pm$ 40
(S19)	772 $\pm$ 4	sanidine of pumice of upper unit and basal airfall unit Bishop Tuff	FCs 27.55 & TCs 27.92 both rel. to MMhb-1 513.9	wm of 23 multigrain laser fusions: $760 \pm 2$ ka. Age for MB by adding 12 kyr based on linear interpolation of sedimentation rate	790 $\pm$ 4
(S23)	774.2 $\pm$ 3.6	sanidine of air fall pumice and ash flow of Bishop Tuff	TCs 27.92 Ma rel. to MMhb-1 513.9	wm of 69 single crystal laser fusions: $758.9 \pm 1.8$ ka. Age for MB by adding 15.3 ( $\pm 2.2$ ) kyr based on linear interpolation of sedimentation rate	791 $\pm$ 4

\* wm = weighted mean; † Authors indicate that they probably dated a MB precursor.

## Astronomical tuning of the K-T boundary (figs. S2, S3a-c, S4)

**Figure S2: Original tuning of (S24) to the eccentricity time series of the Va03\_R7 (S25) solution.**

Dinares-Turell et al. (S24) using the lithological expression of a 2.4 Myr eccentricity minimum (marked by \* around 62 Ma) in their cycle bundles 35-36 as starting point for the tuning. This tuning was extended by matching successive 100-kyr limestone beds to successive 100-kyr eccentricity minima arriving at an K-T boundary age of ~65.8 Ma. The eccentricity time series of the La2004 solution (S26) and corresponding tuning are added for comparison following the same approach with limestone beds 35-36 as starting point and extending the tuning by matching successive 100-kyr limestone beds to successive 100-kyr eccentricity minima now arriving at an K-T boundary age of ~65.6 Ma. Numbers indicated in the column left of the lithological column denote the successive prominent ~100 kyr eccentricity related cycles of (S24) with limestone beds tuned to eccentricity minima in the middle. Note that the position of the boundaries of the 100-kyr cycles differ slightly from the positions indicated in (S24). Crosses to the right of the lithological column mark mid-points of limestone dominated parts of the 100-kyr cycle that correlate with 100-kyr eccentricity minima. The boundaries between the cycles represent mid-points of the more marly intervals of the 100-kyr cycle that correlate with 100-kyr eccentricity maxima. The magnetostratigraphy ranges from top C29r into C27r. Partially filled black shading denotes two short intervals of normal polarities above C27n, which may represent cryptochrons (S24). The K-T boundary is located at 0 m at the base of this part of the section.



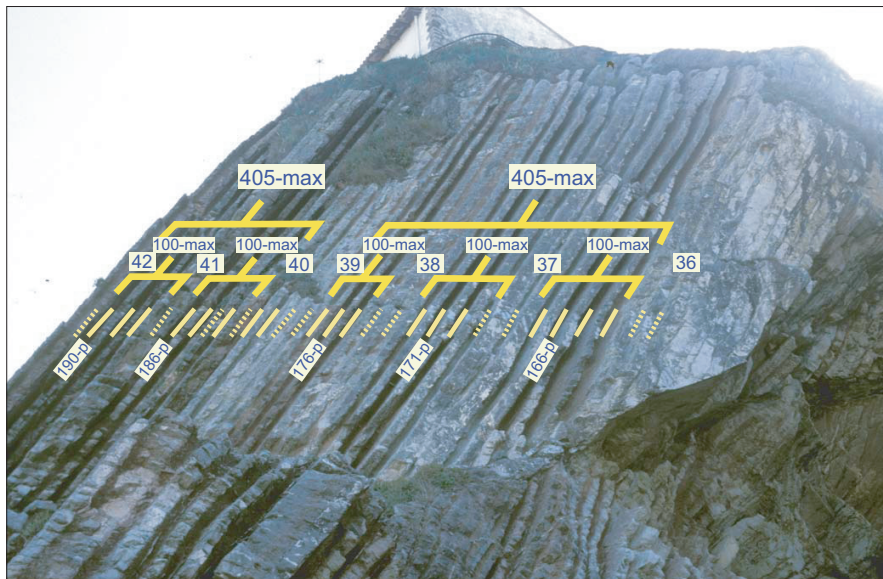


**Figure S3a. Upper part of the Zumaia section of (S24) below the San Telmo chapel.**

In the upper photograph, both 100-kyr limestone beds 29 to 42 of (S24) and large scale clusters of precession-related basic cycles that mark successive 405-kyr eccentricity maxima have been indicated. Lower photograph shows the detailed pattern of the precession-related basic cycles (limestone-marl couplet) in the interval that ranges from 100-kyr limestone bed 36 to bed 42. Solid lines mark distinct to prominent marlbeds of the individual precession related cycles, dashed lines mark less distinct to vague marlbeds. Precession cycle numbers (with a -p) correspond to number as in (S24). The phase relations with the 100- and 405-kyr eccentricity cycles have also been indicated (see also caption to Fig. S4).

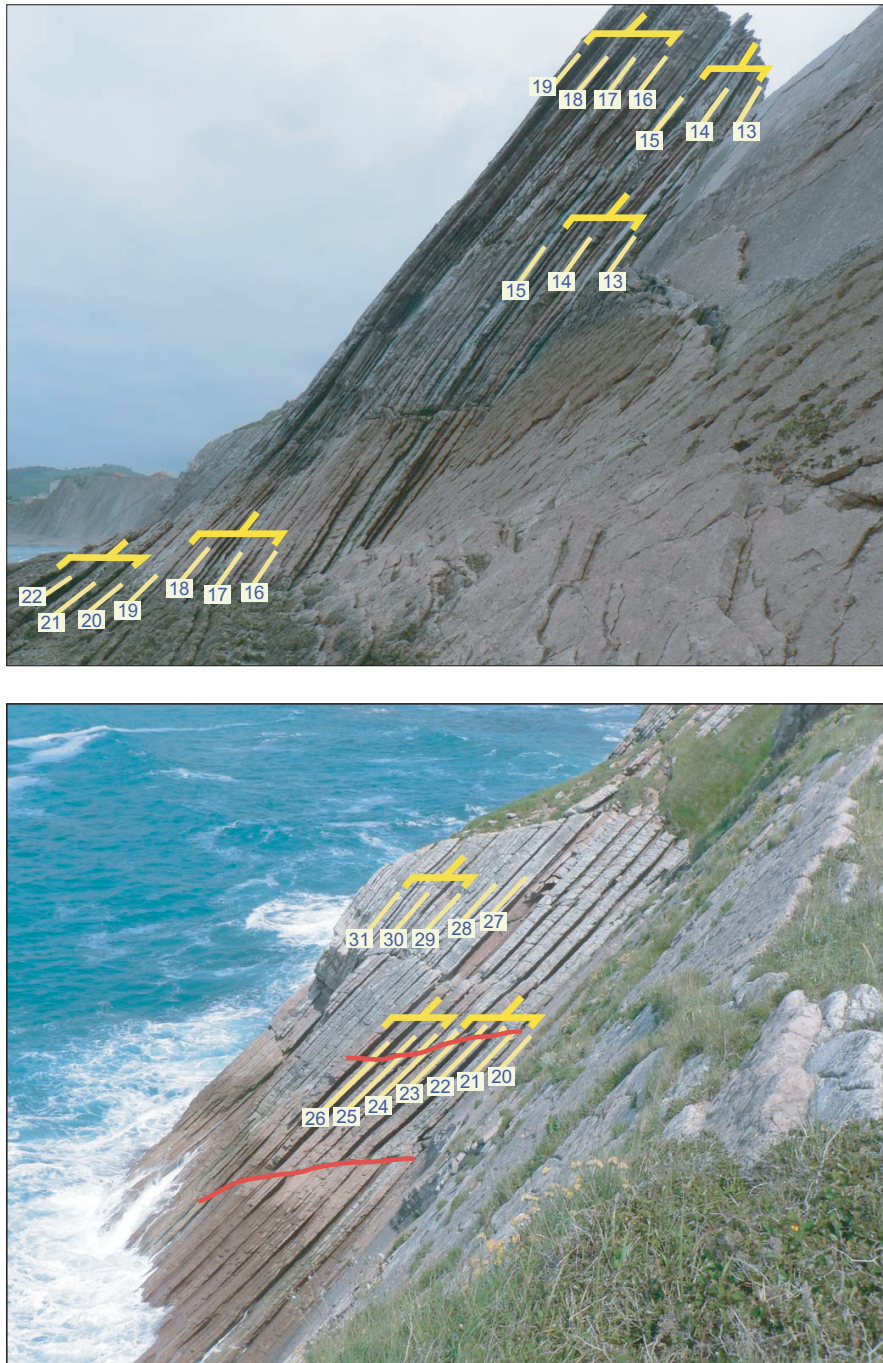


**Figure S3b. Middle part of the Zumaia section (S24).**

The lower photograph shows the interval ranging from 100-kyr limestone bed 21 to 31 of (S24), with a stratigraphic overlap with the upper part of the section shown in Fig. S3a. Also shown are clusters of well-developed 100-kyr marl beds that mark successive 405-kyr eccentricity maxima. Upper photograph shows the interval ranging from 100-kyr limestone bed 13 to 22 of (S24) and the clustering of intervals with well-developed marly layers that mark successive 405-kyr eccentricity maxima. Red lines mark small faults.

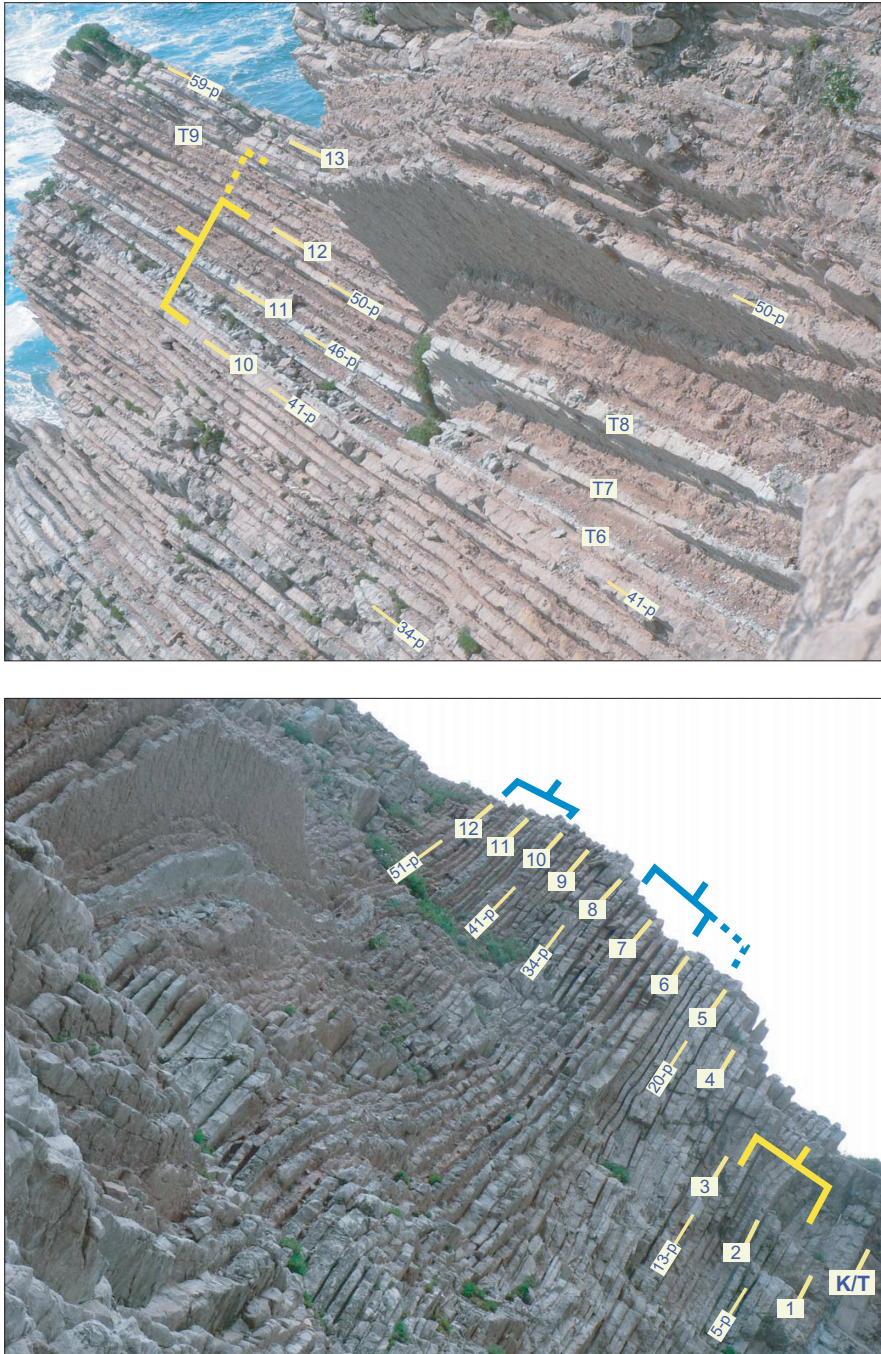
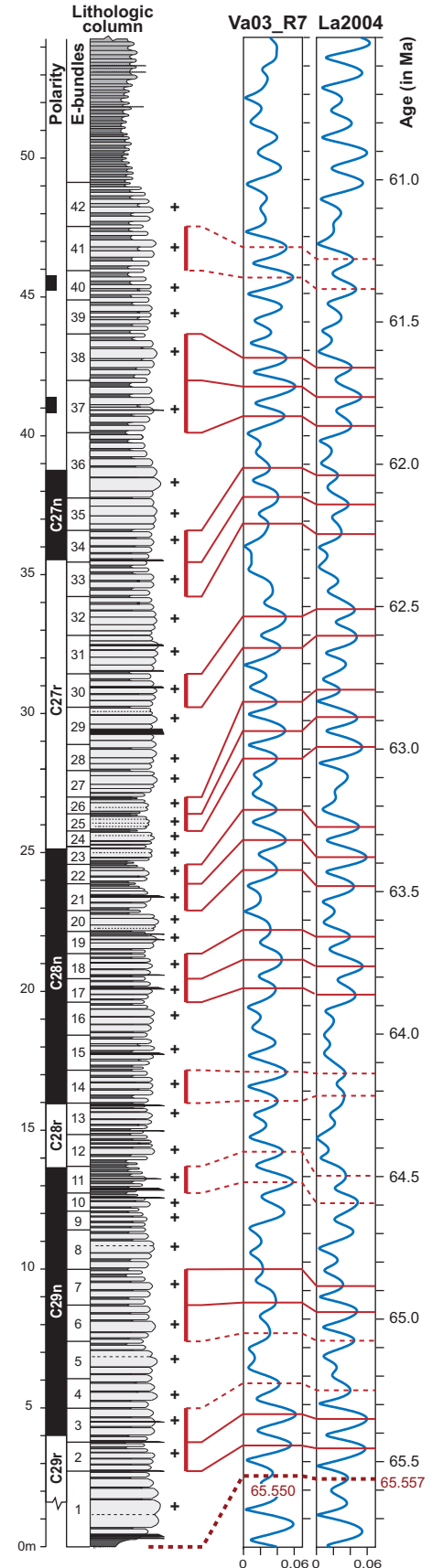


**Figure S3c. Lower part of the Zumaia section of (S24) as exposed on the SW side of the Aitzgorri headland.** The upper photograph shows the interval ranging from 100-kyr limestone bed 10 to 13 of (S24). Also shown is the cluster of well-developed marly layers between 100-kyr limestone beds 10 and 12 (or 13) that corresponds to a single 405-kyr eccentricity maximum. Patterns are less obvious due to the intercalation of several turbidites (T6-9). Lower photograph shows the interval ranging from the K-T boundary up to the 100-kyr limestone bed 12 of (S24) and the clustering of intervals with well-developed marly layers that corresponds to successive 405-kyr maxima. On both photographs, numbers of some characteristic precession-related cycles of (S24) are indicated (with a -p).

**Figure S4: Alternative option to tune the large scale cycles one 405 kyr eccentricity cycle younger.**

This revised tuning is consistent with  $\sim 65.56$  Ma for the K-T boundary, which can be converted to  $\sim 28.02$ - $28.09$  Ma for FCs using the data of (S27-S29) and is more in agreement with the commonly used age of 28.02 Ma (S1) adopted in GTS2004 (S13). Note however, that the absolute uncertainty in  $^{40}\text{Ar}/^{39}\text{Ar}$  ages calculated with  $28.02 \pm 0.28$  Ma is too large to pinpoint the correct 405 kyr eccentricity maximum when all uncertainties are included and is therefore within error consistent with an astronomically tuned age of  $\sim 65.95$  Ma for the K-T boundary (Fig. 4). Tuning one 405 kyr cycle older than our preferred tuning shown in Fig. 4 yields a K-T boundary age of  $\sim 66.43$  Ma which converts to  $\sim 28.38$ - $28.46$  Ma for FCs, coincidentally equivalent to the U/Pb age of FC zircon and titanite of (S30). See further also captions to figs. 4 and S2.



### **Chixculub impact crater and K-T boundary event**

We are aware of the existing and ongoing controversy about relating the Chixculub impact crater to the K-T boundary event. Keller et al. (S31) argue that the Chixculub impact predates the K-T boundary by ~300,000 years, based among others on the presence of alleged planktonic foraminifera of late Maastrichtian age in a 0.5 meter thick laminated limestone between the suevite impact breccia and the K-T boundary in Core Yaxcopoil-1 drilled in the Chixculub structure and the occurrence of multiple tektite layers below the K-T boundary in sections around the Gulf of Mexico. These layers as well as younger tektite layers of Danian age have been interpreted as reworked material from the oldest tektite layer which is supposedly associated with the Chixculub impact, although an additional tektite-producing event is not completely excluded. Smit (S32) opts for a single impact at the K-T boundary arguing that the multiple tektite layers and the sandstone bed (“event deposit”) result from tidal waves generated by the impact. He further mentions the single “dual layer” of impact ejecta observed in continental sections further north in the US and Canada as argument for his scenario; moreover the most complete marine sections do not reveal evidence for a multiple impact history. Evidently this ongoing discussion has consequences for our use of  $^{40}\text{Ar}/^{39}\text{Ar}$  ages from the K-T boundary interval which come both from tektites (Beloc, Haïti), glassy impact melt (Chixculub crater) and from ash layers that closely coincide with the K-T boundary in continental sections in North America.

We therefore preferred to use only single sanidine ages using FCs as main neutron fluence monitor from the Ir-Z and Z-coal bentonites closely associated with the K-T boundary to arrive at an astronomically calibrated  $^{40}\text{Ar}/^{39}\text{Ar}$  age between 65.84 – 65.99 Ma for the boundary (table S4; the limited number of replicate analyses in Izett et al. (S27) are ignored). Note however that the  $^{40}\text{Ar}/^{39}\text{Ar}$  ages of the tektites and Chixculub impact melt (table S4) do not reveal unequivocal differences with this age of the K-T boundary while, according to Keller et al. (S31), the tektites and impact melt should be ~300,000 year older. The fact that these ages are certainly not 300,000 years older than the continental sanidine ages (in spite of some minor discrepancies) actually seems to favour the single event scenario advocated by Smit (S32).

**Table S4: Details on published  $^{40}\text{Ar}/^{39}\text{Ar}$  data of K-T boundary(S27-S29, S33).**

In bold are the ages regarded as best age estimates in original publications. All ages are recalculated to the astronomically calibrated age of  $28.201 \pm 0.046$  Ma for FCs and full absolute errors are given. The K-T boundary as defined in the Western Interior continental sections in northern America is located at the base of lignite or coal beds including IrZ –and Z-coal.

Sample	Method	Standard and standard age (Ma)	Age (in Ma; $\pm 2\text{SE}$ )	Age (in Ma; $\pm 2\text{SE}$ ); FCs = 28.201 Ma
<b>Izett et al., 1991</b>				
Beloc tektite, Haiti	weighted mean of 23 total fusion on single tektites	MMhb-1 513.9 / TCR 27.92 / FCT 27.55	<b>64.48 <math>\pm</math> 0.16</b>	<b>65.98 <math>\pm</math> 0.20</b>
Beloc tektite, Haiti	weighted mean age of 4 incremental heating experiments on single tektites	MMhb-1 513.9 / TCR 27.92 / FCT 27.55	$64.38 \pm 0.36$	$65.88 \pm 0.38$
Beloc tektite, Haiti	1 bulk incremental heating experiment with furnace	MMhb-1 520.4 / TCR 28.20 / FCT 27.80	$64.8 \pm 1.4$	$65.7 \pm 1.4$
HC bentonite in Z-coal, Hell Creek Montana - sanidine	weighted mean of 3 single total fusions	MMhb-1 513.9 / TCR 27.92 / FCT 27.55	$64.57 \pm 0.46$	$66.07 \pm 0.48$
<b>Swisher et al., 1992</b>				
C1 glassy melt rock of Chicxulub crater	weighted mean age of 3 plateau ages on glassy (andesitic) rock chips	FCT 27.84	<b>64.98 <math>\pm</math> 0.10</b>	<b>65.81 <math>\pm</math> 0.14</b>
Beloc tektites (between levels f and g), Haiti	weighted mean age of 5 plateau ages on single tektites (4 tektites did not yield well-defined plateaus)	FCT 27.84	$65.01 \pm 0.16$	$65.84 \pm 0.18$
Beloc and Arroyo el Mimbral microtektites	weighted mean of 3 Beloc and 2 Mimbral total fusion on single tektites	FCT 27.84	$65.07 \pm 0.20$	$65.90 \pm 0.22$
<b>Swisher et al., 1993</b>				
IrZ-coal bentonite - sanidine	weighted mean age of 9 single fusions	FCT 27.84	<b>65.16 <math>\pm</math> 0.08</b>	<b>65.99 <math>\pm</math> 0.12</b>
IrZ-coal bentonite - plagioclase	weighted mean age of 4 single fusions	FCT 27.84	$65.16 \pm 0.78$	$65.99 \pm 0.78$
Z-coal at McGuire Creek - sanidine	weighted mean age of 20 single fusions	FCT 27.84	$65.03 \pm 0.08$	$65.86 \pm 0.12$
Z-coal at Hell Creek State Park Access Road - sanidine	weighted mean age of 13 single fusions	FCT 27.84	$64.96 \pm 0.10$	$65.79 \pm 0.14$
Z-coal combined	weighted mean age of 33 single fusions	FCT 27.84	<b>65.01 <math>\pm</math> 0.06</b>	<b>65.84 <math>\pm</math> 0.12</b>
<b>Dalrymple et al., 1993</b>				
Beloc tektites	weighted mean of 52 total fusion on single tektites in several irradiations (of which 23 in Izett et al., 1991)	MMhb-1 513.9 / TCR 27.92 / FCT 27.55	$64.42 \pm 0.14$	$65.92 \pm 0.18$
Z-coal bentonite - sanidine	weighted mean of 28 single total fusions in several irradiations (of which 3 in Izett et al., 1991)	MMhb-1 513.9 / TCR 27.92 / FCT 27.55	$64.77 \pm 0.14$	$66.28 \pm 0.16$
Z-coal bentonite - sanidine	weighted mean of 25 single total fusions in several irradiations with TCR as standard	TCR 27.92	$64.80 \pm 0.16$	$66.18 \pm 0.16^*$

\*recalculated relative to TCR 28.523 Ma using FC 28.201 Ma and the  $R^{FC}_{TCR}$  of Renne et al. (S1).

## **References in Supporting Online Material**

- S1. P. R. Renne *et al.*, *Chemical Geology* **145**, 117-152 (1998).
- S2. R. H. Steiger, E. Jäger, *Earth and Planetary Science Letters* **36**, 359 (1977).
- S3. J. R. Wijbrans, M. S. Pringle, A. A. P. Koppers, R. Scheveers, *Proc. Kon. Ned. Akad., v. Wetensch.* **98**, 185 (1995).
- S4. K. F. Kuiper, F. J. Hilgen, J. Steenbrink, J. R. Wijbrans, *Earth and Planetary Science Letters* **222**, 583 (2004).
- S5. A. A. P. Koppers, *Computers & Geosciences* **28**, 605 (2002).
- S6. K. J. Cunningham, R. H. Benson, K. Rakic-El Bied, L. W. McKenna, *Sedimentary Geology* **107**, 147 (1997).
- S7. P. Münch *et al.*, *International Journal of Earth Sciences* **95**, 491 (2006).
- S8. S. Roger *et al.*, *Earth and Planetary Science Letters* **179**, 101 (2000).
- S9. K. W. Min, R. Mundil, P. R. Renne, K. R. Ludwig, *Geochimica Et Cosmochimica Acta* **64**, 73 (2000).
- S10. M. A. Lanphere, H. Baadsgaard, *Chemical Geology* **175**, 653 (2001).
- S11. A. Dazé, J. K. W. Lee, M. Villeneuve, *Chemical Geology* **199**, 111 (2003).
- S12. A. K. Baksi, D. A. Archibald, E. Farrar, *Chemical Geology* **129**, 307 (1996).
- S13. F. M. Gradstein, J. G. Ogg, A. G. Smith, *A Geologic Time Scale 2004*, Cambridge University Press (2004), 589 pp.
- S14. A. K. Baksi, V. Hsu, M. O. McWilliams, E. Farrar, *Science* **256**, 356 (1992).
- S15. R. S. Coe, B. S. Singer, M. S. Pringle, X. X. Zhao, *Earth and Planetary Science Letters* **222**, 667 (2004).
- S16. B. S. Singer *et al.*, *Journal of Geophysical Research-Solid Earth* **107** (2002).
- S17. B. S. Singer, M. S. Pringle, *Earth and Planetary Science Letters* **139**, 47 (1996).
- S18. L. L. Brown, B. S. Singer, J. C. Pickens, B. R. Jicha, *Journal of Geophysical Research-Solid Earth* **109** (2004).
- S19. G. A. Izett, J. D. Obradovich, *Journal of Geophysical Research* **99**, 2925 (1994).
- S20. T. L. Spell, I. McDougall, *Geophysical Research Letters* **19**, 1181 (1992).
- S21. L. Tauxe, A. D. Deino, A. K. Behrensmeyer, R. Potts, *Earth and Planetary Science Letters* **109**, 561-572 (1992).
- S22. C. M. Hall, J. W. Farrell, *Earth and Planetary Science Letters* **133**, 327-338 (1995).
- S23. A. M. Sarna-Wojcicki, M. S. Pringle, J. Wijbrans, *Journal of Geophysical Research* **105**, 211,431-21,443 (2000).
- S24. J. Dinares-Turell *et al.*, *Earth and Planetary Science Letters* **216**, 483 (2003).
- S25. F. Varadi, B. Runnegar, M. Ghil, *Astrophysical Journal* **592**, 620 (2003).
- S26. J. Laskar *et al.*, *Astronomy & Astrophysics* **428**, 261 (2004).
- S27. G. A. Izett, G. B. Dalrymple, L. W. Snee, *Science* **252**, 1539 (1991).
- S28. C. C. Swisher, L. Dingus, R. F. Butler, *Canadian Journal of Earth Sciences* **30**, 1981 (1993).
- S29. C. C. Swisher III *et al.*, *Science* **257**, 954 (1992).
- S30. M. D. Schmitz, S. A. Bowring, *Geochimica Et Cosmochimica Acta* **65**, 2571 (2001).
- S31. G. Keller *et al.*, *Earth and Planetary Science Letters* **255**, 339 (2007).
- S32. J. Smit, *Annual Review of Earth and Planetary Sciences* **27**, 75 (1999).
- S33. G. B. Dalrymple, G. A. Izett, L. W. Snee, J. D. Obradovich,  $^{40}\text{Ar}/^{39}\text{Ar}$  age spectra and total-fusion ages of tektites from Cretaceous-Tertiary boundary sedimentary rocks in the Beloc Formation, Haiti, *U. S. Geological Survey Bulletin* (U. S. Geological Survey, Reston, VA, United States, 1993).

**Supporting Online Material**

[www.sciencemag.org](http://www.sciencemag.org)

Materials and Methods

Age and error equations

Text on Chixculub impact and K-T boundary controversy

Tables S1, S2, S3, S4

Figs. S1, S2, S3, S4